Investigating anaerobic metabolism of *Pseudomonas putida* using bioelectrochemical cultivation

Dissertation

zur Erlangung des
Doktorgrades der Naturwissenschaften (Dr. rer. nat.)

der
Naturwissenschaftliche Fakultät I – Biowissenschaften

der Martin-Luther-Universität
Halle-Wittenberg,

vorgelegt von

Herrn Anh Vu Nguyen

Master of Science and Technology
Bachelor of Science and Technology

Gutachter: Prof., Dr. rer. nat., Jens Olaf Krömer
Prof., Dr., Miriam Agler-Rosenbaum
Prof., Dr. sc. nat., Bruno Bühler

Öffentlich verteidigt am **10.07.2024**

Diese Dissertation wurde von

1. Prof., Dr. rer. nat., Jens Olaf Krömer
   Department Umweltmikrobiologie, Helmholtz-Zentrum für Umweltforschung (UFZ);
   Naturwissenschaftliche Fakultät I – Biowissenschaften, Martin-Luther-Universität Halle-Wittenberg

2. Prof., Dr., Miriam Agler-Rosenbaum
   Bio Pilot Plant, Leibniz-Institut für Naturstoff-Forschung und Infektionsbiologie e. V. Hans-Knöll-Institut (HKI);
   Fakultät für Biowissenschaften, Friedrich-Schiller-Universität Jena

3. Prof., Dr. sc. nat., Bruno Bühler
   Department Umweltmikrobiologie, Helmholtz-Zentrum für Umweltforschung (UFZ);
   Naturwissenschaftliche Fakultät I – Biowissenschaften, Martin-Luther-Universität Halle-Wittenberg

bewertet und von der Promotionskommission der MLU Halle-Wittenberg für Veröffentlichung bewilligt.

Eigenständigkeitserklärung

Hiermit versichere ich, dass ich die vorliegende Arbeit selbstständig und nur mit den angegebenen Hilfsmitteln verfasst habe.

Ich erkläre ausdrücklich, dass ich sämtliche in der Arbeit verwendeten fremden Quellen, auch aus dem Internet, als solche kenntlich gemacht habe. Insbesondere bestätige ich, dass ich ausnahmslos sowohl bei wörtlich übernommenen Aussagen (Zitaten) bzw. unverändert übernommenen Tabellen, Grafiken u. ä. als auch bei in eigenen Worten wiedergegebenen Aussagen bzw. von mir abgewandelten Tabellen, Grafiken u. ä. anderer Autorinnen und Autoren (indirektes Zitieren) die Quelle angegeben habe.

Mir ist bewusst, dass Verstöße gegen die Grundsätze wissenschaftlichen Arbeitens im Studium (s. Erklärung über die Beachtung der Grundsätze wissenschaftlichen Arbeitens im Studium) als Täuschung betrachtet und entsprechend der Studien- und Prüfungsordnung des Studiengangs geahndet werden.

Ich versichere, dass ich diese Arbeit bisher nicht in gleicher oder ähnlicher Form bei einer anderen Institution eingereicht habe.

Halle, den 30.07.2024

Anh Vu Nguyen

Author's declaration

This dissertation consists of original work conducted by myself and contains no material previously published or written by another person except where due reference has been made in the text. I certify that, to the best of my knowledge, my dissertation does not infringe upon anyone's copyright nor violate any proprietary rights and that any ideas, techniques, quotations, or any other material from the work of other people included in my dissertation, published or otherwise, are fully acknowledged in accordance with the standard referencing practices. The contributions by others to jointly authored works included in this work are duly acknowledged. I have clearly stated the contribution of others to my dissertation as a whole, including data analysis, significant technical procedures, professional editorial advice, and any other original research work used or reported in my work.

I declare that this is a true copy of my dissertation, including any final revisions, as approved by my doctorate committee and Martin-Luther-University Halle-Wittenberg, and that this dissertation has not been submitted for a higher degree to any other university or institution. The content of this dissertation is the result of works I have conducted since the commencement of my research higher degree candidature and does not include a substantial part of work that has been submitted to qualify for the award of any other degree or diploma in any university or other tertiary institution.

I acknowledge that an electronic copy of my dissertation must be lodged with the University Library and, subject to the policy and procedures of Martin-Luther-University Halle-Wittenberg, the dissertation be made available for research and study in accordance with the German Copyright Act (*Urheberrechtsgesetz*, or *UrhG*) unless a period of embargo has been approved by Martin-Luther-University Halle-Wittenberg. I acknowledge that copyright of all material contained in my dissertation resides with the copyright holder(s) of that material. Where appropriate I have obtained copyright permission from the copyright holder to reproduce material in this dissertation.

Contributions by others to the dissertation

This dissertation includes the original work conducted during my doctorate research. The published or publishing works were drafted in collaborations as stated above. Prof. Dr. Pablo I. Nikel and Dr. Nicolas Thilo Wirth (Systems Environmental Microbiology, Novo Nordisk Foundation Center for Biosustainability, Denmark; Technical University of Denmark) provided the knockout *Pseudomonas putida* KT2440 strains. Caroline Ruhl, Ron Stauder and Dr. Pål William Wallace (Department of Solar Materials, UFZ) offered valuable discussion and technical support regarding the GC-MS and HPLC analytics. Dr. Bin Lai conducted some experiments for strain glcP before the commencement of my own work and provided some data analyses, as well as the calculation and correction of ^{13}C isotope tracing data in Chapter 5, Section 5.1.2. Benjamin Scheer (Department Environmental Biotechnology, UFZ) provided technical support of the operation of nLC-MS/MS. Prof. Dr. rer nat. Lorenz Adrian (Department Molecular Environmental Biotechnology, UFZ; Chair for Geobiotechnology, Institute of Biotechnology, Faculty III - Process Sciences, Technical University Berlin) assisted with data analysis of the proteomics. I acknowledges scholarship support from the Helmholtz Center for Environmental Research – UFZ within the STROMER PhD College and HIGRADE Graduate School. Protein mass spectrometry was done at the Centre for Chemical Microscopy (ProVIS) at the Helmholtz Centre for Environmental Research, which is supported by European regional development funds (EFRE—Europe Funds Saxony) and the Helmholtz Association.

Statement of parts of the dissertation submitted to qualify for the award of another degree

None.

Abstrakt

Die steigende Nachfrage nach kostengünstigen und umweltfreundlichen chemischen Produktionsverfahren erfordert die Entwicklung neuer Fermentationstechnologien. Das Bakterium *Pseudomonas putida* (*P. putida*) ist ein vielversprechender Chassis-Organismus der synthetischen Biologie zur Chemikalienherstellung als Ausgangsmaterial für die chemische Industrie. Ein großer Nachteil dieses Organismus ist allerdings sein obligater aerober Stoffwechsel. Trotz früherer Bemühungen um Anpassung dieses Bakteriums an anoxische Bedingungen durch Gentechnik oder Einsatz eines bioelektrochemischen Systems (BES) blieben die Probleme des zellulären Energiemangels und des internen Redox-Ungleichgewichts von *P. putida* bestehen. Um besser zu verstehen, welches die zugrundeliegenden Ursachen dieses Phänomens sein könnten, zielte diese Doktorarbeit darauf ab, verschiedene Aspekte des Stoffwechsels von *P. putida* wie z.B. den Kohlenstoffaufnahmeweg, den intrazellulären Metabolismus und den Elektronentransfer unter Abwesenheit von Sauerstoff aufzuklären. Durch die BES-Kultivierung verschiedener mutierter *P. putida*-Stämme, deren Kohlenstoffaufnahme jeweils auf bestimmte Stoffwechselwege beschränkt waren, sowie durch die ^{13}C-Isotopenmarkierung von Acetat zeigte sich, dass die Kohlenstoffaufnahme durch die Zytoplasmamembran eher der unter aeroben Bedingungen ähnelt, wenn auch viel eingeschränkter. Es wurde festgestellt, dass die periplasmatische Oxidationskaskade (POC) in der Lage ist, eine Vielfalt von Aldosen zu ihren dazugehörigen Aldonaten und Ketoaldonaten zu oxidieren. Im Vergleich mit Glucose führte die Fructoseoxidation im BES zu einem erhöhten NADPH/NADP$^+$ Verhältnis. Entgegen der beschriebenen Fructoseaufnahme ermöglichte die Isomerisierung von Fructose zu Mannose auch die Oxidation durch Glucose-Dehydrogenase. Dies stellt einen neuen Weg für den Fructosestoffwechsel von *P. putida* im BES dar. Durch vergleichende Proteomik von *P. putida* während der elektrochemischen Experimente wurde eine Hochregulierung der Proteinexpression im zentralen Kohlenstoffmetabolismus sowie der Elektronentransportkette im Vergleich mit Kulturen ohne angelegtes Elektrodenpotential festgestellt. Die Hemmung des Membranproteins TonB wirkte sich negativ auf den elektrischen Strom sowie den Kohlenstoffkatabolismus aus. Dies zeigte prinzipiell, dass TonB eine Rolle bei der Verbesserung des Elektronentransfers spielen kann. Insgesamt stellen diese Ergebnisse nicht nur Wissensgewinn über den anoxischen Kohlenstoffstoffwechsel von *P. putida* in einem anodengesteuerten mikrobiellen Elektrofermentationsprozess dar, sondern sie zeigen auch die Flexibilität dieses Bakteriums bei der Metabolisierung der Kohlenhydrate im BES zum Erhalten eines erweiterten Spektrums von Mehrwertprodukten. Durch die Kombination des aktuellen Wissens mit Strategien des Pathwaydesigns und der Systembiologie könnte dieser

elektrodengestützte Prozess eventuell eine neue robuste Plattform für die Bio-Chemikalienproduktion in der Zukunft sein.

Schlüsselwörter: anodische Fermentation, anoxischer Stoffwechsel, Kohlenhydratoxidation, metabolomische Profilierung, periplasmatische Oxidation, Proteomik, *Pseudomonas putida*, Redox-Stoffwechsel, Transmembranelektronentransport, zentraler Kohlenstoffstoffwechsel.

Abstract

The increasing demand for cost-effective and environmentally friendly chemical production requires the development of new fermentation technology. *Pseudomonas putida* (*P. putida*) – a promising synthetic biology chassis to produce chemicals as feedstock for the chemical industry. A drawback of this organism is its obligate aerobic metabolism. Despite previous endeavours to adapt *P. putida* to anoxic conditions via genetic engineering or the use of a bioelectrochemical system (BES), the problem of energy shortage and internal redox imbalance persisted. In order to better understand what might be the underlying causes for this phenomenon, this dissertation aims to elucidate different aspects of *P. putida*'s metabolism, including carbon uptake, intracellular metabolism, and electron removal under oxygen-limited conditions. Cultivating different mutant *P. putida* strains whose carbon influx is constrained in specific uptake routes in BES, in combination with ^{13}C isotope tracing of acetate, revealed that carbon influx through the cytoplasmic membrane is rather similar to that under aerobic conditions, albeit much more limited. The periplasmic oxidation cascade (POC) was found to be able to oxidize a wide range of aldoses to their corresponding aldonates and ketoaldonates. Fructose oxidation in BES resulted in a higher NADPH/$NADP^+$ ratio compared to glucose. Unexpectedly, the isomerization of fructose to mannose also enabled sugar oxidation by glucose dehydrogenase - a new pathway for fructose metabolism of *P. putida* in BES was uncovered. Comparative proteomics of *P. putida* during BES cultivation showed upregulation of protein expression in the central carbon metabolism as well as the electron transport chain during the electrochemical experiment, compared to controls without applied electrode potential. Inhibiting membrane protein TonB had a negative impact on current output and carbon catabolism, providing a proof-of-concept of the role of this system in facilitating the removal of electrons. Overall, the findings in this dissertation not only provide additional information on *P. putida*'s anoxic carbon metabolism in an anode-driven microbial electro-fermentation process but also demonstrate the versatility of this bacterium in metabolizing carbohydrates under BES conditions for a wide range of value-added carbon products. By combining the current knowledge with metabolic engineering and system biology strategies, this electrode-assisted process could potentially be a new robust platform for the bioproduction of chemicals in the future.

Key words: anodic fermentation, anoxic metabolism, carbohydrate oxidation, central carbon metabolism, metabolic profiling, periplasmic oxidation, proteomics, *Pseudomonas putida*, redox metabolism, transmembrane electron transport.

Acknowledgment

First, I would like to thank the STROMER Ph.D. College for giving me the opportunity to travel to Germany to obtain my Ph.D. degree. I would like to express my sincerest gratitude to my direct supervisor Prof. Dr. rer. nat. Jens O. Krömer, for his immense knowledge, patience, motivation, as well as the continuous support of my doctorate during and after my time working at UFZ. I appreciate the discussions that we have had throughout this Ph.D. journey, through which I have learned a lot as a researcher and a person. Jens always offered his support for my ideas, even though sometimes they weren't the best. There were moments that I had doubt about the path that I am taking, but he always reminded me that the finishing line is within my reach. Outside of work, I was, and will always be, amazed by the adventurous stories of his life and family. I could not ask for a better supervisor and inspiration. To Jens, I don't know what else to say, other than "Thank you for everything!"

I would like to especially thank Dr. Bin Lai, whom I was directly under the mentorship of during my Ph.D. Without his past and present works on bioelectrochemical systems and *Pseudomonas putida*, this dissertation would not come to fruition. To Bin, I just know that you will continue to achieve great success in the future. You are the best!

In addition, I would like to thank Prof. Dr. rer. nat. Andreas Schmid and the Department of Solar Materials (SoMa) for hosting the entirety of my Ph.D. Additionally, I would like to thank Prof. Dr. rer. nat. Lorenz Adrian and his group. Even though juggling between two labs was not an easy task, but I have learned a lot from both. I will always remember the good time and great help that I have received, inside and outside of work. It is my pleasure and honor to know you and work together with you. Great thanks to Ron, Pål, Benny, etc for the technical support. Especially to Lorenz, thank you for being a part of my STROMER direct advisors as well as the (tough) lessons. You reminded me that I should always strive for excellence. (And yes, I still remember every step and structure of every compound in the TCA cycle.)

I would like to extend my thanks to Barbara Timmel and the people of the UFZ International Office, without whom I would still be struggling with the bureaucracy, as well as UFZ's HIGRADE Graduate School and "Do-it" PhD Representatives at UFZ. Your support have made my stay as a foreigner and Ph.D. student in Germany so much easier. All the great events that we have done together will forever stay in my memory.

I would also like to thank all of my old and new friends that I have met along this journey. You guys have made my life in a strange land not so strange anymore. I will forever cherish the good (and crazy) times we have had together. To Caroline Ruhl, friend and colleague, thanks

for all the great helps at work as well as (and sometimes exotic) gifts. I wish you the best of life. To all of my roommates, I wish you all the best, wherever you are now. To my SOMA colleagues, as well as my STROMER fellows – Jieying, Francesco and Johannes, I wish you all the successes with your career. An meine Deutschlehrer*innen und Klassenkameraden, vielen Dank für die tollen Unterrichte!

Last but not least, I would like to thank my family – parents, sister, relatives – for the unrequited love, supports, patience, sacrifices, and above all, for believing in me that I can make this happen. Thank you for being by my side with every step that I have made, even when we were time- and continent-apart. I am very grateful for having you in my life.

This work is dedicated to all of you.

Table of contents

Eigenständigkeitserklärung ..... **I**

Author's declaration ..... **II**

Abstrakt ..... **IV**

Abstract ..... **VI**

Acknowledgment ..... **VII**

Table of contents ..... **IX**

List of figures ..... **XII**

List of tables ..... **XIV**

List of abbreviations and acronyms ..... **XV**

Chapter 1. Introduction **1**

Chapter 2. Literature review **5**

2.1. Physiological features of *Pseudomonas putida* KT2440 5

2.1.1. Genus Pseudomonas: characteristics, distribution and applications 5

2.1.2. Genome 6

2.1.3. Respiration 6

2.1.4. Carbon metabolism 8

2.1.5. Nutrient uptake via TonB complex and TonB-dependent transporters 14

2.2. Aldonic acids and aldonic acid derivatives 15

2.2.1. Chemistry 15

2.2.2. Applications and status of production 17

2.2.3. Challenges of current production processes 20

2.3. Bioelectrochemical systems for industrial processes 21

2.3.1. Basic design 21

2.3.2. Extracellular electron transfer 23

2.3.3. Applications for chemical production 25

2.4. Integrative electrochemical and proteomics approach for strain development of electrogens 30

Chapter 3. Aims, scope and objectives 32

3.1. Aims 32

3.2. Scope 33

3.3. Objectives 33

Chapter 4. Materials and methods 35

4.1. Bioelectrochemical reactor design 35

4.2. Operation and monitoring of bioreactor 38

4.2.1. Media 38

4.2.2. Electrochemical method 39

4.3. Standard operation procedure of bioelectrochemical cultivation 39

4.3.1. Pre-culture preparation 39

4.3.2. Reactor assembly 40

4.3.3. BES cultivation 40

4.4. Analytical methods 40

4.4.1. Gas chromatography – mass spectrometry (GC-MS) 40

4.4.2. High performance liquid chromatography (HPLC) 42

4.4.3. Adenylate and redox molecule assays 43

4.4.4. Differential analysis of protein expression 45

4.5. Calculation of performance parameters 47

4.5.1. Biomass 47

4.5.2. Current density, cumulative charge, and total electron discharge 47

4.5.3. Production yields, rates, carbon and electron balance 47

Chapter 5. Results and Discussion 49

5.1. Carbon flux on cytoplasmic membrane of *Pseudomonas putida* during bioelectrochemical cultivation 49

5.1.1. P. putida mutants channeling carbon through glcP, gaP, and 2kgaP pathway 49

5.1.2. Anaerobic carbon flux distribution on P. putida's cytoplasmic membrane during bioelectrochemical cultivation 53

5.1.3. Discussion 56

5.2. Periplasmic oxidation of aldoses by *Pseudomonas putida* 58

5.2.1. Aerobic oxidation of galactose and arabinose 58
5.2.2. Oxidation of aldohexoses and aldopentoses in BES 59
5.2.3. Discussion 61
5.3. Metabolism of fructose by *Pseudomonas putida* under BES condition 62
5.3.1. Bioelectrochemical performance 62
5.3.2. Extracellular metabolic profile 64
5.3.3. Impact of fructose metabolism on the energy and redox status of the cell 65
5.3.4. Proteomics of Pseudomonas putida under anaerobic cultivation 67
5.3.5. Discussion 73
5.4. Inhibition of TonB decreases the bioelectrochemical activity of *Pseudomonas putida* 78
5.4.1. Effect of TonB inhibitors on P. putida's sugar catabolism under aerobic conditions 78
5.4.2. Effect of TonB inhibitors on the bioelectrochemical activity of P. putida 80
5.4.3. Discussion 82
Chapter 6. Final remarks and future prospects 84
6.1. Summary 84
6.2. Future prospects 85
6.2.1. New protein targets for strain engineering 85
6.2.2. Additional analytical approaches 86
Bibliography i
Appendix xxi
Curriculum vitae xxxi
List of publications during candidature xxxii

List of figures

Figure 1. Electron micrograph of *P. putida* 5

Figure 2. KEGG pathway diagram of *P. putida* strain KT2440's oxidative phosphorylation system 7

Figure 3. Central carbon metabolism in *P. putida* KT2440. 9

Figure 4. Peripheral glucose oxidation and uptake pathways in *P. putida* KT2440 11

Figure 5. Structure, location and function of the energy-transducing TonB-ExbBD complex in Gram-negative bacteria 15

Figure 6. Examples of aldonic acids, ketoaldonic acid, aldonolactones, and bionic acids .. 16

Figure 7. Working principle of bioelectrochemical systems 22

Figure 8. Simplified representations of known electron transfer mechanisms in bioelectrochemical systems. 23

Figure 9. Three objectives to be tackled in this dissertation 34

Figure 10. The assembled BES reactor 38

Figure 11. Schematic representation of sample preparing step for compound detection and identification by GC-MS 41

Figure 12. Selected ion monitoring analysis of acetate 42

Figure 13. Example of an ATP quantification standard curve 43

Figure 14. Example of NADH and NADPH quantification standard curve 44

Figure 15. Consumption of glucose and production of selected secreted metabolites by *P. putida* KT2440 wild-type, glcP, gaP, and 2kgaP strains 52

Figure 16. Current density, consumption of glucose, and production of GA, 2KGA, and acetate of glcP, gaP, and 2kgaP strains under BES condition 54

Figure 17. Enrichment of ^{13}C in extracellular acetate under BES condition by glcP, gaP, and 2kgaP strains 56

Figure 18. Summed fractional labelling of ^{12}C and ^{13}C of extracellular acetate under BES condition by wild-type, glcP, gaP, and 2kgaP strains 58

Figure 19. Aerobic oxidation of D-galactose and L-arabinose by *P. putida* KT2440 59

Figure 20. Comparative performance of *P. putida* KT2440 wild-type and Δ*gcd* in BES with different aldose substrates. 60

Figure 21. GC-MS analysis of extracellular metabolite composition of KT2440 culture in D-galactose, L-arabinose, and D-ribose..... 61

Figure 22. Comparative performance of *P. putida* KT2440 wild-type and Δ*gcd* in BES with fructose as substrate..... 63

Figure 23. GC-MS analysis of *P. putida*'s extracellular sugars and sugar acids during BES cultivation with fructose. 64

Figure 24. NADPH/$NADP^+$ and NADH/NAD^+ ratios of *P. putida* KT2440 in BES..... 66

Figure 25. Relative differences in abundances of detected proteins in *P. putida* under different anaerobic cultivation setups. 68

Figure 26. Changes in protein expression of the central carbon metabolism in *P. putida* KT2440 during bioelectrochemical cultivation in fructose at peak current..... 76

Figure 27. Changes in protein expression of the electron transport chain in *P. putida* KT2440 during bioelectrochemical cultivation in fructose at peak current 77

Figure 28. Aerobic growth of *P. putida* KT2440 with the addition of 2-(((3-chloro-4-methoxyphenyl)amino)methyl)-8-quinolinol, and 3-hydroxy-2-(4-isopropylphenyl)-6-methyl-4H-chromen-4-one 79

Figure 29. Optical densities, absorbances of ferricyanide, and pH values of aerobic cultures of *P. putida* KT2440 with and without TonB inhibitors..... 80

Figure 30. Effect of TonB inhibitors and DMSO on glucose oxidation of *P. putida* under BES condition. 81

List of tables

Table 1. Regulatory proteins of upper glucose catabolic pathways in *P. putida***.** 12

Table 2. Production and application of selected aldonic acids and derivatives. 18

Table 3. Reported examples of chemicals produced via cathodic electro-fermentation..... 27

Table 4. Reported examples of chemicals produced via anodic electro-fermentation. 29

Table 5. Mutant *P. putida* strains used for studying cytoplasmic carbon flux. 50

Table 6. Performance of wild-type and mutant *P. putida* KT2440 strains in aerobic shake flasks 51

Table 7. Process parameters of *P. putida* strains catabolizing glucose in BES. 53

Table 8. Process parameters of anoxic fructose conversion of *P. putida* KT2440 wild-type and Δ*gcd* in BES reactors. 65

Table 9. Comparison of energy and redox ratios of *P. putida* cultivated in anoxic conditions. 66

Table 10. Changes in protein expression of the central carbon metabolism in *P. putida* KT2440 during bioelectrochemical, and open-circuit cultivation in fructose..... 70

Table 11. Changes in protein expression of the electron transport chain in *P. putida* KT2440 during bioelectrochemical, and open-circuit cultivation in fructose..... 72

List of abbreviations and acronyms

Abbreviation	Full name
2KGA	2-Keto-D-gluconic acid/-gluconate
2KGL	2-Keto-L-gulonic acid
A^-	Anion
ABC	ATP-binding cassette
Abs	Absorbance
ADP	Adenosine diphosphate
ATP	Adenosine triphosphate
BES	Bioelectrochemical system
BSTFA	N,O-Bis(trimethylsilyl)trifluoroacetamide
C^+	Cation
CA	Chronoamperometry
cAMP	Cyclic adenosine monophosphate
CB	Carbon balance
CDW	Cell dry weight
CE	Coulombic efficiency
CM	Cytoplasmic membrane
CMPAMQ	2-(((3-chloro-4-methoxyphenyl)amino)methyl)-8-quinolinol
CTAB	Cetyltrimethylammonium bromide
DDA	Data-dependent acquisition
DIA	Data-independent acquisition
DMSO	Dimethyl sulfoxide
DNA	Deoxyribonucleic acid
ED	Entner-Doudoroff
EMP	Embden-Meyerhof-Parnas
F16P	Fructose 1,6-bisphophate
F1P	Fructose 1-phophate
FAD(H_2)	Flavin adenine dinucleotide
FBA	Flux balance analysis
FC	Fold change
FeCN	Ferri-/ferrocyanide
GA	D-Gluconic acid/-gluconate
GA3P	Glyceraldehyde 3-phosphate
Gad	Gluconate dehydrogenase complex
GapDH	Glyceraldehyde 3-phosphate dehydrogenase
Gcd/*gcd*	Glucose dehydrogenase (Protein/gene)
GC-MS	Gas chromatography – mass spectrometry
HCD	Higher energy collisional dissociation

HIPPMC	3-hydroxy-2-(4-isopropylphenyl)-6-methyl-4H-chromen-4-one
HPLC	High-performance liquid chromatography
IC	Ion chromatography
KDPG	2-Dehydro-3-deoxy-phosphogluconate
LB	Lysogeny broth
MEC	Microbial electrolysis cell
MES	Microbial electrosynthesis
MET	Microbial electrochemical technology
MFC	Microbial fuel cell
MOX	Methoxyamine
MTBSTFA	N-methyl-N-tert-butyldimethylsilyl-trifluoroacetamide
NADH/NAD^+	Nicotinamide adenine dinucleotide (reduce/oxidized)
NADPH/$NADP^+$	Nicotinamide adenine dinucleotide phosphate (reduce/oxidized)
(n)LC-(MS/)MS	(Nano-)liquid chromatography-(tandem) mass spectrometry
OC	Open-circuit
OD	Optical density
OM	Outer membrane
OMC	Outer membrane (c-type) cytochrome
ORF	Open reading frame
PEEK	Polyether ether ketone
PEP	Phosphoenolpyruvate
PHA	Polyhydroxyalkanoate
POC	Periplasmic oxidation cascade
POP	Peripheral oxidative pathway
PP(P)	Pentose phosphate (pathway)
PQQ(H_2)	Pyrroloquinoline quinone(quinol)
PTFE	Polytetrafluoroethylene
PTS	Phosphotransferase system
RLU	Relative light unit
(m)RNA	(messenger) Ribonucleic acid
SHE	Standard hydrogen electrode
SIM	Selected ion monitoring
STROMER	Sustainable Transformation by Electrochemical Reactions
TBDMS	*tert*-Butyl dimethyl silyl
TBDT	TonB-dependent transporter
TCA	Tricarboxylic acid
TMS	Trimethyl silyl
WT	Wild-type
UQ(H_2)	Ubiquinone(quinol)
UV	Ultraviolet

Chapter 1.
Introduction

November 15th 2022 marked the 8-billion milestone of the world population, which has been predicted to reach 9.7 billion in 2050, despite the decreasing projection of growth rate to less than 1% per year as of 2020 – the first time since 1950 [1]. With the continuously growing population, the demand for food, energy, and materials, alongside concerns with the environmental impact of human activities, also rise. From 2000 to 2019, the total amount of resources used to meet the demands for goods and services increased by more than 65% globally, amounting to 95.1 billion metric tons in 2019. Therefore, in order to relieve the pressure on the environment as well as its effects on human health and economy, measures to increase resource efficiency, and overall efforts to de-materialize economic growth, are needed [2].

One of the many industries where these measures are most impactful is the production of input chemicals for different economic sectors. In 2021 the world chemical sales reached over €4000 billion, with Europe as the second largest chemicals producer, making up of 14. 7% to the global sales; Germany was one of the two largest European suppliers by contributing more than €171 billion. 56% of total chemical products in Europe were sold for further industrial manufacturing, including rubber and plastics, textiles, construction, computer production, and pulp and paper. Nevertheless, it still relies heavily on oil-based manufacturing and is subject to cumulative cost effects more than other sectors [3, 4]. Bio-based products, on the other hand, can make the economy more sustainable and lower its dependence on fossil fuels. Bio-based products are, wholly or partly, derived from materials of biological origin; by using fermentation and bio-catalysis instead of traditional chemical synthesis, higher process efficiency could be obtained, and with proper design and management, has the potential for generating fewer toxic by-products and less waste than traditional chemical manufacturing. For this reason, the EU has declared the bio-based products sector to be a priority area with high potential for future growth and re-industrialization [5, 6]. Thus, industrial fermentation has become the center of attention for production of bio-based chemicals.

Fermentation is traditionally (and narrowly) defined as the process where cells generate energy from breaking down carbohydrates in the absence of oxygen. But in a general sense, especially in the area of industrial microbiology, it is referred to as the biotransformation of a substrate by microbes or their enzymes to a desired product, regardless if oxygen is required (i.e., aerobic fermentation) or not (anaerobic fermentation). This is one of the oldest and most sustainable food processing and preservation methods, and throughout the history of

humankind various types of fermentation have been employed [7]. During the 20th century, the first industrial-scale fermentation processes were established for the production of chemicals, including acetone, butanol, and citric acid [8]. Today, the range of products that comes from fermentation includes antibiotics, organic acids, amino acids, polysaccharides, vitamins, enzymes, etc. [9, 10].

In larger-scale bioproduction or remediation, aeration can become cost-intensive as scaling-up of the aerobic process is significantly limited by the oxygen transfer rate [11-14]. Furthermore, facultative anaerobes, such as *Escherichia coli*, might, during oxygen limitation, form large amounts of by-products, such as acetate, which can inhibit the growth and fermentation performance of the bacteria [15-17]. On the other hand, strictly aerobic bacteria, such as *Pseudomonas putida* do not form such fermentative by-products. *P. putida* has previously demonstrated hallmark features of an interesting microbial chassis for industrial and environmental processes [18-21], due to its versatile metabolism towards a wide range of carbon sources [22, 23] and high resistance to environmental stresses [24]. Like any other obligate aerobes, however, this bacterium requires oxygen not only as an electron sink but also as a reagent of oxygenation reactions. Recently, oxygen-dependent enzymes essential for biomass production were replaced with non-oxygen-associated alternatives [25]. Nevertheless, the published efforts to include selected fermentative or anaerobic respiratory pathways to establish anaerobic electron balancing in the cells still relied on fermentation by-products or co-substrates as electron sinks [26-28]. Even though these strategies were able to improve the bacterium's survival under anoxic conditions, along with minimal carbon turnover, no substantial anaerobic growth was observed, as well as a persisting problem of energy shortage, and redox imbalance.

An approach to decouple the electron balance from the carbon balance, or depletable external electron acceptors is the use of microbial electrochemical technologies (METs). Here, electrodes take up excess electrons from respiratory pathways or fermentation reactions. In recent years, various bioelectrochemical system (BES) designs have been utilized for anodic cultivation of *P. putida* under oxygen-deprived conditions. In brief, an electrode (anode) was provided as the terminal electron sink for the cells via redox mediators, such as ferricyanide $Fe[CN]_6^{3-}$ [29-31], or self-secreted phenazines [32-34] to drive anaerobic carbon metabolism. The recorded current response provides a direct measurement of catabolic reactions occurring in the system, as electrons are released during substrate oxidation.

Unfortunately, there is still a long way to go until bioelectrochemical production can meet industrial requirements. There is a general recognition that scale-up is an important and difficult barrier to overcome, as the industrial scale reactors need to achieve similar

performances as laboratory scale reactors, while the productions need to remain economically feasible and environmentally friendly [35-37]. As a consequence, reactor design and operational parameters are crucial elements, as well as potential limiting factors, for the upscaling process [38]. Moreover, the rates of electron transfer (as well as diffusion of substrate and products, and advection) are determining factors to the intrinsic rates of substrate utilization; for this reason, there have been many different approaches to electrode designs and materials to optimize electron transfer [39]. However, for biofilm-based electrodes, current density still does not scale up linearly with the active surface area, in order to meet the demand of high-capacity processes [40]. Many characteristics of biofilms – such as morphology, thickness, physical properties, and composition – all have a significant contribution to the performance of the bioelectrode; yet, our current knowledge of electron transfer between electrodes and microbial metabolism are still limited to a mainly few metal-reducing bacteria [41, 42].

The goal of the PhD College STROMER (Sustainable Transformation by Electrochemical Reactions) at Helmholtz Center for Environmental Research (UFZ) was to understand and engineer physical, chemical, and biological heterogeneities in electrochemical processes and reactors, which can be utilized and steered using electrochemical potentials, e.g., for synthesis, degradation, and sensing [43]. Connected by the fundamentals of using electrons as a universal currency for (bio)electrochemical reactions and the materials and methods used for their study, the project consisted of four projects:

1. **Electrode process:** How to develop carbon-based electrodes and electrode processes for optimal control of enrichment, mobility and conversion of chemicals?
2. **Biofilm electrodes:** How can microbial structure-function relationships be used for bioelectrochemical systems?
3. **Metabolism:** How are electrons transferred across biological membranes and which proteins are involved?
4. **Engineering:** How can scalable (bio)electrochemical reactor systems be designed and implemented?

Our project 3, "*Electro-chemical control of cellular metabolism*", aimed to decipher the metabolic and molecular basis of METs, providing fundamental information on spatial and temporal heterogeneities needed for engineering materials, microbial strains, and reactors. By using *P. putida* as model organism, we anticipated identifying key nodes in the metabolism to elucidate the link between external electrodes and intracellular metabolism.

Dissertation outline

To further support the current and future research of *P. putida* as a host for anaerobic biotransformation of organic chemicals, this dissertation will focus on three different aspects of cellular metabolism: carbon uptake, carbon catabolism, and electron removal in *P. putida*, all under the context of BES. Although some elements of this work (e.g., reactor setup, cultivation procedure or some analytical methods) have been established in earlier works from other colleagues [30, 31, 44, 45], the expansion of knowledge and understanding of *P. putida*'s physiology in BES lies within the following novel approaches: i) the BES cultivation of mutant strains that only have specific carbon uptake pathways for ^{13}C-tracing analysis; ii) the use of alternative carbon substrates in order to overcome previously hypothesized limitations caused by glucose metabolism under anoxic conditions; and iii) the inhibition of certain transmembrane transport system that is suspected to be involved in the removal of electron of *P. putida* in BES. The main content of this dissertation consists of 7 chapters in total:

Chapter 1 and **2** provide the current knowledge of the model organism *P. putida* strain KT2440, as well as the implication of bioelectrochemical reactors in research and industrial applications;

Chapter 3 outlines the scope, aims, and objectives of this dissertation;

Chapter 4 gives a detailed description of the experimental procedure, including bioreactor setup, operation, and protocols used for analysis;

Chapter 5 presents the results of the conducted experiments to elucidate the objectives of this dissertation, as well as discusses inferences from the obtained results;

Chapter 6 concludes this dissertation with future prospects and suggestions for further studies.

Chapter 2.
Literature review

2.1. Physiological features of *Pseudomonas putida* KT2440

2.1.1. Genus Pseudomonas: characteristics, distribution and applications

Pseudomonads belong to the class of Gammaproteobacteria, including nearly 300 taxa with validly published and correct names [46]; approximately 10 new species in the genus have been described yearly in the last decade [47]. The genus consists of rod-shaped, Gram-negative, lophotrichous bacteria with free or smooth swimming, which is best described by the type species *Pseudomonas aeruginosa* [48] (**Fig. 1**). Another characteristic that is generally found in *Pseudomonas* include the production of siderophores, notably the fluorescent yellow-green pyoverdine under iron-limiting conditions [49], and other siderophores in some species such as thioquinolobactin and pyocyanin to create competitive ecological advantages [50, 51].

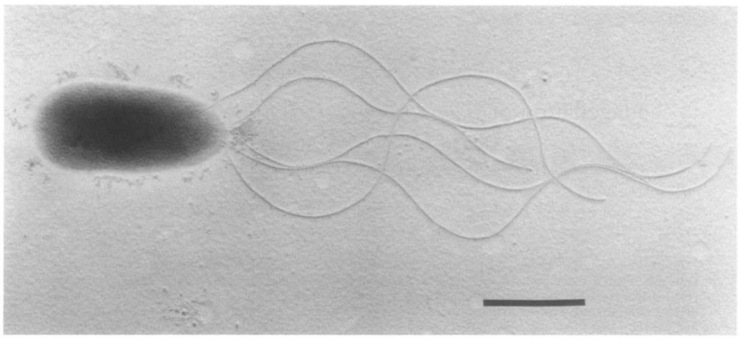

Figure 1. Electron micrograph of *P. putida* PRS2000. Figure was reproduced from a publication by Harwood, et al. [52]. The scale bar is 1 μm.

Pseudomonads are present in and able to adapt to different physicochemical and nutritional niches, from being found in water, soils, and hydrocarbon-polluted sites, to colonizing on plant surfaces or in rhizospheres, as well as in animals like insects or humans [53]. Being in such diverse environments, *Pseudomonas* species play an important role on their surroundings and display many features that are interesting for biomedical, agricultural, and industrial biotechnology. The most notorious species is *P. aeruginosa* – an opportunistic pathogen in humans, which possesses the ability to resist many antibiotic treatments; the roles of its virulence factor and biofilm have been the focus of biomedical research [51, 54]. Other species are also focused on, like *P. syringae* due to their pathogenicity against plants [55], or *P. fluorescens* for its growth-promoting properties in plants or occasional involvement in causing diseases in humans [56, 57]. From an industrial perspective, the species *P. putida* is

one of the most interesting microorganisms from the genus *Pseudomonas*, as it lacks undesirable traits (such as pathogenicity and virulence), while retaining several beneficial qualities including catalytic vigor and versatile metabolism. These characteristics include a high tolerance for oxidative stress [21, 58], and certain strains are able to withstand high concentrations of organic solvents [59-61], which is currently making it an interesting host for the production of fine chemicals [62-65].

In this work, *P. putida*'s, particularly of the model strain KT2440, versatile metabolism toward monosaccharides and their derivative sugar acids, is under investigation, as well as the subsequent effect of their catabolism on the cells under anaerobic conditions in a bioelectrochemical reactor. As a consequence, the following section will focus mainly on prominent characteristics relevant to the study conducted in this dissertation.

2.1.2. Genome

P. putida KT2440 is a plasmid-free strain derived from toluene-degrading bacterium *P. putida* mt-2; it has lost the chromosomally encoded restriction systems and the authentic pWW0 toluene-catabolic plasmid [66, 67]. Its single circular chromosome contains 6181873 bp in length with an average G+C content of 61.5%. A total of 5420 open reading frames (ORFs) with an average length of 998 bp were identified. The non-coding regions account for 11.5% of the *P. putida* genome and contain 7.5% of repeated sequences. Only nine non-coding regions of more than 1 kb have been identified. Comparative genome analysis with the currently completed microbial genomes revealed that 85% of ORFs of the KT2440 genome have homologs in the *Pseudomonas aeruginosa* PAO1 genome, with 61% having their best hit to predicted proteins in PAO1 [68-70].

2.1.3. Respiration

Due to the non-fermentative lifestyle and the lack of necessary proteins for anaerobic respiration [25, 71], *P. putida* is classified as an obligate aerobe, with oxygen as the sole final electron acceptor. Furthermore, the cell requires oxygen molecules for several reactions, including benzoate [72], heme, NAD(P), and pyrimidines metabolism [25].

As for its electron transport chain, *P. putida* possesses a proton-pumping complex type I NADH dehydrogenase, two non-proton-pumping type II NADH dehydrogenases, two ubiquinol oxidases (cytochrome bo3 and a cyanide-insensitive bd-type oxidase CIO), a cytochrome bc1 complex and three cytochrome c oxidases (cytochrome aa3 and two cytochrome cbb3 oxidases) [68, 69, 73, 74]

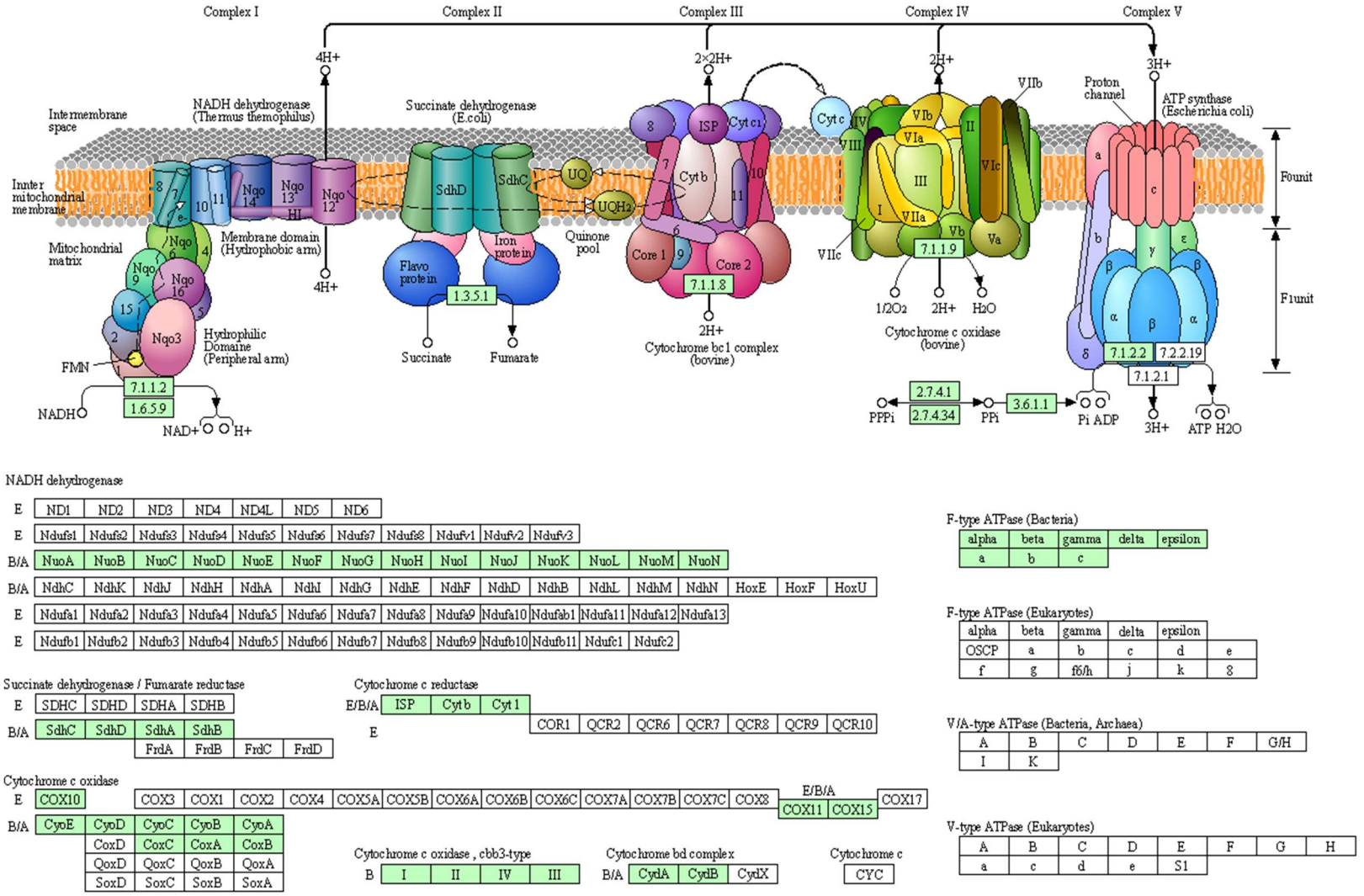

Figure 2. KEGG pathway diagram of *P. putida* strain KT2440's oxidative phosphorylation system (https://www.genome.jp/pathway/ppu00190). In the upper part the five respiratory chain complexes with the corresponding E.C. numbers are shown. In the bottom part, as rectangles, the subunits of each respiratory chain complex are indicated; boxes highlighted in green are subunits found in the strain.

2.1.4. Carbon metabolism

As a ubiquitous saprotrophic bacterium that colonizes the rhizosphere, *P. putida* is adapted to the complex nutrients present in its surrounding environment. Genomic data reveal the capability of the cell to metabolize a wide range of naturally occurring carbohydrates and sugar alcohols such as D-glucose, D-fructose, D-mannose, D-ribose, and glycerol; moreover, it is capable of using a wide variety of organic acids, including citrate, succinate, lactate, and acetate as carbon source [19, 24, 68, 69, 75] (**Appendix A**). Under laboratory conditions, the bacterium can grow on complex media, such as lysogeny broth (LB) [22]. Like many pseudomonads, *P. putida* can selectively assimilate a preferred compound among a mixture of several potential carbon sources via carbon catabolite repression, during which transcriptional expression of genes required for the degradation of less-preferred substrates is repressed in the presence of the preferred substrate [76]. Interestingly, *P. putida* favors central carbon metabolism's organic acids or amino acids over glucose [22, 77, 78], and this has been associated with an iron-scavenging strategy in *P. putida* KT2440 under iron-deficient conditions [79, 80].

The central carbon metabolism that links to the consumption of some carbohydrates, of the strain KT2440, is demonstrated in **Fig. 3**. Glycolysis in *P. putida* is divided into two sets of pathways. The upstream reactions consist of four different pathways:

- the Embden-Meyerhof-Parnas (EMP) pathway, with 6-phosphofructokinase missing;
- the Entner-Doudoroff (ED) pathway, where carbon flux almost exclusively passes through [77, 81];
- the oxidative pentose phosphate (PP) pathway; and
- the peripheral oxidative pathway (POP), with the periplasmic oxidation cascade (POC) responsible for glucose catabolism in the periplasm.

Following the node glyceraldehyde 3-phosphate (GA3P) is the substrate-level phosphorylation, which consists of five reactions that lead to pyruvate. The glycolytic pathways is connected to the tricarboxylic acid (TCA) cycle and the glyoxylate shunt via a linking reaction of the pyruvate dehydrogenase complex, by converting pyruvate to acetyl-coenzyme A, as well as several anaplerotic reactions [77]. The TCA cycle consists of eight reactions that convert citrate to isocitrate, isocitrate to 2-ketoglutarate, 2-ketoglutarate to succinyl-coenzyme A, succinyl-coenzyme A to succinate, succinate to fumarate, fumarate to (L-)malate, (L-)malate to oxaloacetate, and oxaloacetate back to citrate; four of which involve redox co-factors. Also, both *P. putida* KT2440's isocitrate dehydrogenase paralogs (Icd and Idh) are NADP-dependent, instead of NAD [68, 69].

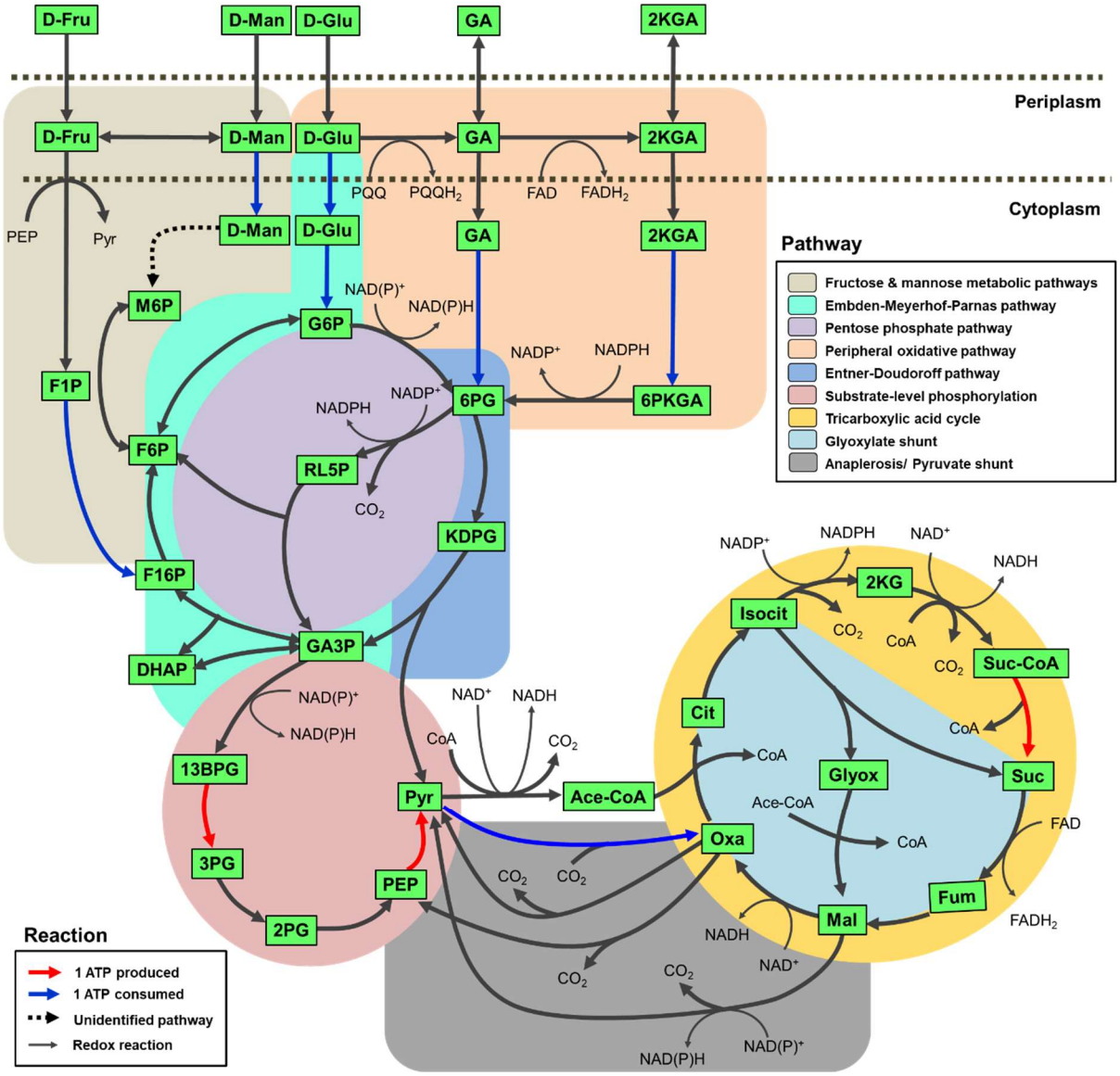

Figure 3. Central carbon metabolism in *P. putida* KT2440. Each green box represents an intermediate metabolite of the pathway. All reactions occuring before/toward the node GA3P are considered upper carbon metabolism, while the ones after GA3P are considered lower carbon metabolism. D-Fru, fructose; F1P, fructose 1-phosphate; D-Man, mannose; M6P, mannose 6-phosphate; D-Glu, glucose; G6P, glucose 6-phosphate; F6P, fructose 6-phosphate; F16P, fructose 1,6-bisphosphate; DHAP, di-hydroxyacetone phosphate; RL5P, ribulose 5-phosphate; GA, gluconate; 2KGA, 2-ketogluconate; 6PKGA, 6-phospho 2-ketogluconate; 6PG, 6-phosphogluconate; KDPG, 2-dehydro-3-deoxy-phosphogluconate; GA3P, glyceraldehyde 3-phosphate; 13BPG, 1,3-bisphosphoglycerate; 3PG, 3-phosphoglycerate; 2PG, 2-phosphoglycerate; PEP, phosphoenol-pyruvate; Pyr, pyruvate; Ace-CoA, acetyl coenzyme A; Cit, citrate; Isocit, isocitrate; 2KG, 2-ketoglutarate; Suc-CoA, Succinyl coenzyme A; Suc, succinate; Fum, fumarate; Mal, (L-) malate; Oxa, oxaloacetate; Glyox, glyoxylate.

2.1.4.1. Glucose metabolism

Glucose – the most frequently used carbon source in laboratory cultivation, was found predominantly metabolized through the periplasmic oxidation pathway and the ED pathways [81]. The missing 6-phosphofructokinase in its genome renders the strain unable to metabolize glucose through the EMP pathway, which would produce twice as much ATP during substrate-level phosphorylation. This “setback”, however, allows carbon to flow in a cycle known as the ED-EMP cycle, where the cell can regenerate its NADPH pool [77]. A rich NADPH pool allows the cell not only to perform vigorous anabolic reactions, but also enables detoxification under oxidative stress [82]; in fact, Chavarría, et al. (2013) attempted to rewire the central carbon metabolism of KT2440 by introducing 6-phosphofructokinase from *E. coli*, and knocked out the ED pathway: the mutant strain was found to have lower growth rate and redox stress tolerance due to a decreased pool of NADPH [83]. In this dissertation, the oxidation of sugar on the cytoplasmic membrane is primarily focused on.

2.1.4.1.1. Peripheral oxidation pathway in *P. putida*

The peripheral oxidation pathway (POP) of sugars is common amongst aerobic and facultative anaerobic bacterial species, including *P. putida*. In addition to the uptake through the EMP pathways (glcP), which consists of the ATP-binding cassette (ABC) transporter (GtsABCD, PP_1015-1018) and the enzyme glucokinase (Glk, PP_1011), POP is responsible for the incomplete oxidation of glucose into its derivative sugar acids – gluconate (GA) and 2-ketogluconate (2KGA), in the periplasm, and the uptake of these sugar acids into the cytoplasm [84-86]. The POP is made of two smaller branches: gaP, consisting of the pyrroloquinoline quinone (PQQ)-dependent glucose dehydrogenase (Gcd, PP_1444), two gluconate transporters GntT (PP_3417) and PP_0625, and the gluconokinase (GnuK, PP_3416); and the rather unique 2kgaP, consisting of the membrane-binding gluconate dehydrogenase complex (Gad, PP_3382-3384), a 2-ketogluconate transporter (KguT, PP_3377), a 2-ketogluconate kinase (KguK, PP_3378), and an NADPH-oxidizing 2-ketogluconate-6-phosphate reductase (KguD, PP_3376).

Under aerobic conditions, as carbon is channeled almost exclusively via ED pathway, gaP is especially a more favorable route of entrance for glucose into the central carbon metabolism [77, 81]. One of the two key enzymes involved in this pathway is Gcd (the other is GnuK), whose specificity toward different monosaccharides will be explored in section 5.2. Gcd catalyzes the oxidation of D-glucose to D-glucono-1,5-lactone, which is further spontaneously or enzymatically converted (by gluconolactonase) into GA, releasing two protons and transferring two electrons via PQQ to ubiquinone (UQ) in the cytoplasmic membrane and eventually to the electron transport chain [87, 88]. Similarly, the Gad complex, consisting of

three polypeptides: (i) a flavoprotein subunit, (ii) a cytochrome c_1 subunit, and (iii) a peptide of unknown function [89], further oxidizes GA to 2KGA, releasing another two electrons, which are captured and transferred to the electron transport chain [90], and two protons are released into the periplasm. For this reason, the POC allows *P. putida* to produce energy even before the carbon frame of the sugar molecule is getting processed in the cytoplasm, and hence, both gaP and 2kgaP pathways have a higher net ATP yield in comparison with glcP.

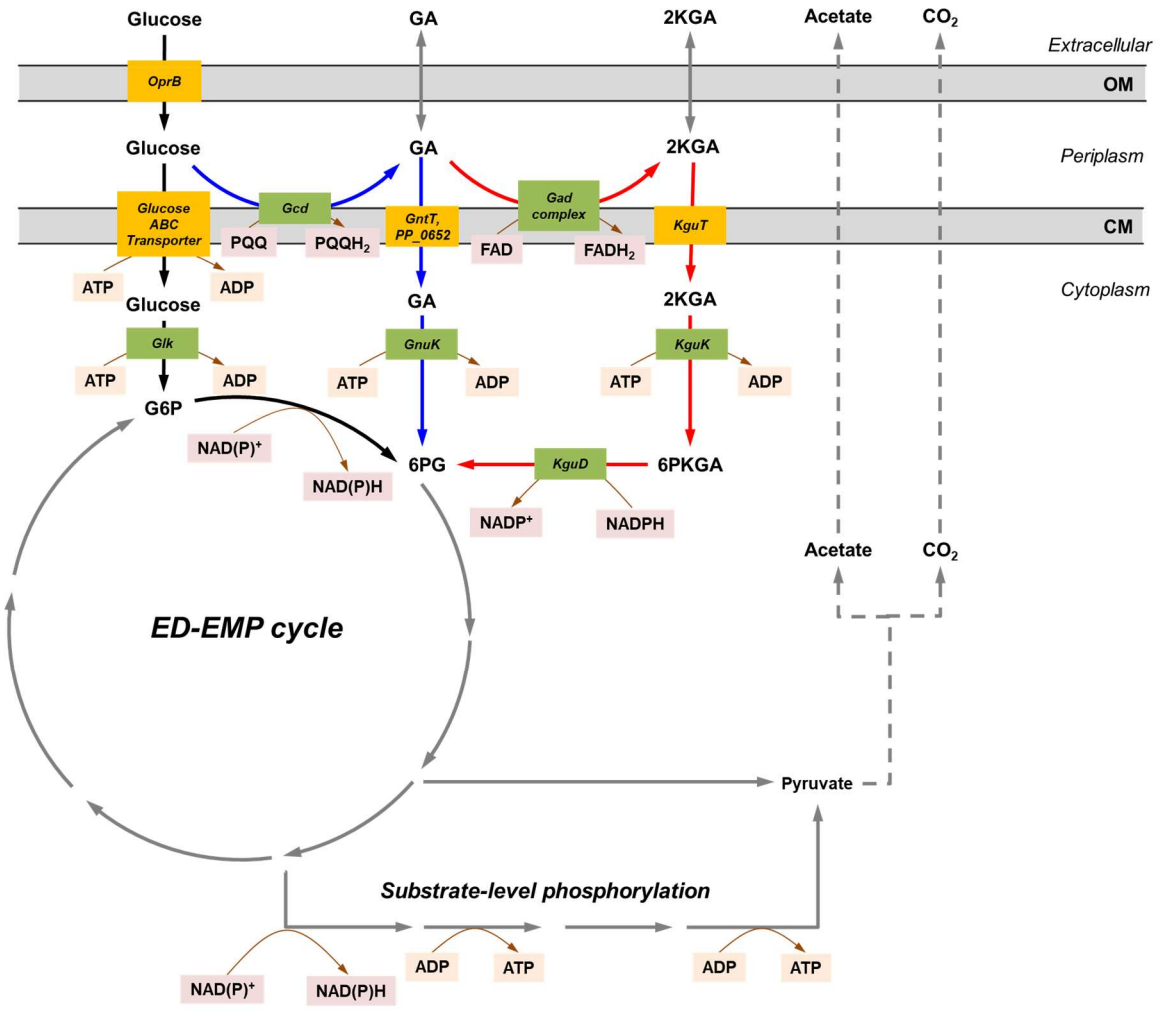

Figure 4. Peripheral glucose oxidation and uptake pathways in *P. putida* KT2440 that lead to the "crossroad" upper-glycolytic metabolite gluconate 6-phosphate (6GP), including direct glucose uptake pathway (glcP, black arrows), uptake via conversion to GA (gaP, blue arrows) and to 2KGA (2kgaP, red arrows). Gray solid arrows represent unspecified glycolytic reactions; gray dash arrows represent unspecific pyruvate degradation to acetate and CO_2. OM, outer membrane; CM, cytoplasmic membrane.

Under aerobic conditions, glucose enters the cell through all three previously described branches in the periplasm, but mainly through the gaP, and exclusively through the ED pathway in the cytoplasm to the central carbon metabolism [77, 81]. However, the cell's

behavior deviates under oxygen-limited (i.e., BES) conditions, despite none of POP proteins being recognized to be oxygen-dependent: the carbon was found channeled mostly through the periplasmic cascade, while very little through the cytoplasm's metabolic pathways [30]. On the other hand, it was shown in a study by Yu, et al. (2018) that expression of Gad might have been stimulated by overexpressing only Gcd and overproducing GA [31], demonstrating that the periplasmic oxidation cascade might be self-regulated. The remaining portion of the POP is found to be controlled by a versatile set of transcriptional regulators; some are responsible for multiple pathways of the central carbon metabolism (also known as global regulators). Since expression of these proteins relies mostly on availability of the sugar acids produced in the periplasm and intermediates of the ED pathways (**Table 1**), accumulation of GA and 2KGA, in theory, should also induce expression of the pathways for uptake of these molecules.

Table 1. Regulatory proteins of upper glucose catabolic pathways in *P. putida.*

Regulator	Function	Effector	Target gene/operon	Reference
GltR-II	Activator	2KGA/6PG	*oprB*, gtsABCD**	[91, 92]
HexR	Repressor	KDPG	*gap-1, edd-glk*-gltR-2, zwf*-pgl*-eda*	[91, 93-95]
GntR	Repressor	GA/6PG	*gntT*, PP_3415* (*gntR*)	[96]
PtxS	Repressor	2KGA	*ptxS, kguEKTD*, PP_3382-3384* (*gadCBA*)*	[91, 94, 97]
FnrA	Repressor/Activator	Unknown	*gap, edd, hexR*	[98]

* gene/operon directly involved in the POP. GA, gluconate; 2KGA, 2-ketogluconate; KDPG, 2-keto-3-deoxy-6-phosphogluconate; 6PG, 6-phosphogluconate.

2.1.4.1.2. Biological functions of gluconate and 2-ketogluconate

Many bacteria of the genus *Pseudomonas* are capable of producing GA and 2KGA, and this benefits those microorganisms in many ways. First, it creates a competitive advantage by producing carbon compounds that can only be used by microorganisms possessing sugar acid metabolism, as well as playing a possible role of biological control [99]. Metabolically, there is also a possible gratification for yielding energy via oxidative phosphorylation by producing sugar acids extracellularly as previously described; however, most research associates this process to the scavenging of phosphate by solubilizing mineral phosphate in the soil [100-103]. Although GA production is usually attributed to mineral phosphate solubilization by bacteria, 2KGA might also play a similar role; for instance, transformed *Enterobacter asburiae* PSI3 – a known rock phosphate solubilizer – overexpressing Gad from *P. putida* KT2440 showed increase in mineral phosphate solubility [104]. GA and 2KGA are

capable of acting as Ca^{2+} chelators under appropriate physicochemical conditions, and the protons released from periplasmic oxidation of sugars provide the acidification of the external environment necessary to dissolve the poorly soluble calcium phosphates [102]. In turn, phosphate concentration in the environment was found to contribute to the modulation of PQQ-dependent Gcd's expression [100, 105]. Finally, increasing phosphate availability is not the only benefit for both the host plants and the microbes in their symbiotic relationship [106]: by lowering environmental pH it could also help suppress root immunity, facilitating root colonization of *Pseudomonas* spp. [107].

2.1.4.2. Fructose metabolism

2.1.4.2.1. Phosphoenolpyruvate-dependent phosphotransferase system (PTS)

Unlike the ATP-binding cassette (ABC) transporter, which is energized via ATP hydrolysis, the PEP-dependent PTS separately phosphorylates the sugar molecule as a step prior to their import, controlled by the intracellular PEP/pyruvate ratio. In this way, an internal metabolic signal (i.e., the PEP/pyruvate ratio) decides the efficiency of sugar intake. In *E. coli*, both glucose and fructose can be taken up via PTS transporter, whereas *P. putida* utilizes non-PTS (i.e., ABC transporter, POP) for the import of glucose, and fructose is captured using a dedicated PEP-dependent PTS [77, 108, 109]. This fructose-only transport system involves three proteins: the membrane-bound permease EIIBC (FruA), the cytoplasmic phosphocarrier EI/HPr/EIIAFru polyprotein (FruB), and a cytoplasmic phosphokinase (FruK) which further phosphorylate the fructose 1-phosphate (F1P) to the ED-EMP metabolite fructose 1,6-bisphophate (F16P) (Fig.); all three components are encoded by the operon *fruBKA* [109, 110]. Interestingly, the *fruBKA* operon is modulated only by F1P, which acts as an inducer against the catabolite repressor-activator Cra^{Fru} [111]. Not only the expression of the PTS is affected, but so is the one of the glyceraldehyde 3-phosphate dehydrogenases (PP_3443), that involves in the control of carbon flux in central carbon metabolism [108].

2.1.4.2.2. Intracellular carbon distribution during fructose metabolism

One of the pseudomonads' features is the lack of the enzyme 6-phosphofructokinase, which prevents the EMP pathway to function in both directions, leading to the unique ED-EMP pathway that operates in a cyclic manner. When fructose enters the central carbon metabolism through the F16P node, it could go to either downstream via aldolase activity, or upstream to the ED and oxidative pentose phosphate branches. As a result, the cells channel around 48% of the carbon through EMP and PP pathways when fed with fructose, compared to only ~4% with glucose [109]. Since the NADPH regenerating reactions of the central carbon metabolism are mostly located in these pathways, feeding *P. putida* cell with fructose could potentially be a solution for overcoming redox imbalance that has been a predicted constraint for *P. putida*

F1 on glucose under BES conditions [30]. Moreover, unlike POP, the PTS system is not NAD(P)H-dependent, and the enzyme PP_3443 also displayed dual $NAD(P)^+$ specificity, which could further help to boost NADPH regeneration.

2.1.5. Nutrient uptake via TonB complex and TonB-dependent transporters

In Gram-negative bacteria, like *P. putida*, the outer membrane acts as an additional barrier and hinders the uptake of essential nutrients. The lack of ATP-energizing translocation on the outer membrane limits the non-diffusible uptake of large molecules and nutrients at low concentrations. In order to transport those substrates that could not be transported via facilitated diffusion, a system of a protein complex that transduces energy from the cytoplasmic membrane to the outer membrane is needed. The TonB-ExbBD complex, "powered" by the proton motive force created on the cytoplasmic membrane, was discovered to be responsible for the import of a wide range of compounds, from the well-known ferric iron and ferric iron-binding molecules to newly identified substrates such as vitamins (cobalamin, thiamin), metals (nickel, copper, cobalt), or dissolved organic matters (saccharides, peptides, glycosaminoglycan), and for each substrate, a specialized TonB-dependent transporter (TBDT) located on the outer membrane is required [112-116]. TBDTs are β-barrel proteins with a ligand-binding site facing outside of the cell, and a disordered protein domain facing the periplasm, also known as "plug", which could change conformation upon ligand-receptor and TonB-TBDTs interaction [117, 118]. The TonB complex, on the other hand, consists of three protein units: TonB, ExbB and ExbD (**Fig. 5**). The 26-kDa unit TonB has three distinctive domains: the membrane-binding domain at the N-terminus, a cross-peptidoglycan domain which is rich in proline, and a C-terminal domain that interact with the plug domain TBDTs on the outer membrane, which has been hypothesized to induce opening of the gate for ligand entrance by mechanical force [118-120]. The 26-kDa ExbB and 17-kDa ExbD are also indispensable for TonB to conformationally respond to proton motive force and association of TonB with the cytoplasmic membrane [119, 121, 122]. In addition to TonB complex's and TBDTs' function in iron acquisition, the ability to assimilate iron-binding ligands that they do not produce, especially in *Pseudomonas* spp. [123-125], leads to our belief that the complex might also be responsible for the intake of iron-based artificial mediators across the outer membrane of the model organism *P. putida* KT2440.

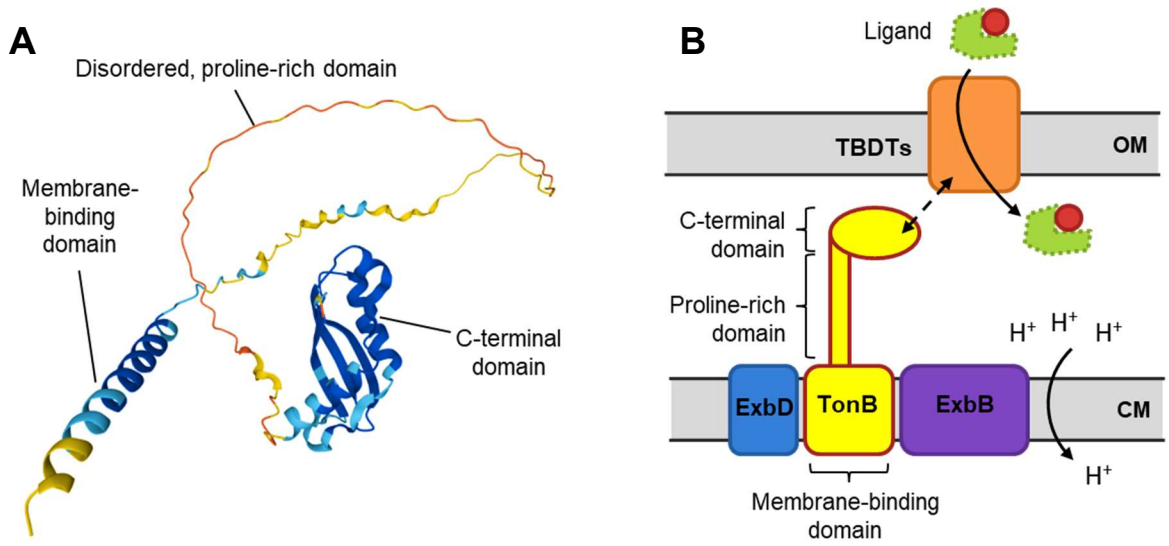

Figure 5. Structure, location and function of the energy-transducing TonB-ExbBD complex in Gram-negative bacteria. (**A**) Predicted 3D model of TonB protein generated by AlphaFold; dark blue: very high structure confidence, light blue: high confidence, yellow: low confidence, orange: very low confidence. (**B**) Simplified drawing of complex organization and mechanism of action of TonB-ExbBD and TBDTs; OM, outer membrane; CM, cytoplasmic membrane.

2.2. Aldonic acids and aldonic acid derivatives

As mentioned previously, GA and 2KGA play an important role in the physiological function and ecological fitness of the microorganisms producing those metabolites. In addition, these sugar acids, alongside many other aldonic acids and their derivatives, have also been found to be valuable for different human uses since the early 20th century. This section will further discuss the role and implication of these sugar acids, as well as different aldonic acids, in human activities and industries.

2.2.1. Chemistry

2.2.1.1. Chemical structure

An aldonic acid is any of a family of sugar acids obtained by oxidation of the aldehyde functional group of an aldose to form a carboxylic acid functional group. This distinguishes aldonic acids from other sugar acids such as ulronic acids (the hydroxymethyl group at the terminal end of an aldose or ketose is oxidized) and aldaric acids (both the aldehyde group and hydroxymethyl group at the terminal end of an aldose are oxidized) [126, 127]. Different derivatives of aldonic acids include aldonolactones, ketoaldonic acids, and bionic acids. Aldonolactones are produced via esterification of the carboxyl group with one of the remaining hydroxyl groups of the aldonic acid. Ketoaldonic acids are aldonic acids that include one or

more keto groups in their structure. If an additional sugar is attached to the aldonic acid, the molecule becomes a bionic acid.

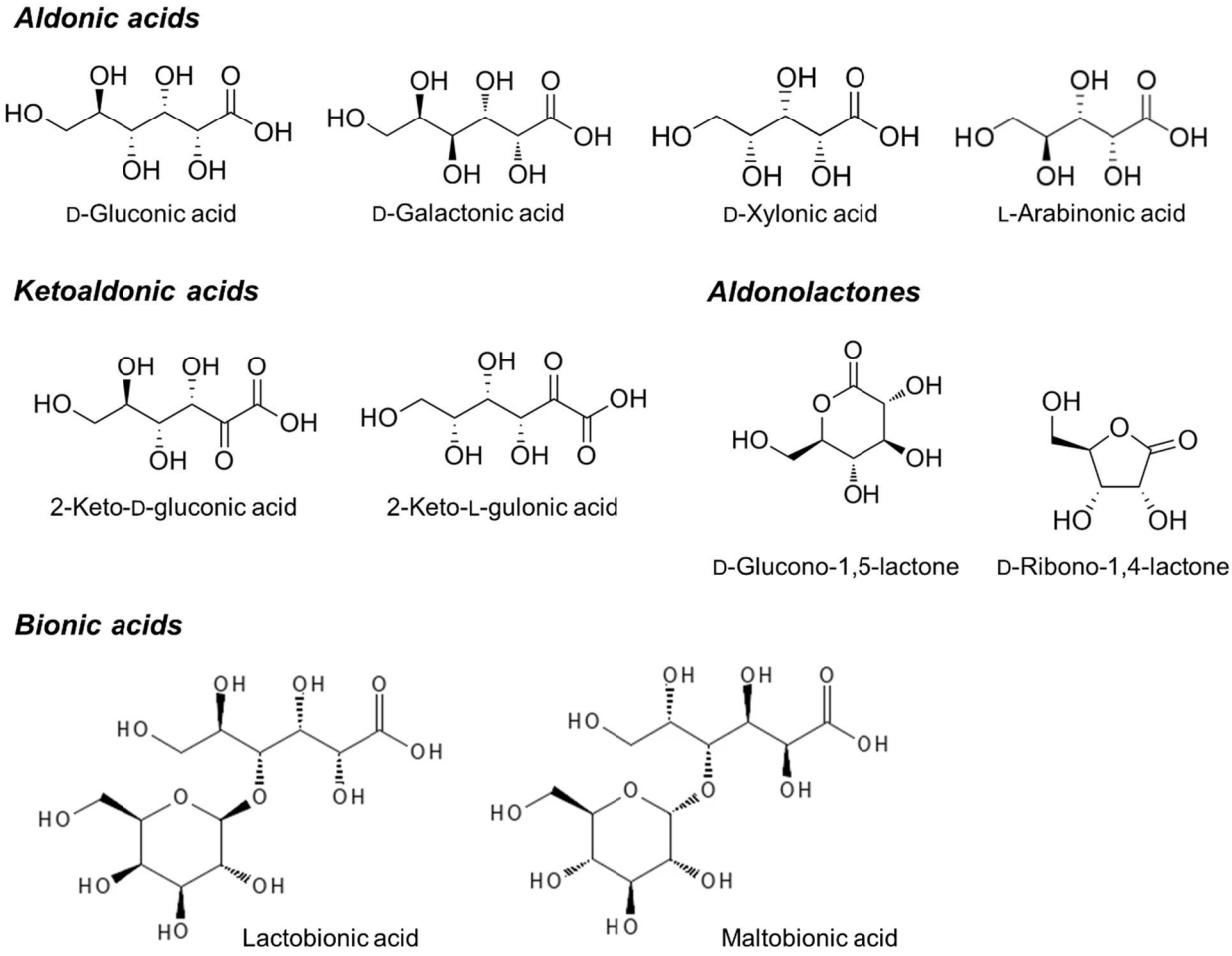

Figure 6. Examples of aldonic acids, ketoaldonic acid, aldonolactones, and bionic acids with practical and commercial value.

2.2.1.2. Chemical and biological synthesis

Aldonic acids (and other polyhydroxycarboxylic acids) are known to be produced by electrochemical or chemical oxidation. The most widely used chemical method for preparing aldonic acids is the oxidation of the unprotected aldose with bromine or other halogen oxidants in aqueous solution, and the aldonic acid is usually isolated as the lactone. Many electrochemical methods for the oxidation of sugars have also been developed, including direct electron transfer between the electrode and the substrate, or by indirect electrolysis, whereby an electrocatalyst mediator is used [127, 128]. As a result, several drawbacks exist, such as harsh reaction conditions, prolonged reaction process, high production cost, and complications in the downstream processing; on the other hand, biological methods, especially by heterogeneous catalytic oxidation, feature milder reaction conditions, simpler

reaction processes, high catalyst efficiency and recycling, and easier purification of target products [129].

The biological production of sugar acids relies on the fact that heterotrophic microorganisms not only have a variety of substrates in nature, especially those living in close association with primary producers, but they also possess enzymes and enzyme systems that are specific for each target compound, surpassing that of synthetic chemistry [130]. In most industrial sugar acid production processes involving at least one microbial component, sugar oxidases or dehydrogenases play a key role in converting the raw material (sugars) into the desired products (sugar acids). One of the most prominent enzymes is glucose dehydrogenase (in bacteria) or glucose oxidase (in fungi), which catalyzes the oxidation of glucose in the presence of co-factors like NAD(P), PQQ, or FAD, to gluconic acid. This one-step oxidation reaction can be found in many microbes, including *Pseudomonas* spp., *Escherichia* spp., *Klebsiella* spp., *Gluconobacter oxydans*, etc., and in eukaryotes such as *Penicillium* spp., *Aspergillus niger,* and *Aureobasidium pullulans* [131-133].

2.2.2. Applications and status of production

Sugar acids, particularly aldonic acids and derivatives, have a well-known, wide range of applications in food, cosmetics, medicine, pharmaceutics, chemical, and material industries [126, 127]. Aldonic acids are usually derived from oxidization of five common aldoses, including xylose, glucose, mannose, arabinose, and galactose [134]. In the following **Table 2**, the production and applications of selected aldonic acids and derivatives from aldohexoses, aldopentoses, or disaccharides is summarized.

2-Keto-L-gulonic acid (2KGL) is an example of an aldonic acid derivative produced at a commercial scale by combining both microbial fermentation and synthetic chemistry. This precursor of ascorbic acid has been historically (and still being) manufactured using the Reichstein process, which involves one fermentation step and at least three chemically catalyzed transformations from D-glucose [135]. Ascorbic acid (Vitamin C) is one of the most important antioxidants in food, cosmetics, and pharmaceutics. The global market for vitamin C and its derivatives reached USD 1.24 billion in 2022 with the most important exporters being China (USD 773 million), the United States (USD 86.1 million), and the United Kingdom (USD 81.6 million) [136]. Over the years, each of the chemical catalysts has been proposed to be replaced by a biological one, i.e., an enzyme or a microorganism that can carry out a similar reaction, to produce 2KGL, which can be transformed to ascorbic acid by esterification and lactonization [135]. Furthermore, the desire to reduce environmental hazards as well as to utilize cheaper raw materials led to the development of new synthesis pathways using different

Table 2. Production and application of selected aldonic acids and derivatives.

Compound	Application	Substrate	Method of production	Reference
Aldonic acids and ketoaldonic acids				
D-Gluconic acid	pH regulator in food; calcium and heavy metal sequestering agent; corrosion inhibitor; concrete dispersant; metal supplements: antioxidant	D-Glucose	(Bio)Chemical conversion Microbial (electro)fermentation [a]	[126, 127, 132, 137, 138]
2-Keto-D-gluconic acid	Precursor for ascorbic acid (Vitamin C) and isoascorbic acid production; stabilizing agent; antioxidant	D-Glucose	Microbial (electro)fermentation [a]	[30, 31, 135, 139-144]
2-Keto- L-gulonic acid	Precursor for ascorbic acid (Vitamin C) production	D-Sorbitol, D-glucose	Microbial fermentation [a] (with/without additional chemical conversion steps)	[127, 135, 136, 140, 145-148]
D-Galactonic acid	Calcium sequestering agent	D-Galactose	Microbial fermentation	[126, 149, 150]
D-Xylonic acid	Platform chemical for synthesis; fabric material; concrete dispersant; pharmaceutical precursor	D-Xylose	(Bio)Chemical conversion Microbial fermentation [a]	[126, 129, 151-153]
L-Arabinonic acid	Concrete dispersant; precursor of industrial chemicals; cosmetics additive	L-Arabinose	Chemical conversion Microbial fermentation	[150, 154]
Aldonolactones				
D-Glucono-1,5-lactone	Food additive, preservative, tablet excipient	D-Glucose	(Bio)Chemical conversion Microbial fermentation [a]	[127, 132, 137, 138, 155]
D-Ribono-1,4-lactone	Pharmaceutical precursor, herbicidal precursor	D-Ribose, lignocellulose	Chemical conversion	[156, 157]
Bionic acids				
Lactobionic acid	Food and cosmetics additive; pharmaceutics	Lactose, whey	Chemical conversion Microbial fermentation [a]	[149, 158-160]
Maltobionic acid	Food and cosmetics additive	High-maltose corn syrup	Microbial fermentation [a]	[149, 161]

[a] Processes involving a *Pseudomonas* sp., wild-type or genetically modified, as fermenter.

host organisms [162]. Hence, other purely fermentative processes have been developed, some even utilizing engineered strains to reduce the multiple conversion steps in a mixed-culture system into a single, whole-cell catalyst [145, 148], while others involve fermentation through other intermediates, for instance, GA, and 2KGA – a stereoisomer of 2KGL [140, 147]. The Reichstein process, a two-step fermentation with a single culture or with a mixed culture, and a one-step fermentation have achieved the highest process yield of 60%, ~95% and >81%, respectively. During the two-step fermentation process, the yield of L-sorbose from D-sorbitol reached ~98%, while the yield of 2KGL from L-sorbose reached >97%; as a result of the high conversion ratios, this is now the only purely biological route applied for the industrial-scale production of ascorbic acid [136, 163].

Sugar acids derived from glucose (GA, KGA, gluconolactones) are naturally occurring polyhydroxy carboxylic acids commonly found in humans and other organisms, which are non-toxic, non-corrosive, mildly acidic, less irritating, and easily degradable [133]. Thus, GA and derivatives are extensively used in chemical, pharmaceutical, food, beverages, and construction industries [126, 127, 132]. The huge market consumption of GA and derivatives has spurred interest in the development of an effective and economical system for their production [137]. Industrial production of D-gluconic acid is mainly performed by *A. niger*, achieving approximately 96% production yield, and with a worldwide annual production level of approximately 90,000 tons in 2016 [137, 164]. However, the system-specific requirements in glucose fermentation contribute to the high price of GA and its derivatives [137].

An alternative source of carbohydrates for sugar acid production may come from lignocellulosic biomass, which can be recovered from forestry and agro-industrial waste or agricultural residuals [165]. Pentoses like D-xylose and L-arabinose alongside hexoses like D-mannose and D-galactose, which are the main constituents in hemicelluloses, represent in general 15–35% of plant biomass [166, 167]. Sugar acid derived from these monosaccharides were shown to have similar ranges of application in comparison with glucose-derived sugar acids [126, 150, 151]. Out of these molecules, D-ribono-1,4-lactone notably has one of the highest value, as it is used as a precursor for the synthesis of various natural or synthetic bioactive molecules relevant to medicinal chemistry and chemical biology [157, 168]; nonetheless, production of D-ribono-1,4-lactone remains a costly process and it is still achieved through purely chemical syntheses [156].

Lactobionic acid and maltobionic acid are examples of bionic acids – a group of value-added chemicals derived from aldonic acids, which have also gained attention for medical, pharmaceutical, food, chemical, and cosmetic applications due to their excellent properties, such as antioxidant, non-toxic, biocompatible, and biodegradable [159, 161]. While bionic

acids are traditionally produced using high-energy metal catalysts [160], other biological methods of production were also under intensive investigation. For instance, *Pseudomonas* species like *P. fragi* and *P. taetrolens* were found to be efficient producers of not only bionic acids, but also other aldonic acids as well [149, 158, 161]. These examples have demonstrated that *Pseudomonas* sp. could be employed as biocatalysts for such processes; but furthermore, species from this genus could also play the role of host organism for an engineered (homologous or heterologous) catalytic system [144, 149, 169, 170].

2.2.3. Challenges of current production processes

Despite already being available for industrial application, the production of sugar acids using purely biological systems still encounters various bottlenecks. Firstly, the physiology of the inoculum plays a role that could make or break the fermentation process. An example is the use of *A. niger* to produce GA by industrial fermentation, which was patented by Blom in 1952 [171]; even though fungal fermentation features a high yield and less by-product [172], the filamentous fungus exhibits a diverse morphology in liquid media, and thus, prevents biomass recycling owing to difficult separation from other macro-sized components [173]. In addition, excess mycelia formation during fermentation could occur with high-concentration carbon sources, which in turn decreases the yield due to increase of media viscosity and reduced airflow, leading to failure in employing the widely used continuous fed-batch setup in industrial fermentation [174, 175]. Bacteria, on the other hand, are prone to by-product formation, which requires effective inhibition of various by-products in the fermentation process and the purification of the target products in downstream processes [133].

In order to lower the final production cost, in addition to minimizing the hazardous effects on the environment, multiple endeavors of reducing fermentation steps have been made. Nonetheless, the journey to create new and improved methods at a larger scale rivaling the efficiency of the current industrial process has not yet been achieved. For instance, to replace the classical two-step fermentation used in ascorbic acid production with a single-strain one-step process, Wang, et al. (2018) proposed that multiple aspects should to be taken into consideration: (i) formation of unwanted intermediates and by-products, which are difficult to separate from each other; (ii) identification of highly efficient enzyme homologs and optimal combinatorial expression in one single, suitable chassis; (iii) transmembrane transport efficiency of substrate/product; (iv) optimization of the global metabolic network; (v) electron transfer rate and regeneration of redox co-factors; and (vi) potential degradation pathways of the target product in the host cell [163].

Finally, all current biological processes to produce sugar acids and derivatives at an industrial scale required oxygen to operate; however, there are several setbacks regarding aerobic processes. Aerobic oxidation of glucose produces approximately 10 times more ATP compared to fermentation [176] – resulting in higher growth rate and productivity. It also leads to higher carbon loss in the form of CO_2 through the TCA cycle, as well as heat generation, since the free energy for glucose oxidation with O_2 (-2870 kJ $mol^{-1}_{glucose}$) exceeds that for glucose fermentation (-218 kJ $mol^{-1}_{glucose}$) [177]. Furthermore, aeration can become cost-intensive [11-13] as scaling-up of the aerobic process is significantly limited by the oxygen transfer rate [14], thus, needs higher energy input through increasing stirring speed and gas flow. A possible solution is to increase gas pressure to improve the dissolved O_2 concentration in the liquid phase; yet, an elevated concentration of O_2 results in a higher generation of reactive oxygen species, leading to increase cellular damage to the microorganism [178]. Therefore, aerobic scale-ups are generally considered more difficult, while it is possible to achieve larger scale-up factors and overall volumes for anaerobic processes [179]. As a consequence, there is an increased desire for an alternative reactor setup that could yield high product titer as well as have reduced operational costs.

2.3. Bioelectrochemical systems for industrial processes

2.3.1. Basic design

In biotechnological transformations, a separation of growth and production is desired and streamlined metabolic pathways are designed to minimize energetic and material costs. Meanwhile, redox imbalance and by-product formation are often challenging for large-scale applications. Microbial electrochemical technologies (METs) - a relatively new approach to industrial processes - promise to solve these issues. After starting to gain public attention in the 1990s, METs have taken part in boosting advances in the identification and use of microorganisms, systems configuration, and material science; within the last two decades, METs have experienced an exponential increase in the number of scientific publications, covering diverse biological and environmental domains [180, 181].

The first MET to emerge was a microbial fuel cell (MFC), dating back to the early 1960s from the works of Sisler [182] and Davis [183], which provided a proof of concept for the generation of electricity using different microorganisms. As the research progressed, other concepts were developed and derived from MFC to fit a specific field of application, from microbial electrolysis cells (MECs) for hydrogen production [184], to most recently the microbial electrosynthesis cells for targeted production of value-added chemicals [185]. Although with different names,

all the above concepts were encompassed under the term bioelectrochemical system (BES), as they are all based on the electron transfer between microbes and solid electrodes.

A BES operates based on the exchange of metabolic electrons with solid-state electrodes; some microorganisms can oxidize organic substances using an anode as metabolic electron acceptor, while others accept electrons from a cathode and utilize them for metabolic reactions such as simple redox transformations or to generate metabolic reducing equivalents. In most cases, the anode and cathode reactions are separated by a semipermeable barrier to allow counter ion exchange, to separate fuel and oxidant, as well as to prevent short circuit reactions. By providing appropriate electrode potentials, the microorganisms can use the electrodes as electron acceptors for the oxidation of more complex compounds to simpler ones (anodic oxidation), or as electron sources for the reduction of the substrates to desired products (cathodic reduction) [181, 185]. This process can be uncoupled from cellular carbon metabolism providing a universal system to perform redox-controlled biotransformation. Several elements including the electrode surface, microbial kinetics, reactor configurations, and the electrogenic microorganisms used to construct the device all play a critical role in the system to function properly [186]. The working principle of BES is illustrated in **Fig. 7**.

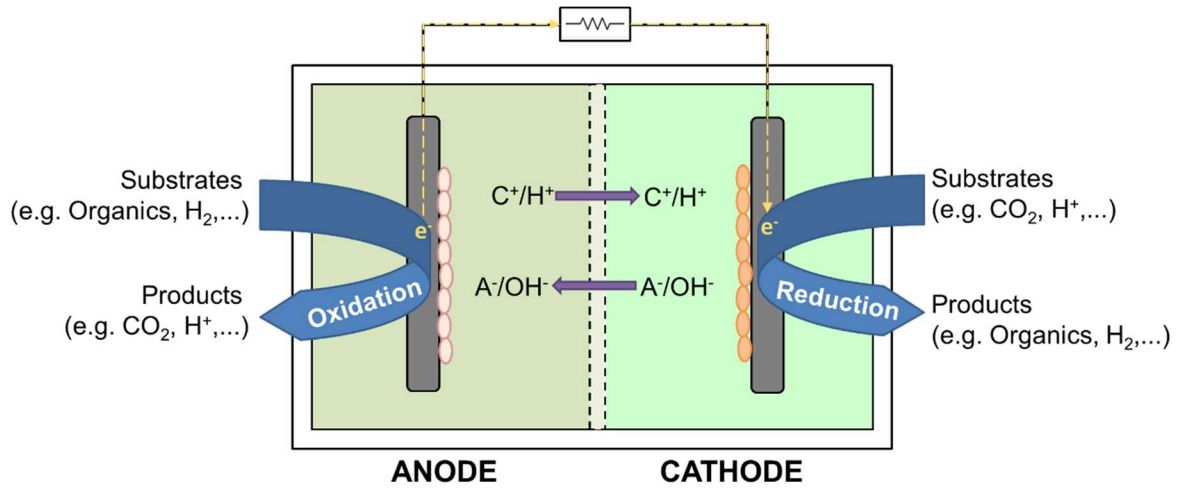

Figure 7. Working principle of bioelectrochemical systems. The electrodes can either play the role of an anode, which receives electrons from substrate oxidation by the microorganisms or as a cathode, which feeds the microorganisms electrons for reduction reactions. Anion/cation-exchange membranes are typically used to separate the chambers, and a power source can also be utilized to supply electrical energy.

2.3.2. Extracellular electron transfer

Understanding electron transfer is fundamental for the performance of BES, and later, process engineering and improvement. A lot of effort has been invested into the investigation of the electron transfer routes in different electroactive microorganisms, and more mechanisms for extracellular electron transfer compared to what was believed so far have been observed [187]. The mechanisms of electron exchange between cells and electrodes vary amongst species of electrogens; nonetheless, the interaction between biological components and electrode material, in general, can be classified into two categories: either by organisms using electrode surface as active growth substratum (direct electron transfer), or by planktonic organisms using organic or inorganic electron shuttles (indirect electron transfer) (**Fig. 8**). The most intensively investigated electrogens with better-understood electron transfer systems include *Geobacter* and *Shewanella*. However, these microbes often have a limited range of applications due to their specific use of substrate under bioelectrochemical conditions. More environmentally ubiquitous and metabolically robust microorganisms, such as *Pseudomonas* spp., show more potential for industrial applications, yet only a few species within this genus with natural redox mediator-secreting systems demonstrate electrogenesis [188]. In most, if not all, cases, the molecular players of the electron transfer between external electrodes and the internal redox metabolism, as well as the effect of external electron transfer on the intracellular metabolism have not been investigated in depth. Hence, it is necessary to identify key nodes in the metabolism to be able to manipulate such nodes, for instance, using metabolic engineering.

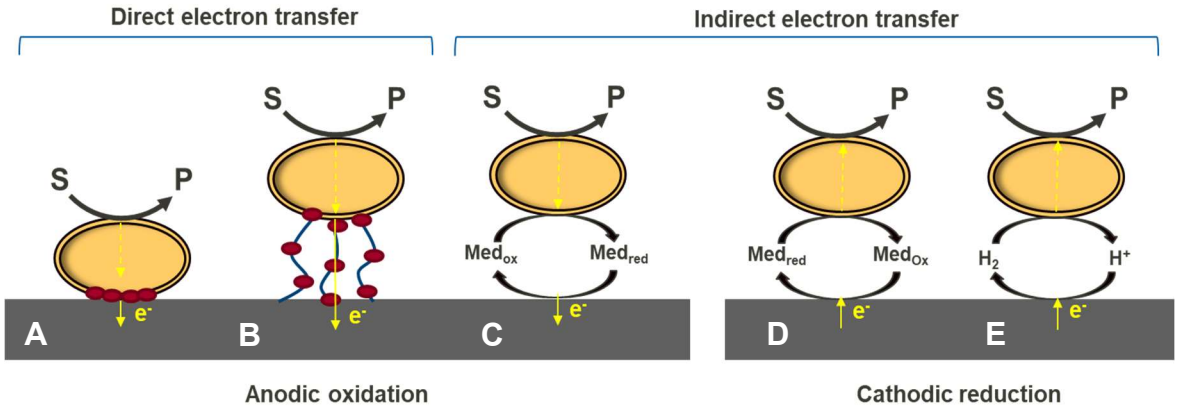

Figure 8. Simplified representations of known electron transfer mechanisms from microorganisms to the electrodes (i.e., anodic oxidation), or vice versa (cathodic reduction), in bioelectrochemical systems. Direct electron transfer occurs via (**A**) membrane-bound cytochromes and/or (**B**) electrically conductive pili; indirect electron transfer occurs via (**C, D**) soluble redox mediator and/or (**E**) oxidation of hydrogen by microorganisms. S, substrate; P, product; $Med_{red/ox}$, mediator (reduced/oxidized form).

2.3.2.1. Direct electron transfer

The anodic respiration via direct electron transfer (i.e., direct contact between the cell and the electrode) pathways has been intensively studied in *Geobacter sulfurreducens* and *Shewanella oneidensis*. *Geobacter*'s ability to convey electrons to a solid substrate is due to a complex system of outer membrane c-type cytochromes (OMCs). OmcB, OmcE, and OmcZ, along with type IV pili, are found to be more abundant in and genetically upregulated in current-harvesting biofilms compared with biofilms grown on fumarate as the electron acceptor, suggesting a role for these proteins in extracellular electron transport. The OmcB complex appears to be the major route in the electron transfer connecting periplasmic cytochromes and extracellular electron acceptors. OmcE and OmcS, nonetheless, are believed to be located on the cell surface where they are suggested to transfer electrons to electrically conductive type IV pili [189, 190]. Two mechanisms for electron transfer in *Geobacter* are proposed: the metallic-like conduction model and the super-exchange model. In the metallic-like model, conductivity is conferred by the π-stacking of aromatic residues in pilin, which may allow electron delocalization. In the super-exchange model, electrons are transported through sequential redox reactions between aligned redox cofactors, driven by the potential gradient produced by the simultaneous reduction of redox mediators and their oxidation at the anode surface [191]. Moreover, extracellular cytochromes appear to have a more important role in *Geobacter*'s direct interspecies electron transfer than type IV pili [190]. Meanwhile, *Shewanella* also shows to have a complex electron transfer system consisting of OMCs and nanowires yet with different components [189]. The OMCs of *Shewanella* responsible for iron (III) oxide reduction are MtrC and OmcA, and the nanowires are extensions of the outer membrane and periplasm instead of pilin-based structures [192].

2.3.2.2. Indirect electron transfer

Another method of electron transfer is indirect electron transfer, where electrons are delivered from the electrogens to the electrode (or vice versa) using soluble redox substances in a cycling change between their oxidized and reduced forms. Many redox compounds are effective for this process, including both artificially synthesized chemicals and biologically excreted metabolites produced by the organisms. *Shewanella* is known to secrete flavin mononucleotide and riboflavin extracellularly to act as electron shuttles [193]. Another example of secreted redox mediators are phenazines – a group of secondary metabolites produced by both Gram-positive and Gram-negative bacteria that play multiple roles and contribute to the behavior and competitiveness of their producers [194]. The most studied phenazine is pyocyanin, which is produced by *P. aeruginosa* [195]. This compound induces redox stress within its target by promoting the generation of reactive oxygen species such as

superoxide [196]. Pyocyanin, alongside phenazine-1-carboxylic acid, were investigated as redox mediator for *P. aeruginosa* in BES [197], and they can also act as an electron shuttle for the non-electroactive *P. putida* that heterologously produces these phenazines [32-34], by possibly transferring electrons from Gcd oxidizing glucose to the electrode [198].

Mediated electron transfer can also be carried out with exogenous redox molecules that interact with and act as electron shuttle between the electrode and the biological component, without being degraded or metabolized. For a redox mediator to be an effective electron shuttle, its standard redox potential (also known as formal or midpoint potential, E'_0) should be somewhere between those of the two half reactions (i.e., electron donating and accepting reactions) [199]. Neutral red, methyl red, methyl viologen, methylene blue, anthraquinone disulfonate, cobalt(III)tris-2,2′-bipyridine, ferricyanide are examples of artificial redox mediators used in both anodic and cathodic reactions [200, 201]. Ferricyanide, or $[Fe(CN)_6]^{3-}$ consists of a Fe^{3+} center bound in octahedral geometry to six cyanide ligands, and its most widespread use is as a single electron acceptor or donor respectively due to the well-known $[Fe^{III/II}(CN)_6]^{3-/4-}$ reversible couple. The advantages of ferricyanide is that its redox potential is quite stable with time, and its use allows the employment of relatively simple spectro-photometric methods for quantification [202]. In a BES reactor utilizing *P. putida*, only those redox molecules whose electrochemical mid-point potentials were above 0.207 V (vs standard hydrogen electrode) could successfully shuttle electrons from microbes to the anode, and with a midpoint potential of 0.416 V in the given setup, ferricyanide proved to be a suitable mediator for *P. putida* [30]. It was shown that ferricyanide interacted with cytochrome c reductase (complex III) in the electron transport chain of the bacterium [45], but the mechanism of electron transfer between the cell and ferricyanide still needs to be further elucidated.

2.3.3. Applications for chemical production

For the last two decades, the potential of METs has drawn much interest and its inspiration for novel concepts has quickly flourished in many areas of biotechnological application, including electro-fermentation and bioproduction of value-added products, bioelectricity, self-powered implantable biomedical devices, biosensors, bioremediation, and wastewater biorefinery for compost, energy, nutrient, and water recovery, etc [181, 203]. In the case of MFCs and MECs, the difference in redox potential between anode and cathode results in net electrical energy produced; however, for the former, O_2 is reduced on the cathode side, while protons are reduced to produce H_2 in the latter. If an external energy input is required to drive the intended reactions, the microbial BES is referred to as a microbial electrosynthesis (MES) cell. These systems can be combined with each other for multi-purposed reactors, for example, bioproduction of H_2O_2, alcohols, bioplastics from CO_2 and wastewater [185, 204-

208], with the combination of a chemical anode or bioanode with a biocathode or a cathode that indirectly drives a biological reaction.

2.3.3.1. Cathodic reduction

One of the main goals of employing cathodic reduction via BES is to capture and utilize CO_2 – one of the main greenhouse gasses and contributor to global warming, in order to reduce the amount of atmospheric CO_2, as well as to relieve the energy crisis [209]. This electricity-driven microbial conversion of CO_2 is mainly conducted via MES, and while the majority of all MES studies have focused mostly on methane and acetate production [210], the product spectrum has broadened in recent years, including ethanol, n-butyric acid, n-butanol, hexanoic acid, and n-hexanol [211, 212]. Nevertheless, low value, low rate/titer and limited diversity of cathodic products, as well as high production cost [213], still hinder MES from industry-scale application.

To expand the product diversity and obtain higher value products, one approach is chain elongation; species of the *Clostridium* family can elongate short-chain carboxylic acids (produced from MES) to long-chain products (up to C8) with different alcohols as co-substrates [214, 215]. Polyhydroxyalkanoates (PHAs) are another group of value-added products that spark interest in incorporating CO_2 fixation in biopolymer production via the bioelectrochemical route [206], especially with the recent isolation of the electroactive, PHA-producing *Kyrpidia spormannii* [216-218]; however, there were in general very few reports on the electro-fermentation of PHAs, and the product titers at laboratory scale remain low [219, 220]. A summary of reported examples of chemical production via cathodic electro-fermentation is shown in **Table 3**.

Table 3. Reported examples of chemicals produced via cathodic electro-fermentation.

$E_{electrode}$ (V vs. SHE)	Microorganisms	Substrate	Product	Coulombic efficiency (%)	Production rate (mg h^{-1}) [c,d]	Titer (g L^{-1}) [c]	Reference
+0.045	*Clostridium pasteurianum DSM 525*	Glucose	Butanol	16	11.26 ± 2.25	1.00 ± 0.20	[221]
			Butyrate	41	42.72 ± 6.74	3.80 ± 0.60	
		Glycerol	Butanol		26.91	2.87	
			1,3-Propandiol		44.39	4.74	
-0.401	*Clostridium saccharoperbutylacetonicum N1-4*	Glucose	Acetone			2.4	[222]
			Butanol			5.8	
			Ethanol			0.4	
-0.451	Engineered *Escherichia coli* T110	Glucose	Succinate			3.61 ± 0.15	[223]
		+HCO_3^-/CO_2	Acetate			0.55 ± 0.01	
-0.801	Mixed consortium from anaerobic digester	Lactate	Propionate	82.8 [e]	~39.8 [f]	0.96	[224]
			Acetate		~18 [f]	0.43	
			Butyrate		~4.04 [f]	0.10	
-0.7	*Methanococcus maripaludis*	CO_2	Methane	58.9 ± 0.8	5.89 ± 0.34		[225]
-0.65	Enriched methanogenic culture	CO_2	Methane	>80	~1		[226]
-1.1 to -1.3	Enriched acetogenic culture	CO_2	Acetate	33.2 ± 2.3		0.74 ± 0.05	[227]
-0.4	*Moorella thermoautotrophica*	CO_2	Acetate	65 [e]	145.6		[228]
			Formate		121.2		
-0.59	Co-culture of *Methanobacterium* spp. and *Acetobacterium* spp.	CO_2	Methane	~84 [e]	~1.06–4.67 [f]	~0.112	[229]
			Acetate		~2.50–10.0 [f]	~0.24	
-0.4	*Sporomusa ovata*	CO_2	Acetate	86 ± 21		~0.3	[230]
-0.6	*Clostridium* spp.-dominated electroactive consortium	CO_2	Acetate	44	6.0	4.9	[231]
			Butyrate		3.0	3.1	
			Butanol		1.5	0.8	
			Isobutyrate		1.8	1.6	
			Isobutanol		0.3	0.2	
			Caproate		1.6	1.2	
			Hexanol		0.4	0.2	
3.0 [a]	*Ralstonia eutropha* Re2133-pEG12	CO_2	Isopropanol			0.216 ± 0.017	[232]
-0.625	*Kyrpidia spormannii* EA-1	CO_2	Polyhydroxyalkanoates	2.9	4.0 –4.88 [f, g]		[219]
-1.06 [b]	Abiotic	CO_2	Formate		90.1 ± 1.9	2.18 ± 0.05	[233]
	Cupriavidus necator	Formate	Poly-3-hydroxybutyrate			0.056	

[a] whole cell voltage, [b] vs. reverse hydrogen electrode (RHE), [c] data recalculated based on the reporting data, [d] specific production rate, unless otherwise specified, [e] overall efficiency for all listed products, [f] maximum production rate, [g] per m^2 of cathode surface.

2.3.3.2. Anodic oxidation

As there is still only a limited number of known microorganisms with the capability of catalyzing biotransformation or biosynthesis of complex molecules via cathodic processes, an advantage of anodic processes is the more diverse range of products with a higher market value – e.g., hydroxycarboxylic acids, sugar acids, polyalcohols, amino acids, and surfactants (**Table 4**), which presents itself as a more attractive option for industrial applications. Nevertheless, the low product titer, as well as issues with reactor scale-up, still pose a challenge for bioanodic production to rival current industry-scale fermentations. One of the key resolutions to these issues is to develop a proper electrochemically active strain and its corresponding metabolic pathway.

The central focus of anodic oxidation is currently to employ MFCs for recovery of nutrients and energy from wastewater, by converting chemical energy from organic/inorganic compounds into electrical energy [234, 235]. Mixed cultures of electrogenic and electrotrophic microbes are known to be more effective in the production of current compared to pure cultures of bacteria [236]. Yet, while microbial consortia have the ability to adapt to changing environments and robustly perform various tasks, the complex interspecies interaction often leads to difficulties in characterizing and controlling their metabolic networks [237]. On the other hand, bacteria that perform advanced electrochemical activities through better-understood mechanisms, such as *Geobacter* or *Shewanella*, are typically employed as pure anode microorganisms, but they are generally limited to oxidation of the carbon source to biomass, CO_2, and few other minor products with low added value [238, 239]. Therefore, the adaptation of model strains to the electrochemical conditions via strain engineering, especially with microorganisms with readily available synthetic biology tools, e.g., *E. coli* or *Pseudomonas* [19, 240-242], instead of developing metabolic engineering platforms for currently used electrogens, is generally preferred as an alternative approach. Other microbes, including *Bacillus subtilis* and cyanobacteria, are also emerging as potential synthetic biology chassis for their robust metabolism and tractable genetics, even though the toolkits developed for these bacteria remains limited [243-245].

Table 4. Reported examples of chemicals produced via anodic electro-fermentation.

$E_{electrode}$ (V vs. SHE)	Microorganisms	Substrate	Product	Coulombic efficiency (%)	Production rate (mg h^{-1}) [b,c]	Titer (g L^{-1}) [b]	Reference
+0.4	Engineered *Shewanella oneidensis*	Glycerol	Ethanol			~1.30	[246]
			Acetate			~0.32	
+0.45	Co-culture of *Clostridium cellobioparum* and *Geobacter sulfurreducens* PCA	Glycerol	Ethanol			~10	[247]
+0.2 [a]	Engineered *Escherichia coli*	Glycerol	Ethanol		12.12 ± 1.70	55.25 ± 7.76	[248]
			Acetate		8.94 ± 0.52	40.75 ± 2.37	
+0.2 [a]	Engineered *Escherichia coli*	Glucose	Acetoin	20.2–93.4		0.86 ± 0.02	[249]
0	Engineered *Shewanella oneidensis*	Lactate	Acetoin		0.91	0.24	[250]
+0.7	Engineered *Bacillus subtilis*	Glucose	Acetoin	85.48 ± 2.65 [d]	25.55 ± 1.76	1.69	[251]
			Lactate		26.12 ± 3.60	0.70	
			Acetate		4.80 ± 0.60	0.19	
			2,3-Butanediol		25.23 ± 2.70	1.14	
+0.7	*Klebsiella pneumoniae* L17	Glycerol	3-Hydroxypropionate			1.27 ± 0.19	[252]
			1,3-Propanediol			2.08 ± 0.36	
			2,3-Butanediol			0.61 ± 0.01	
	Engineered *Klebsiella pneumoniae* L17	Glycerol	3-Hydroxypropionate			1.94 ± 0.20	
			1,3-Propanediol			0.72 ± 0.27	
			2,3-Butanediol			1.79 ± 0.03	
+0.697	Engineered *Pseudomonas putida* KT2440	Citrate	4-Hydroxybenzoate		0.41 [e, f]	0.036	[29]
+0.697	*Pseudomonas putida* F1	Glucose	2KGA	93.3 [d]	62.12 ± 11.65 [e]	1.47 ± 0.27	[30]
			Acetate		3.06 ± 0.60 [e]	0.07 ± 0.01	
+0.697	*Pseudomonas putida* KT2440	Glucose	2KGA	96.0 ± 5.0	7.57 ± 0.39 [e]		[31]
	Engineered *Pseudomonas putida* KT2440	Glucose	2KGA	95.4 ± 2.5	29.32 ± 2.14 [e]		
+0.697	*Pseudomonas putida* KT2440	Fructose Aldoses	Mannonate (keto)Aldonates	85.0 ± 5.4	4.47 ± 1.30 [e]	0.59 ± 0.05	[253]
+0.697	Engineered *Corynebacterium glutamicum*	Glucose	L-Lysine	96.08 ± 6.74 [d]	29.56 ± 0.33	0.32 ± 0.04	[254]
			L-Alanine		9.69 ± 0.41	0.08 ± 0.01	
			Glycine		1.56 ± 0.18		
+0.197	Engineered *Pseudomonas putida* KT2440	Glucose	2KGA [g]			0.72 ± 0.1	[34]
			Rhamnolipids [g]		1.27 ± 0.02	0.030 ± 0.001	
			Mono-rhamnolipids [h]			0.030 ± 0.005	

[a] vs. normal hydrogen electrode (NHE), [b] data recalculated based on the reporting data, [c] specific production rate, unless otherwise specified, [d] overall efficiency for all listed products, [e] per g_{CDW}, [f] maximum production rate, [g] produced in 1-L bioreactors, [h] produced in 500-ml benchtop reactors.

2.4. Integrative electrochemical and proteomics approach for strain development of electrogens

In the field of synthetic biology, organisms are often redesigned for useful purposes by engineering them to have new abilities [8]. In terms of MES, as discussed before, there are two routes that we could take regarding engineering of the biological elements: engineering naturally electroactive bacteria for the production of desired chemicals, or engineering non-electroactive bacteria, that are already endowed with production pathways, for the unnatural electrochemical cultivation conditions. In either case, there is a need for fundamental understanding of the cell's biological processes and the identification of key components, in order to select targets for the development of highly efficient strains for electrosynthesis. As biological systems usually exhibit robustness to environmental perturbations, as well as complex networks of interaction within themselves and with each other [255], integrative analysis using different techniques is essential to acquire a comprehensive overview of cell behavior under a given condition. These integrative data sets from different molecular levels would help to understand the metabolic activities occurring in the organism as well as to identify the limiting steps and potential engineering targets for strain development of electrogens.

The foremost approach to qualification/quantification of metabolism of a biological system is metabolic profiling, which is referred as the measurement of low-molecular-weight metabolites and their intermediates that reflects the dynamic response to external stimuli, or in relation to inherent biological variations [256]. Metabolic profiling can be "targeted" (i.e., measurement of specific metabolites of known identity) or "non-targeted" (simultaneous measurement of as many metabolites as possible in a biological specimen) [257]. There are different methods available, such as liquid or gas chromatography coupled to MS, or nuclear magnetic resonance; each has their own advantages and drawbacks, and their application (as well as combination of methods) should be considered depending on the purpose of the experiment. For instance, the most common high-performance liquid chromatography (HPLC) detectors, e.g., refractive index, ultraviolet (UV) or fluorescence, provide little or no structural information; consequently, structure elucidation requires additional off-line spectroscopy [258]. Gas chromatography (GC) retention times, on the other hand, are robust and reproducible even on different machines and thus can be used in database searches to identify unknown metabolites. However, even when combining with mass spectrometry, it has limited mass range and the molecular ion is often not detected due to fragmentation which hinders identification of unknown compounds [259].

Non-growing bacteria that are metabolically active are valuable for industrial biotechnology, because non-growing cells could maximize yield by converting the substrate into the desired product instead of biomass [260]. This could also be the case for *P. putida* in BES; so far, no growth could be achieved under anoxic conditions, yet the cultures still displayed catabolic activities [29-31]. Nonetheless, data on global gene expression of non-growing BES cultures is still very limited. Transcriptomics is referred to as the study of an organism's transcriptome – "a snapshot in time of the total transcripts present in a cell" [261], offering a global picture of gene expression at a certain time point. Despite this, when it comes to a population of non-growing cells, analyzing the transcriptome profile of cultures can become extremely challenging due to the small number of viable cells and short mRNA lifetime. Also, the metabolic objectives of non-growing cells are not as well-defined compared to exponentially growing cells as a result of a wide range of stimuli leading to growth arrest [260, 262, 263]. On the other hand, the half-life of a protein is approximately two orders of magnitude longer than mRNA's half-life, which allows most proteins to persist in a bacterial cell long after the mRNAs that encoded them have been degraded [264]. Hence, proteome analysis might be a better tool to investigate dynamic responses of the cell to external and internal conditions that result in zero growth, by providing important information on the state of a biological system that is not readily apparent from the level of RNA expression [265].

There are different high-throughput technologies for the global or targeted analysis of proteins in a biological system, one is the use of mass spectrometry (MS), through which proteins are identified by a combination of peptide mass fingerprinting and amino acid sequencing via tandem MS [266, 267]. In general, MS-based proteomics is divided into two approaches: top-down and bottom-up. While top-down MS ionizes intact proteins directly, bottom-up MS requires proteolytic digestion of proteins and is the standard approach to large-scale or high-throughput analysis of highly complex samples [268]. When bottom-up is performed on a mixture of proteins it is called shotgun proteomics; peptide identification is achieved by comparing the tandem mass spectra derived from peptide fragmentation with theoretical tandem mass spectra generated from *in silico* digestion of a protein database. Protein inference is accomplished by assigning peptide sequences to proteins [269].

Chapter 3.
Aims, scope and objectives

3.1. Aims

Metabolism is generally defined as “all the biochemical reactions that occur in a cell or organism”. The study of cellular metabolism comprises of investigating “the chemical diversity of substrate oxidations and dissimilation reactions […], which normally function in bacteria to generate energy”, and “the uptake and utilization of the inorganic or organic compounds required for growth and maintenance of a cellular steady state (assimilation reactions)” [270]. In order to cover both aspects of microbial metabolism, and more specifically, the metabolism of the model organism *P. putida* KT2440 in BES condition, three major questions need to be answered:

1. Which pathways are responsible for sugar uptake during carbohydrate catabolism?

2. How does it affect the internal metabolism of the cell when the sugar is taken up into the cytoplasm?

3. How does the cell dispose of excess electrons in the absence of oxygen?

To each of the questions mentioned above and based on the finding of several preceding works, the following points are addressed:

1. The carbon uptake is hypothesized to be constrained by internal redox imbalance [30], which is simultaneously the cause and consequence of carbon flux redirected toward periplasmic oxidation. Identifying the pathway(s) where carbon intake is restricted and their energy and redox requirement provides proof-of-principle of the role of the said redox co-factor(s).

2. The intracellular activity of the cell is limited by the low carbon flux toward the central carbon metabolism [30, 31]. By steering carbon flux away from the usual periplasmic oxidation pathway, we could at least alter the internal redox state and recover some intracellular activities.

3. The direct interaction of the redox mediators with the electron transport chain of *P. putida* is responsible for the removal of electrons when oxygen is unavailable [45]. In addition to the intrinsic biologic activities of microbial cells, the performance of *P. putida* in BES is also determined by the mass transfer across the membrane. However, the

transport of redox mediators across the outer membrane is yet to be elucidated, but it is hypothesized to be linked to the cell's ability to import iron and iron-based compounds, considering the similarity in their structure. By targeting the machinery that is responsible for the uptake of iron, we could manipulate the turnover of oxidized mediator in the periplasm, and thus, inhibit or improve anaerobic respiration in *P. putida*.

3.2. Scope

So far, there has been no successful attempt to engineer a strain of *P. putida* that is capable of growth under strictly anaerobic conditions [26-28], and it is possible that up to 57 additional genes and 3 externally added vitamins are required to achieve such feat [71]. Therefore, this work focuses mainly on the behavior of the wild-type strain KT2440 within the scope of bioelectrochemical cultivation, while growth and metabolic perturbation as a result of oxygen limitation are not further discussed. Various biological aspects of *P. putida*, including the sugar transformation and uptake on the cytoplasmic membrane, the effect of culture conditions on the performance of the cell, and the adaptation strategy of the cell toward anoxic conditions, such as the transport of artificial electron shuttles across the outer membrane, are thus under investigation. The knowledge gained from this dissertation would be an expansion of the current understanding of *P. putida*'s metabolism, as well as serving as a prerequisite for future technological development of *P. putida* engineering and cultivation.

3.3. Objectives

Three main objectives have been defined to address the three research questions (**Fig. 9**).

For question 1, we selected acetate to measure enrichment of ^{13}C, as this metabolite is known to be produced intracellularly but accumulated extracellularly during bioelectrochemical cultivation [30, 31, 33]. Quantification of ^{13}C abundance in acetate produced by each strain might reveal (i) if and how much acetate was coming from catabolizing extracellular substrate, versus from catabolizing intracellular carbon (e.g., polyhydroxyalkanoates, glycogen and β-glucans, which are known carbon storage compounds in pseudomonads [22, 271]), and (ii) which POP branch(es) is/are responsible for carbon uptake under BES condition. Mutant strains of each branch of the POP, named glcP, gaP and 2kgaP were generated (**Fig. 4**). ^{13}C isotope tracing has previously been used to model carbon flux in *P. putida and P. aeruginosa* [81].

For question 2, in addition to the characterization of cellular function, including electrochemical measurement, metabolite profiling and bioassay for quantification of ATP and redox ratios, mass spectrometry-based proteomics of the cell, in particular proteins involved in the central carbon metabolism, were also conducted. Proteomic analysis could further reveal (i) if the cell remains active under the given condition, and (ii) how perturbed cellular metabolism is in comparison with when no electrode potential is provided (i.e., open-circuit mode). This step could be helpful in identifying any potential metabolic targets that can be altered to overcome metabolic barriers or avoid the limiting co-factors under anaerobic conditions.

For question 3, in order to assess the role of TonB protein complex and TBDTs without severely compromising the viability of the cells, the work of Lai, et al. (2020) was adapted; this study employed electron transport chain inhibitors to reveal which respiratory complex ferricyanide could interact with to remove electron from the chain [45]. Similarly for TonB protein, two different TonB inhibitors, which were identified via high-throughput screening for *E. coli* [116], were tested. To make sure that the compounds also work on *P. putida*, experiments were conducted via aerobic as well as BES cultivation.

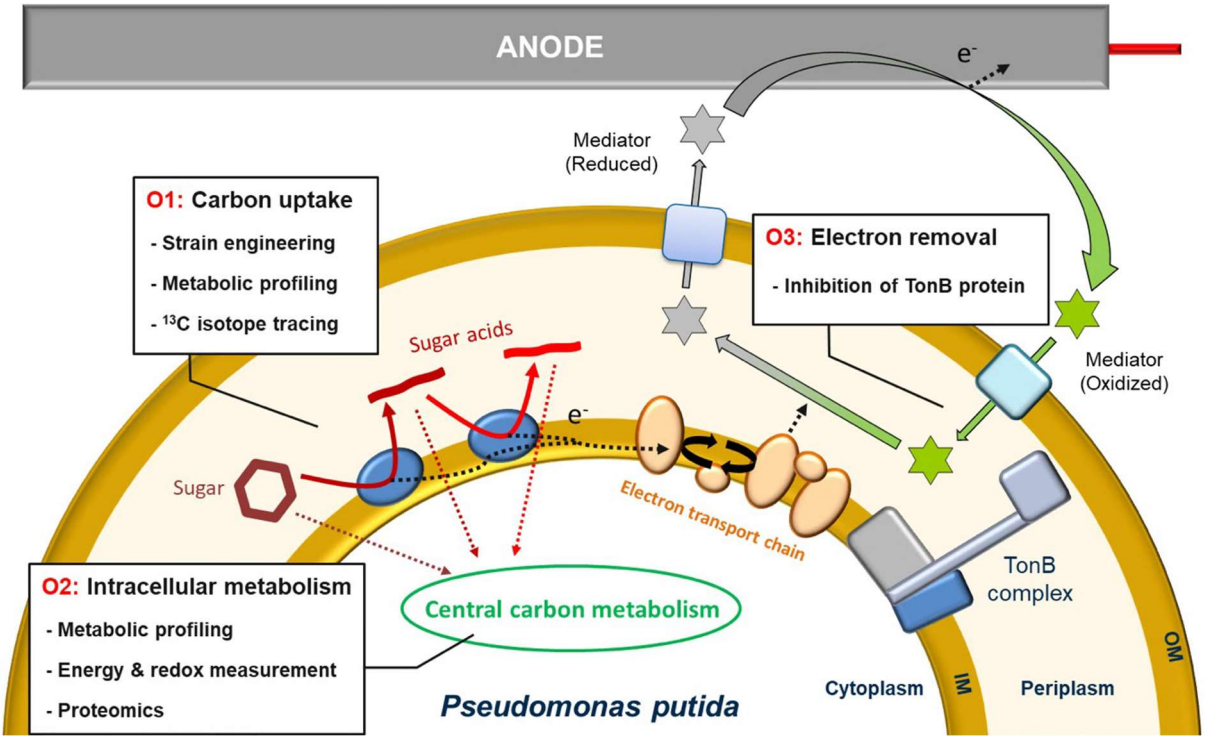

Figure 9. Three objectives to be tackled in this dissertation and their respective approaches. OM, outer membrane; IM, inner membrane.

Chapter 4.
Materials and methods

4.1. Bioelectrochemical reactor design

In theory, any type of BES reactor should able to be used for this study if it meets the following criteria: (i) it is sealable and autoclavable to prevent contamination; (ii) provides defined conditions for the working chamber (anodic chamber) where *P. putida* cells will be cultivated, which means it needs to be separated from the counter chamber (cathodic chamber) by an ion exchange membrane and parameters, especially temperature and mixing, can be controlled. An additional bonus would be sufficient working volume for multisampling and enough space for external plug-in sensors (e.g., pH, pO_2, redox, etc.).

Based on these considerations, a double-jacketed cylinder-like glass reactor sealed with polyether ether ketone (PEEK)-made lids and plugs, was previously designed [29, 30]. A quick release clamp was used to tighten the lid with the glass vessel. The connections are using the DN60 standard size (Duran Group, Germany). The schematic diagram of the reactor is shown in **Fig. 10**, and also elsewhere [30]. Detailed description of the reactor can be found below.

- **Glass vessel**: the working chamber is surrounded by an outer layer for temperature control connected to a heating water bath, and one injection port (GL14 screw size) is also designed on the glass vessel for such as inoculation and supplementary of medium.
- **Lid**: the lid is made from PEEK material because of its stability and resistance against thermal, chemical and climate stresses. All the measuring and controlling units are plugged into the working chamber through the lid with screw plugs sealed with O-rings. Seven open ports were designed on the lid; while six of them have an inner diameter of 12 mm, the remaining port (in the center) only has a 2-mm diameter hole for working electrode cable.
- **Screw plugs**: the plugs are also made from PEEK. Four different designs are present: (i) plug with 12-mm diameter hole in the center for connecting glass tubes and sensors; (ii) solid plug used as sealing stoppers; (iii) plug with 2-mm diameter hole for working electrode cable; (iv) plug with four holes of 3.2-mm diameter for gassing, pH controlling and sampling (via autoclavable teflon tubing with outer diameter of 3.2 mm).
- **Condensers**: the glass condenser is used to reduce the water loss caused by N_2 gas sparging. It has a membrane filter (0.22 µm pore size) to keep the reactor sterile and is connected to a chiller (4-8 °C) to recover the moisture in the off-gas. In this case, roughly

0.09 ml/h water loss would be detected with about 30 ml min^{-1} nitrogen flow through the headspace of the reactor [30], but this number needs to be determined case by case.

- **Bridging tube**: a glass tube with outer diameter of 12 mm was used as bridging tube to connect the reference electrode with the working chamber. This connection allows for minimizing voltage losses while still ensuring that the reference electrode is not being contaminated by the electrolyte in the working chamber. On the top end of the tube, a GL14 open-top cap is used to connect the reference electrode (the red cap shown in Figure 1), and on the other end, the tube is sealed with a porous glass/ceramic frit (pore size of ≤1 μm, projected diameter of ~3 mm). Frits could also be fixed via heat shrink polytetrafluoroethylene (PTFE) tube, but this sometimes falls off during or after autoclaving.
- **Counter electrode compartment**: it is a hollow glass tube with also the outer diameter of 12 mm. The top-end is open and the bottom end (which will be plugged into the working chamber) is sealed by a membrane (to be discussed below in number 10) with GL14 open-top cap and O-ring.
- **Membrane**: membrane is an essential unit of the BES reactor in our case. Different types of membrane will affect the anion and/or cation exchange between anode and cathode chambers, especially protons and the corresponding pH changes in each chamber [272]. However, this will not be an issue while (i) a pH control system is applied for the anode chamber and/or (ii) short batch experiments are conducted (< 10 mM glucose substrate). Only the anodic half-cell reaction (i.e., the interaction of *P. putida* cells and anode) is significant for the BES cultivation of *P. putida*.
- **Working electrode (anode)**: it is the key component of the BES reactor. Normally carbon material is used, due to its stability and biocompatibility. Here carbon cloth was chosen as the working electrode material. The raw carbon material is normally quite hydrophobic on the surface which is not good for the (bio)electrochemical reactions. Hence, pretreatment of the material prior to use is required. Many methods were developed in the past decades [273]. But for cultivating *P. putida*, it requires a working electrode which can work at high positive potential because of the mediator used. Successful method tested in our lab was using cetyltrimethylammonium bromide (CTAB) to treat the carbon cloth: soaking in 2 mM CTAB solution overnight (about 16 h, 40 °C, 200 rpm of shaking) or running cyclic voltammetry for 100 cycles in 2 mM CTAB solution. Identical performance can be observed for both methods. The working potential window, defined as no significant oxygen evolution observed (otherwise oxygen would be produced through electrochemically oxidation of H_2O), for the treated carbon cloth can be over 0.8 V (vs SHE), which is sufficient for the case of using $K_3[Fe(CN)_6]$ as mediator. Unsuccessful pretreatment

method tested was electrolysis in acids, which gave a strong background noise from blank electrode.

- **Reference electrode**: it is used to control the potential of the working electrode. Different types of reference electrodes can be employed depending on the purpose of the experiment or the setup. Saturated Ag/AgCl electrodes are easier and safer to handle, and have higher stability at various operating conditions.
- **Counter electrode (cathode)**: the cathode material does not affect the anodic cultivation. In general, an electrode with low overpotential for hydrogen evolution or oxygen reduction will be recommended to improve the energy efficiency of the whole reactor, such as a platinum electrode. But considering the cost and the main purpose of our experiment, stainless steel mesh is chosen for the reasons of good conductivity, stability, and high specific surface area. Other materials, e.g. carbon fiber or graphite, can also be used as well depending on the availability on site.
- **Electric connecting wire**: titanium wire is selected to connect electrodes to the external potentiostat, because it meets the following requirements: (i) it is long-term stable against corrosion in a moist environment; (ii) it is biocompatible but does not interact with microorganisms.
- **Agitator:** magnetic stir plate placed at the bottom of the reactor is used for mixing, with a cross-shaped stir bar of 25 x 25 x 9 mm in the working chamber.
- **Sparger:** the BES reactor is continuously flushed with nitrogen gas in the headspace with a speed controlled by a gas flow meter. Previous results confirmed the dissolved oxygen was lower than 15 ppm (the lower detection limit of the sensor (OXY-4 mini, Presens, Germany)) with our reactor design and operating parameters for the whole batch.
- **Temperature controlling system:** a recirculating heater is used to control the temperature of the working electrode chamber (i.e., anodic chamber) and another recirculating chiller is used to recover the moisture loss due to the gas pumping.
- **pH controlling system** (optional depending on the purpose): while up to 1.5 g L^{-1} glucose is used as sole carbon source in BES and the BES is running in short-term batch mode, pH control is not compulsory. However, it will become essential if (i) higher concentration of glucose is added; (ii) long-term (≥ 2 weeks) or fed-batch processes are targeted where acidic products accumulate in the broth; or (iii) a quantitative physiology characterization requiring metabolic steady-state is conducted, such as flux balance analysis, omics' analysis, etc. The pH value will change the glucose uptake rate significantly.

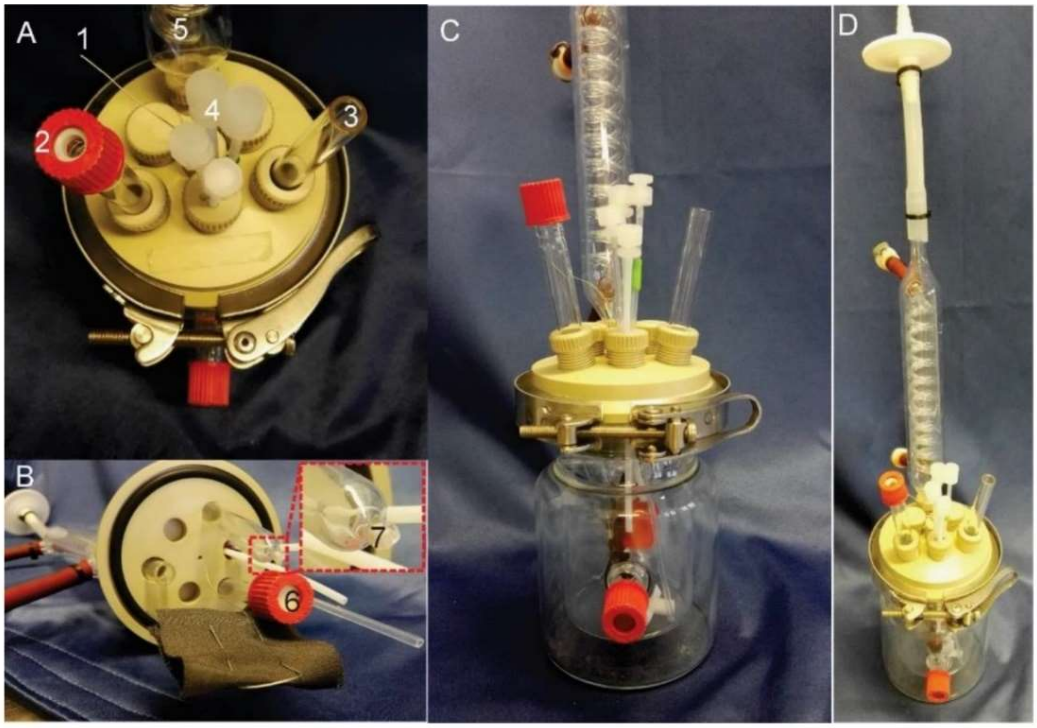

Figure 10. The assembled BES reactor. Figure was reproduced from a publication by Lai, et al. [274]. (**A**) top-view; (**B**) bottom view of the lid; (**C**) and (**D**) overview from the side. 1, working electrode electric wire; 2, top-end of the bridging tube; 3, top-end of the counter electrode compartment; 4, four-port plug for gassing, sampling and feeding; 5, condenser; 6, bottom-end of the counter electrode compartment, sealed by an ion exchange membrane; 7, bottom-end of the bridging tube, sealed by porous glass frit (pore size of < 1 µm).

4.2. Operation and monitoring of bioreactor

4.2.1. Media

Two media used for pre-culture cultivation are:

- **Lysogeny broth (LB)**: tryptone 10 g L^{-1}, yeast extract 5 g L^{-1} and NaCl 10 g L^{-1}. For solid media, agar (15 g L^{-1}) is added to LB broth, and
- **Defined mineral medium (DM9):** Na_2HPO_4 6 g L^{-1}, KH_2PO_4 3 g L^{-1}, NH_4Cl 1 g L^{-1}, $MgSO_4 \cdot 7H_2O$ 0.10 g L^{-1}, 1 ml L^{-1} of $CaCl_2 \cdot 2H_2O$ stock solution (15 g L^{-1}) and 1 ml L^{-1} of trace elements stock solution. The trace element solution contains: $FeCl_3 \cdot 6H_2O$ 1.5 g L^{-1}, KI 0.18 g L^{-1}, H_3BO_3 0.15 g L^{-1}, $CoCl_2 \cdot 6H_2O$ 0.15 g L^{-1}, $MnCl_2 \cdot 4H_2O$ 0.12 g L^{-1}, $Na_2MoO_4 \cdot 2H_2O$ 0.12 g L^{-1}, $ZnSO_4 \cdot 7H_2O$ 0.12 g L^{-1}, $CuSO_4 \cdot 5H_2O$ 0.03 g L^{-1}, EDTA (acid form) 10 g L^{-1}, and $NiCl_2 \cdot 6H_2O$ 0.023 g L^{-1}. Glucose of 5 g L^{-1} is used as sole carbon source.

Three buffers used in the bioelectrochemical system during the BES cultivation are:

- **Anodic buffer (DM9A)**: A modified DM9 medium (as described above for the pre-culture preparation) was used: (i) glucose concentration was adjusted to 2 g L^{-1}; (ii) a final concentration of 1 mM mediator such as $K_3[Fe(CN)_6]$,was added.

- **Cathodic buffer (DM9B)**: A modification of the DM9A buffer was used in the cathode compartment: (i) no added glucose; (ii) no trace element solution and no $CaCl_2 \cdot 2H_2O$; (iii) no mediator added.

- **Reference buffer**: saturated KCl was used as the buffer filled into the bridge tube for the reference electrode. A few crystals were added into the liquid phase to maintain the concentration.

4.2.2. Electrochemical method

Cyclic voltammetry was used to determine the redox potential of the added mediator and thus to define the working electrode potential. Based on the previous results published elsewhere [30], 0.5 V vs Ag/AgCl/KCl_{sat} was set for the case $K_3[Fe(CN)_6]$. Chronoamperometry (CA) was used to control the working electrode potential to the desired value against reference electrode.

4.3. Standard operation procedure of bioelectrochemical cultivation

4.3.1. Pre-culture preparation

Achieving anaerobic growth of *P. putida* is the ultimate target of applying this electrode-based cultivating technique. But at this stage, pre-growth of working biomass under aerobic conditions is still required. A classic microbiology cultivation procedure starting from cryostock with defined and identical cultivating parameters, to minimize the batch effects, is applied for each batch.

In brief, the cryostock was firstly streaked on an LB agar plate to grow single colonies for liquid culture. A single colony was then inoculated into DM9 medium and cultivated in a shake flask at 30°C and 200 rpm (with 2.5 mm orbit) overnight (15-16 h). After that, the cells were quantified by OD_{600} measurement and harvested by centrifugation (30 °C, 5000 *g*, 10 min), resuspended in about 15 ml DM9B buffer and injected into the BES reactor.

To maintain identical cellular status after overnight cultivation for each batch, the LB agar plate culture should be used within 24-36h; otherwise, a longer lag phase in the liquid phase cultivation would possibly be observed and thus change the growth status of cell pellets for BES inoculation. The flasks were filled with medium to a maximum volume of ≤ 20% (identical amount for all batches) of the nominal volume of the vessel.

4.3.2. Reactor assembly

The reactor was constructed based on the functions described above and autoclaved. Before autoclaving, DM9B buffer was filled into the working chamber as well as the counter electrode compartment. The bridging tube was filled with saturated KCl solution. In addition, the reactor should be checked for air tightness before autoclaving.

4.3.3. BES cultivation

4.3.3.1. Condition set-up

Water used to circulate the reactor's jacket needs to be maintained at the optimal growing temperature of *P. putida*, by adjusting the heating circulator (e.g., pumping rate, heating power, etc) to ensure the value is 30 ± 0.5 °C for all reactors connected in series, while the condenser's temperature is approximately 6-8°C to minimize liquid loss through evaporation. The stirring speed of the agitator was set to 400 rpm. CA method for potentiostat was set up with the following parameters: the working electrode potential of "0.5 V" against reference electrode when ferricyanide was later used as mediator; current recording intervals of every 6-10 min for the whole batch; and "Auto" resolution for the current range.

4.3.3.2. Reactor operation

After an abiotic run for 5-8 hours for the fresh medium and a flat background signal was achieved (0 mA fluctuating within a maximum of ±10 µA range), a final concentration of 1 mM sterilized mediator is injected into the working chamber, the reactor continued to run for another 14-16 hours. When a flat background signal was achieved (most likely fluctuating between 0-10 µA), the BES reactor was inoculated with biomass from the pre-culture, then the current was recorded until manually stopped. The reactor was sampled at least once every two days and supernatant and/or cell pellets were collected depending on the analytic purposes.

4.4. Analytical methods

4.4.1. Gas chromatography – mass spectrometry (GC-MS)

4.4.1.1. Sample preparation

4.4.1.1.1. For detection and identification of acetate

120 µl of culture supernatant was blow-dried with pure N_2 gas. The dried sample was dissolved in 50 µl of 100% pyridine and derivatized with 20 µl of N-methyl-N-tert-butyldimethylsilyl-trifluoroacetamide (Macherey-Nagel, Düren, NRW, Germany) at 70°C for 1 hour. Automated derivatization was carried out using the TriPlus™ RSH autosampler (Thermo Scientific).

4.4.1.1.2. For detection and identification of unknown sugars and sugar acids

15 nmol of adonitol was added in 5-10 µl of culture supernatant as internal standard and then blow-dried with pure N_2 gas. The dried sample was derivatized with 50 µl of MOX reagent (2% Methoxyamine·HCl in pyridine, Thermo Scientific) at 40°C for 1 hour, followed by 50 µl of SILYL-991 (N,O-Bis(trimethylsilyl)trifluoroacetamide:chlorotrimethylsilane 99:1, Macherey-Nagel, Düren, NRW, Germany) at 80°C for 2 hours.

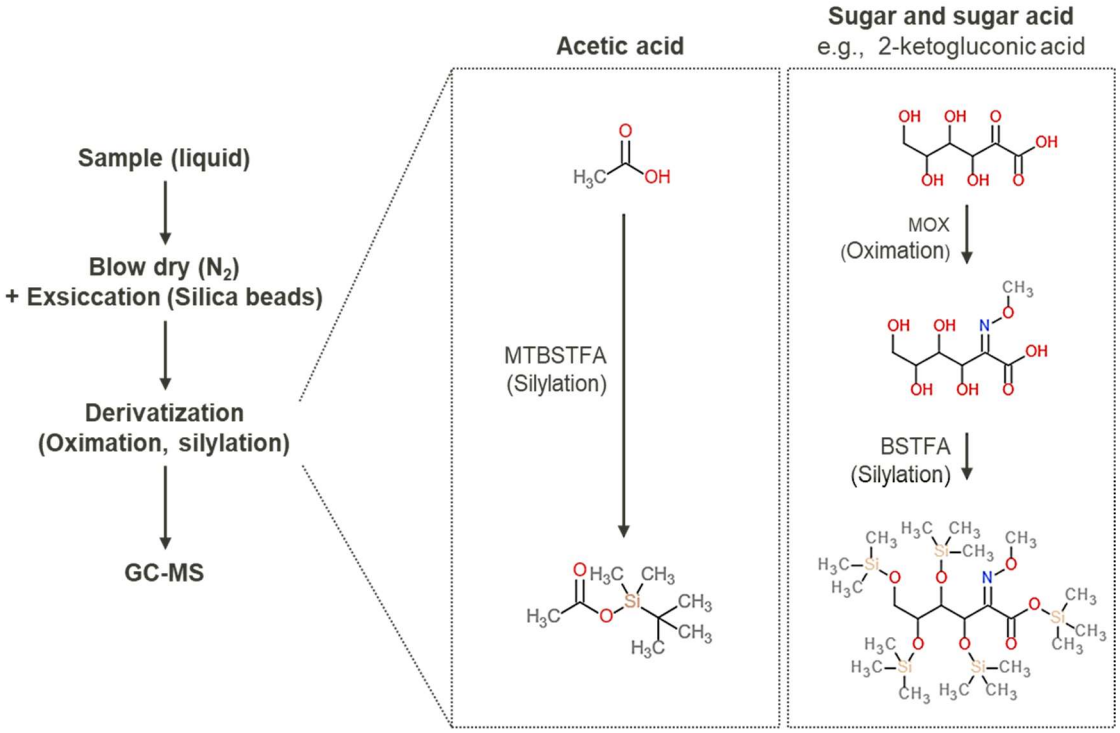

Figure 11. Schematic representation of sample preparing step for compound detection and identification by GC-MS. MOX, methoxyamine: MTBSTFA; N-methyl-N-tert-butyldimethylsilyl-trifluoroacetamide; BSTFA, N,O-Bis(trimethylsilyl)trifluoroacetamide.

4.4.1.2. Operation

4.4.1.2.1. Equipment

Extracellular metabolites were identified by a GC-MS system (ISQ™ LT Single Quadrupole, Thermo Scientific, Waltham, MA, United States) equipped with an off-axis discrete dynode electron multiplier and electrometer (Dynamax™ XR detection system), a TR-5MS GC Column (30 m × 0.25 mm, Thermo Scientific), operated with He as the carrier gas. Derivatized sample was injected in splitless mode.

4.4.1.2.2. Selected ion monitoring (SIM) mode for detection of acetate-1TBDMS

The temperature profile setting was as follows: 40°C (1 min), 40-150°C (5 min^{-1}), 150-320°C (100°C min^{-1}), and hold at 320°C for 20 min. Only three m/z peaks were targeted: 117.1, 118.1,

and 119.1, corresponding to [U-^{12}C]acetate-, [1-^{13}C]acetate-, and [1,2-$^{13}C_2$]acetate-1TBDMS, respectively. Retention time and m/z spectrum of acetate-1TBDMS were validated using unlabeled external standard (i.e., 99% sodium acetate anhydrous, which underwent the same treatment as the samples). The measured mass spectral data were corrected for other naturally occurring stable isotopes based on the elemental composition of the derivatized acetate molecule [275, 276].

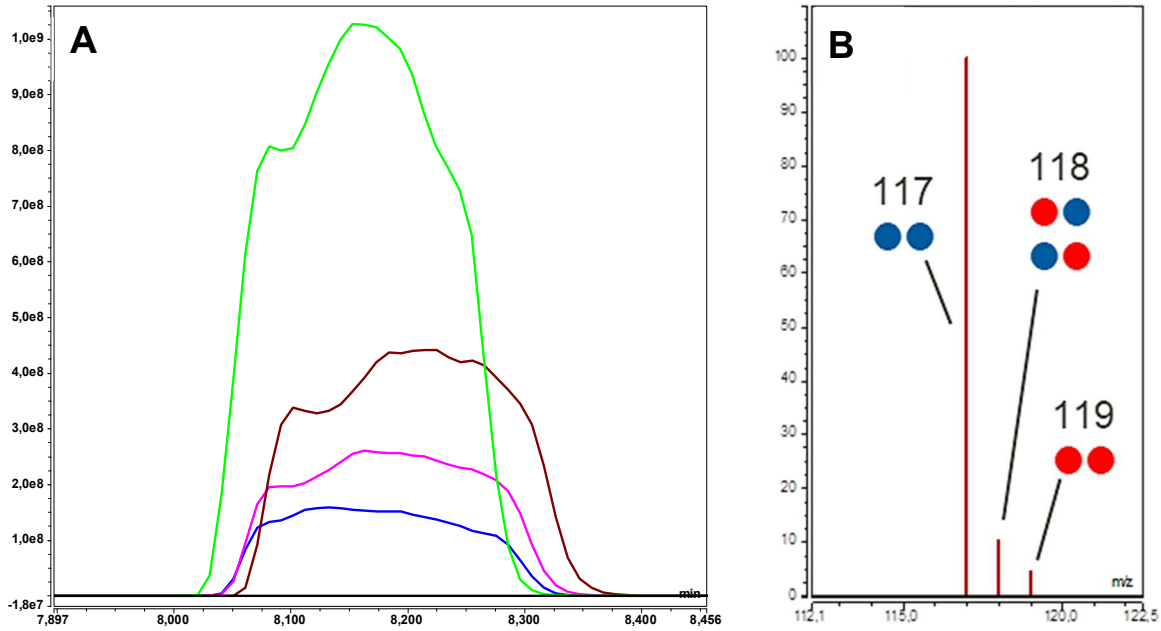

Figure 12. Selected ion monitoring analysis of acetate (external standard). (**A**) GC peaks of acetate-1TBDMS of prepared standard samples (in absolute amount): 2.5 µmol (green), 1 µmol (brown), 0.5 µmol (magenta), 0.25 µmol (blue). (**B**) Isotopomer distribution of acetate-1TBDMS; only three m/z peaks were targeted: 117.1, 118.1, and 119.1, corresponding to unlabeled, half-labeled and fully labelled acetate molecule.

4.4.1.2.3. Full scan mode for separation and detection of sugars and sugar acids

The temperature profile setting was as follows: 60°C (1 min), 60-270°C (8.5°C min^{-1}), and 270-325°C (70°C min^{-1}). Products were validated using external standard compounds and ready-made MS libraries from the National Institute of Standard and Technology (NIST, Gaithersburg, MD, United States).

4.4.2. High performance liquid chromatography (HPLC)

The BES cell cultures were centrifuged at 4°C, 17000 *g* for 10 minutes and the supernatants were collected. High-performance liquid chromatography (HPLC) was conducted using HPLC system (Dionex UltiMate 3000, Thermo Scientific) operated with a Hi-Plex H column (300 mm × 7.7 mm, 8 µm particle size, Agilent, Santa Clara, CA, United States). The quantification method of extracellular sugars and organic acids was previously described by Lai, et al. [44],

with additional calibrations of D-mannose, and D-mannonate from hydrolyzed D-mannono-1,4-lactone (abcr GmbH, Karlsruhe, Germany) for this study.

4.4.3. Adenylate and redox molecule assays

4.4.3.1. ATP quantification

Liquid culture was drawn out of the reactor and centrifuged at 4°C, 17000 *g* min^{-1} for 10 minutes in a Sigma™ micro-centrifuge pre-cooled to 4°C. The supernatant was completely discarded, and 250 µl of PB and 250 µl of extraction buffer were added, vortexed, and incubated on ice for 20 minutes. The mixture was then centrifuged again at the same condition; the supernatant was collected and neutralized with KOH 1M solution. The sample was then 20-fold diluted in reaction buffer. Conversion of ADP to ATP was carried out using pyruvate kinase (Merck), based on the irreversible reaction:

$$PEP + ADP \xrightarrow{Pyruvate\ kinase} Pyruvate + ATP$$

ATP was quantified using ATP determination kit, PRO (Biaffin GmbH & Co KG, Kassel, Germany). For the ATP assay, each culture was made into technical replicates, measured alongside a standard series of ATP dilutions. 50 µl of sample was added in each well of a 96-well Nucleon flat white plate, and then mixed with 50 µl of bioluminescent reagent. Before measurement, the plate was incubated at 37°C for 570 seconds while shaken 2 mm orbitally and then hold for 30 seconds. The luminescence gain was set to “Auto”.

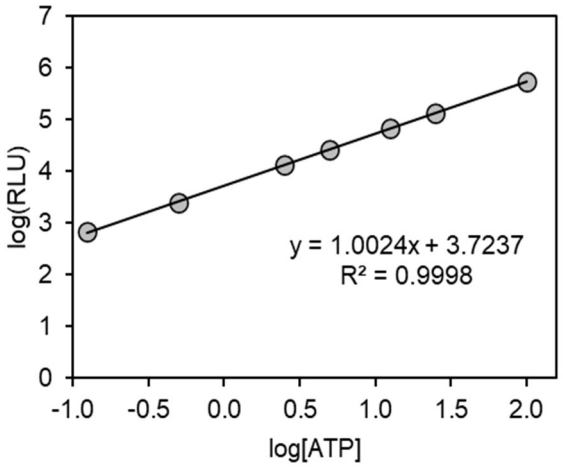

Figure 13. Example of an ATP quantification standard curve.

The standard curve (i.e., $\log_{10}$[RLU] versus $\log_{10}$[ATP]) was used to determine the amount of experimental ATP corresponding to the measured RLU (**Fig. 13**). The initial amount of ATP was determined as below:

$$ATP_{initial} = \frac{ATP_{experiment}\ (\mu mol) \times \text{dilution fold}}{100\%\text{- Luminescence inhibited by TCA (\%)}}; \quad \textbf{(1)}$$

with the percentage of luminescence inhibited by TCA according to the dilution rate determined previously by Lai, et al. [30]. The normalized amount of ATP per gram cell was determined as follows:

$$ATP_{normalized} = \frac{ATP_{initial}\ (\mu mol) \times \text{Volume}_{\text{ATP sample}}\ (ml)}{\text{Reaction volume (ml)} \times \text{Culture volume (ml)} \times \text{Cell content (g ml}^{-1})} \quad \textbf{(2)}$$

The value of total (ATP+ADP) was obtained by quantifying the total ATP amount in the sample after conversion by pyruvate kinase. The ATP/ADP ratio was then calculated as following:

$$\text{ATP/ADP ratio} = \frac{ATP}{\text{Total (ATP + ADP) - ATP}} \quad \textbf{(3)}$$

4.4.3.2. NAD(P)H quantification

Approximately 50 mg of cells were prepared for the following assays by washing with a cold phosphate buffer (pH 7.75, pre-cooled to 4 °C) and collected by centrifugation at 4°C, 17000 *g* for 1 minute. Metabolism was quenched by rapid freezing of cell pellets in liquid N_2. Commercial assay kits of NADH and NADPH (K338 & K349, BioVision Inc., Milpitas, California) were used and the extraction and quantification of respective co-factors were conducted following the manufacture's description. Total amount of NAD(P) molecules was obtained by omitting the heat degradation step in the standard protocol.

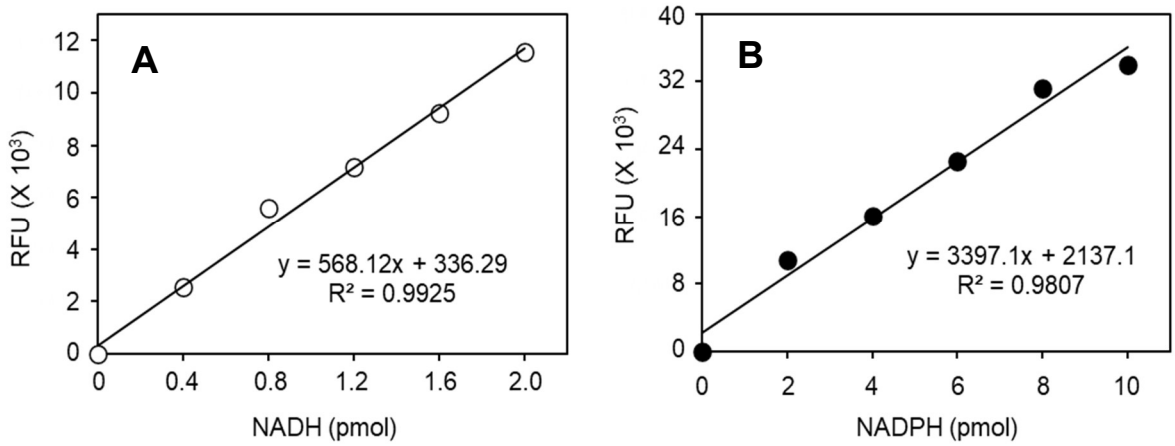

Figure 14. Example of a (**A**) NADH and (**B**) NADPH quantification standard curve.

The redox ratio (Red/Ox) for both molecules was calculated as following:

$$\text{Redox ratio} = \frac{C_{NAD(P)H}}{C_{NAD(P)}^{total} - C_{NAD(P)H}} \quad \textbf{(4)}$$

With $C_{NAD(P)H}$: concentration of the reduced form in the sample, and $C_{NAD(P)}^{total}$: total concentration of NAD(P) in the sample.

4.4.4. Differential analysis of protein expression

4.4.4.1. Sample preparation

Approximately 200 µg cell pellets were harvested by centrifugation (4°C, 17 000 g, 10 min) at inoculation time (t_0), at the time of peak current (t_1), and 414 h after inoculation (t_2). Cells were washed in 50 mM ammonium bicarbonate and disrupted with 3 cycles of flash freezing-thawing in liquid N_2. Glyceraldehyde 3-phosphate dehydrogenase (GapDH) from *Staphylococcus aureus* Mrsa252 was added to each sample as the internal standard. The samples were then reduced with 10 mM dithiothreitol in 50 mM ammonium bicarbonate for 1 h at 30°C. Subsequent alkylation of cysteine residues was performed using 100 mM iodoacetamide in 50 mM ammonium bicarbonate for 1 h at room temperature in the dark. Trypsin digestion was carried out by incubation overnight at 37°C with slight shaking using a final concentration of 0.1 µg $µl^{-1}$ sequencing-grade modified trypsin (Promega Co., Madison, WI, United States). Peptide samples were desalted using C18 Zip Tip columns (Merck Millipore, Darmstadt, Germany).

4.4.4.2. Shotgun proteomics

Each biological sample was divided into three technical replicates, prior to analysis via nano-liquid chromatography-tandem mass spectrometry (nLC-MS/MS) using an Orbitrap Fusion Tribrid mass spectrometer (Thermo Scientific) equipped with a nanoLC system (Dionex Ultimate 3000RSLC; Thermo Scientific). Peptides were separated on a Acclaim PepMap100 C18 column (250 mm × 0.075 mm, 3 µm particle size, Thermo Scientific) at a flow rate of 0.3 µl min^{-1} by applying the following settings with eluent A (0.1% formic acid in water) and eluent B (80% (v/v) acetonitrile and 0.1% formic acid in water): column equilibration for 1 min at 4% B, then followed by a gradual increase to 10% B within 4 min, to 35% B within 95 min, to 55% B within 20 min, to 90% B within 10 min, and finally hold at 90% B for 5 min.

Eluted peptides were ionized via an electrospray ion source (TriVersa NanoMate, Avion) operated in positive mode and scanned continuously between 350 and 2,000 m/z by the

Orbitrap mass analyzer with a resolution of 120,000, and a maximum ion injection time of 50ms. The two most intense ions with charge between 2+ and 7+ were picked for fragmentation with the quadrupole set to a window of 1.6 m/z and subjected either to higher energy collisional dissociation (HCD) mode with a collision energy of 30%. Fragment ions were analyzed in the ion trap mass analyzer. Dynamic exclusion was enabled for 45 s after fragmenting a peptide ion to prevent repeated fragment analysis of the same ion.

4.4.4.3. Proteomic data analysis

Protein identification was conducted by Proteome Discoverer (v2.4, Thermo Fisher Scientific) using the SequestHT as a search engine with the UniProt database of *P. putida* KT2440 with the following settings: cleavage enzyme trypsin, peptide length of 6-144 residues, allowing up to two missed cleavages, precursor mass tolerance, and fragment mass tolerance were set to 3 ppm and 0.1 Da, respectively. Oxidation of methionine residues and carbamidomethylation of cysteine residues were selected as dynamic modification and static modification, respectively. The false discovery rate of identified peptide sequences was kept to < 0.01 using the Percolator node. The abundance of proteins and peptides was calculated by label-free quantification based on area counts using the Minora node implemented in Proteome Discoverer. The relative protein abundance or relative peptide abundance was normalized to the abundance of the internal standard. The abundance of each protein at each sampling point was calculated as the average of the abundances in all replicates. Log fold change (FC) of protein expression during the cultivation was calculated as the fold change of the abundance at a time point (t_i, i =1 or 2) versus the abundance at time t_0:

$$\log_2(FC) = \log_2\left(\frac{\text{Abundance } (t_i)}{\text{Abundance } (t_0)}\right) \quad \textbf{(5)}$$

One-tailed paired t-test was used for computing p-values of two dependent sets of abundances. Volcano plots were generated from significance ($-\log_{10}$(p-value)) against $\log_2$(FC). The following color signals are used for data presentation: red, upregulated; blue, downregulated, black, not significantly changed. As some proteins were undetected/ unquantified at either inoculation and/or cultivation points, their respective abundance ratios (i.e., fold changes) were either undefined or equal to 0; these data were labeled with the color gray.

4.5. Calculation of performance parameters

4.5.1. Biomass

To calculate the cell dry weight (CWD) of *P. putida*, KT2440 culture at OD_{600} of 1 was deposited on a PTFE membrane (pore size of 0.22 µm) by filtration, washed, and dried until the total weight of the membrane became unchanged. The conversion coefficient, which was assumed for all *P. putida* strains used in this dissertation, was then empirically determined using the following formula:

$$\text{Coefficient} = \frac{\text{Total dry weight - (Dry salt weight + Dry membrane weight)}}{V_S \times OD_{600\ \text{sample}}} \quad \textbf{(6)}$$

yielding a value of 0.476 g L^{-1} per one OD measured at λ=600 nm.

The CDW (in g) was then approximated from measured OD_{600} as following:

$$CDW = 0.476 \times OD_{600} \times V_S \quad \textbf{(7)}$$

with V_S: volume of the sample (in L).

4.5.2. Current density, cumulative charge, and total electron discharge

To calculate the current density (j, in mA cm^{-2}) at time t, the following formula is applied:

$$j_t = \frac{I_t}{A} \quad \textbf{(8)}$$

with I: current output recorded by the potentiostat (in mA), and A: the projected area of the carbon electrode, which was 25 cm^2 in all experiments.

The cumulative charge (Q_t, in mC, or mA s) at time t after k recording steps was calculated as:

$$Q_t = \frac{1}{2}\sum_{k=1}(I_k + I_{k-1})(t_k - t_{k-1}) \quad \textbf{(9)}$$

Total electron discharge (n_e, in mmol) during the time interval $t_i - t_0$ (in s) was calculated using the following formula:

$$n_e = \frac{\int_{t_0}^{t_i} It\ dt}{F} \quad \textbf{(10)}$$

with F: the Faraday's constant (96485.3 C mol^{-1}).

4.5.3. Production yields, rates, carbon and electron balance

The absolute quantity of a metabolite (n_M, in mmol) at a specific sampling point was calculated as following:

$$n_M = C_M \times (V_R + V_S) \quad \textbf{(11)}$$

with C_M : concentration of the metabolite quantified by HPLC (in mM), V_R: volume of the remained medium in the reactor (in L), and V_S: sampling volume (in L).

The molar yield coefficients (Y) are determined as the slope of a plot of mol product versus mol substrate converted. The specific rate of metabolites (r_P, mmol g_{CDW}^{-1} h^{-1}) is then calculated based on the following equation:

$$r_P = r_s \times Y_{P/S} \quad \textbf{(12)}$$

with $Y_{P/S}$: the yield coefficient of specific metabolite (mmol product per mmol sugar), and r_S: the specific substrate uptake rate (in mmol g_{CDW}^{-1} h^{-1}).

For those BES fermentations with acetate and/or pyruvate, lactate, formate as by-products, the yield of CO_2 can be assumed as a constant ratio to acetate (one mol CO_2 per one mol acetate). Therefore, the carbon balance (in %) is calculated based on the molar yield:

$$\text{Carbon balance (CB\%)} = 100 \times \frac{\sum (Y_{P/S} \times n_p^c)}{6} \quad \textbf{(13)}$$

with n_p^c: the number of carbon atoms of the corresponding compounds, and 6: the carbon atom number per hexose molecule.

The coulombic efficiency, that is the efficiency in the transfer of electric charge during the conversions, was then determined using the formula:

$$\text{Coulombic efficiency (CE\%)} = 100 \times \frac{Y_{e/S}}{\sum (Y_{P/S} \times n_p^e)} \quad \textbf{(14)}$$

with $Y_{e/S}$: the yield of electrons to the electrode from sugar catabolism (mmol electrons per mmol hexose), and n_p^e: the number of electrons released by forming specific metabolites.

Chapter 5.
Results and Discussion

5.1. Carbon flux on cytoplasmic membrane of *Pseudomonas putida* during bioelectrochemical cultivation

As a heterotrophic microorganism, *P. putida* needs organic carbon substrates for biomass formation. The first question to address in this dissertation is, under anoxic condition of BES, through which pathway(s) carbon is taken up from outside of the cell into the central carbon metabolism. As indicated in previous studies, even though most of the glucose was transformed into extracellular sugar acids including GA and 2KGA through the POC, there was an accumulation of a few metabolites that could only be produced intracellularly, such as acetate [30, 31]. It was, however, unknown if the acetate was the result of catabolism of the fed substrate, or if the cell had to compensate by breaking down its carbon reserves to obtain glucose [22]. Answering this question, will not only provide a crucial understanding of glucose uptake for the engineering of *P. putida* that acclimatizes to, and grows in anaerobic cultivation, but also help pinpoint which internal bottleneck(s) are hindering carbon flux.

5.1.1. P. putida mutants channeling carbon through glcP, gaP, and 2kgaP pathway

5.1.1.1 Bacterial strains and cultivation condition

Three mutant strains were generated to direct the carbon flux toward specific pathways as indicated in section 2.1.3.1.1 (**Fig. 3**, **Table 5**). All strains were constructed at the Systems Environmental Microbiology group of Dr. Pablo I. Nikel at the Novo Nordisk Foundation Center for Biosustainability, Denmark. Cryostocks were initially activated at 30°C in LB medium before pre-culture cultivation. Pre-cultures of *P. putida* KT2440 strains were prepared as previously described in **Chapter 4**, using unlabeled glucose as substrate. The reactors, on the other hand, contained 2.0 g L^{-1} of fully-labeled glucose (≥99 atom % ^{13}C D-Glucose-$^{13}C_6$, Sigma-Aldrich). Another set of reactors using unlabeled glucose as substrate was used as control.

Table 5. Mutant *P. putida* strains used for studying cytoplasmic carbon flux.

Name	Descriptions	Pathway
P. putida KT2440	Wild-type	
P. putida KT2440 Δ*gcd*	Knockout mutant of glucose dehydrogenase (*gcd, PP_1444*)	**glcP**
P. putida KT2440 Δ*glk* Δ*gtsABCD* Δ*gad*	Knockout mutant of glucose ABC transporter (*gtsABCD*, *PP_1015, PP_1016, PP_1017, PP_1018*), glucokinase (*glk*, *PP_1011*) and gluconate dehydrogenase (*PP_3382, PP_3383, PP_3384*)	**gaP**
P. putida KT2440 Δ*glk* Δ*gtsABCD* Δ*gnuK* Δ*gntT* Δ*PP0652*	Knockout mutant of glucose ABC transporter *(gtsABCD, PP_1015, PP_1016, PP_1017, PP_1018*), glucokinase (*glk*, *PP_1011*) and gluconate transporters (*gntT, PP_3417; PP_0652*) and gluconokinase (*gnuK, PP_3416*)	**2kgaP**

5.1.1.2. Strain validation

First, the performance of each mutant strain was evaluated with aerobic cultivation. Each strain was initially cultivated overnight in the minimal medium supplemented with glucose from a single colony. Then, each strain was cultivated in a shake flask in triplicates, and their growth and extracellular carbon were monitored for approximately 8-10 hours where the entire exponential phase is typically observed for the wild-type strain (**Appendix B**, **Fig. 15**). On the growth curve of strain KT2440 (WT) and gaP, a pre-exponential phase (0-2 hours after inoculation), an exponential phase (~2-8 hours after inoculation), and a deceleration phase (after ~8 hours until the end of experiment) could be observed, whereas for the other two strains, pre-exponential phase lasted until ~3-4 hours after inoculation, and then presumably grew exponentially until the end of their respective experiments (**Appendix B**). The result is summarized in **Table 6**. The biomass yield and maximal growth rate of the WT and gaP strains were similar, whereas strain glcP and 2kgaP grew at a similar rate, but nearly twice as slow as the other two. Interestingly, strain 2kgaP consumed glucose twice as fast compared to the other strains, but had the lowest biomass yield, as glucose was mostly converted to extracellular GA and 2KGA instead. Strain glcP did not produce any GA nor 2KGA, while strain gaP only produced GA as extracellular sugar acid (**Fig. 15B-C**). All these results confirmed that the knockout mutations were indeed successful.

Table 6. Performance of wild-type and mutant *P. putida* KT2440 strains in aerobic shake flasks. Data are average from biological triplicates (n=3); the values are depicted as "mean ± standard deviation of the sample mean".

Strain	WT	glcP	gaP	2kgaP
μ_{max} (h^{-1})	0.559 ± 0.026	0.371 ± 0.003	0.675 ± 0.067	0.353 ± 0.004
$r_{glucose}$ (mmol g_{CDW}^{-1} h^{-1})	-10.76 ± 0.63	-8.09 ± 0.39	-10.00 ± 1.34	-16.75 ± 1.68
r_{GA} (mmol g_{CDW}^{-1} h^{-1})	0.312 ± 0.087	0	0.876 ± 0.252	0.813 ± 0.173
r_{2KGA} (mmol g_{CDW}^{-1} h^{-1})	0.845 ± 0.152	0	0	5.350 ± 0.008
$Y_{x/s}$ (g_{CDW} $g_{glucose}^{-1}$)	0.287 ± 0.010	0.254 ± 0.012	0.374 ± 0.034	0.117 ± 0.012
$Y_{GA/glucose}$ (g g^{-1})	0.027 ± 0.006	0	0.077 ± 0.012	0.036 ± 0.005
$Y_{2KGA/glucose}$ (g g^{-1})	0.074 ± 0.008	0	0	0.240 ± 0.008

In addition to GA and 2KGA, five other metabolites – 2-ketoglutarate (2KG), pyruvate, formate, acetate and lactate, which are produced intracellularly and secreted extracellularly, were under observation (**Fig. 15D-H**). Overall, the metabolism of these five compounds was correlated with biomass formation, with WT and gaP strains sharing similar trends in production and re-consumption over time. More specifically, these two strains showed higher extracellular accumulation of 2KG, pyruvate, formate, acetate, and lactate. Interestingly, the only difference between WT and gaP strains was their metabolism of 2KG: while 2KG was suddenly accumulated extracellularly in both strains after the 6-hour mark, it was immediately re-consumed by WT strain as it entered stationary phase, strain gaP showed a delay in re-uptake. On the other hand, glcP and 2kgaP strains also had similar production curves of these five metabolites to each other, albeit lower than the other two strains; at the same time, there were differences observed between these strains as well. For instance, strain 2kgaP had a significantly higher extracellular pyruvate production throughout the experiment, which was comparable with WT and gaP. Furthermore, glcP and 2kgaP strains showed a much higher level of formate carry-over from their inocula at the beginning of the cultivation compared to WT and gaP strains.

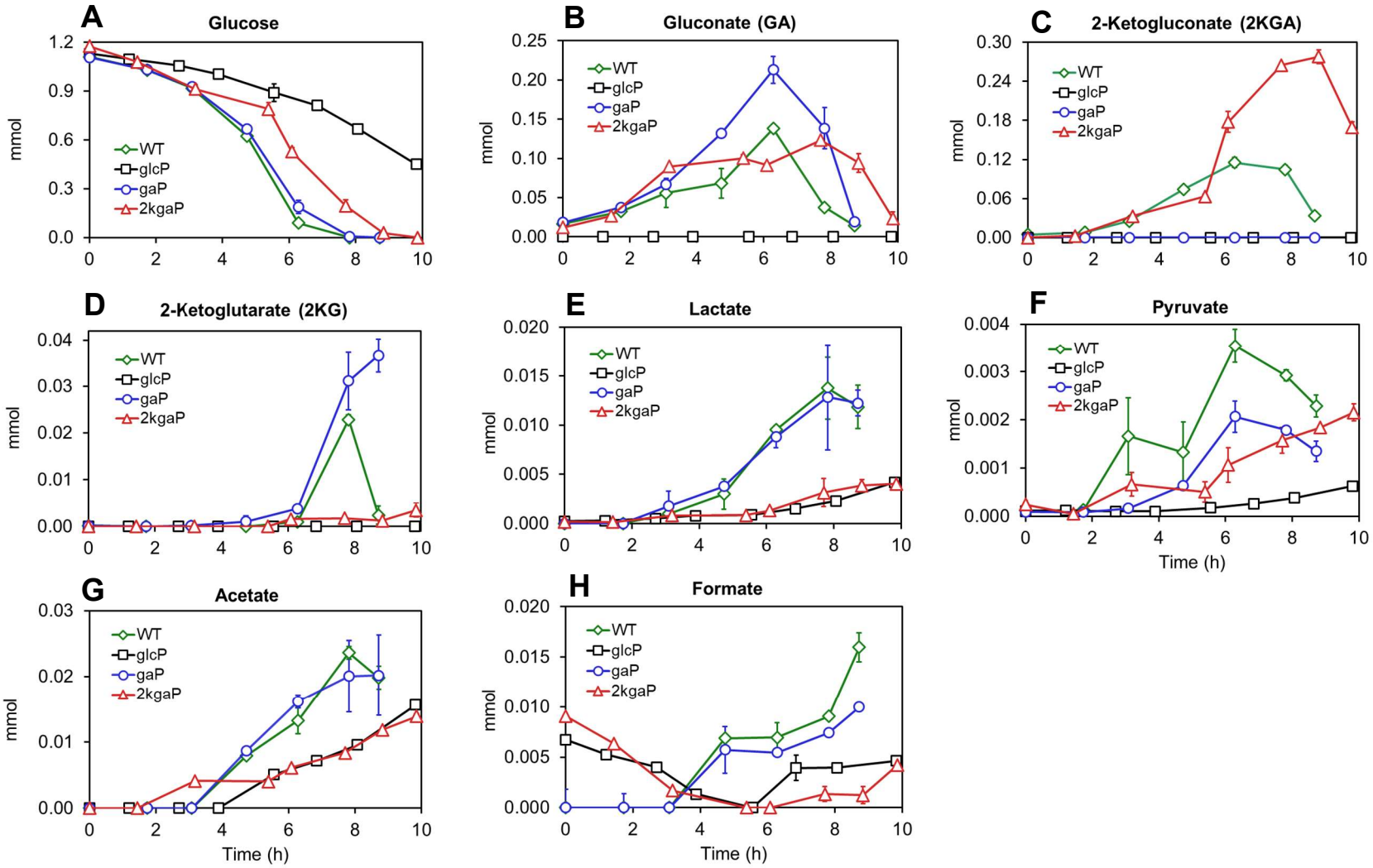

Figure 15. (**A**) Consumption of glucose and production of selected secreted metabolites including (**B**) GA, (**C**) 2KGA, (**D**) 2KG, (**E**) lactate, (**F**) pyruvate, (**G**) acetate, and (**H**) formate by *P. putida* KT2440 wild-type (green), glcP (black), gaP (red) and 2kgaP (blue) strains. Data are averages of biological triplicates, the error bar on each data point represents the standard deviation of the sample mean (n=3).

5.1.2. Anaerobic carbon flux distribution on P. putida's cytoplasmic membrane during bioelectrochemical cultivation

5.1.2.1. Strain performance

Unlike in aerobic cultivation, none of the strains showed an increase in planktonic biomass in BES, which is consistent with previously conducted studies [30, 31]. Strains gaP and 2kgaP produced a significant amount of current, with the respective $Y_{e\text{-}/glucose}$ values of 2.12 ± 0.06 and 3.73 ± 0.34 mol mol^{-1}. Moreover, strain 2kgaP in general produced roughly twice as much electron compared to gaP, whereas strain glcP only produced a small current density that peaked no higher than 0.005 mA cm^{-2} (**Fig. 16A**, **Appendix C**). Concurrently, both the gaP and the 2kgaP strains displayed a much higher consumption rate of glucose compared to strain glcP; at the same time, all strains consumed glucose much slower in the BES setup compared to the aerobic counterpart (**Fig. 16B**, **Table 7**). Under BES conditions, all three mutant strains had a similar extracellular sugar acid profile to aerobic cultures, signifying that the strains were correctly generated. However, strain gaP and 2kgaP showed a significantly higher yield of gluconate and 2-ketogluconate, respectively (**Fig. 16C-D**, **Table 7**), indicating that in BES they were accumulated over time in the medium, while these organic acids were relatively quickly consumed when oxygen was present. On the other hand, despite having a higher acetate production rate compared to strain glcP, strain gaP, and 2kgaP had a 2.3 – 3 times lower acetate yield overall (**Fig. 16E**, **Table 7**). As the evaluating ^{13}C isotope enrichment in acetate was focused on in the next step, measurement of other secreted metabolites was therefore left out.

Table 7. Process parameters of *P. putida* strains catabolizing glucose in BES. Data are the average from biological triplicates (n=3); the values are depicted as "mean ± standard deviation of the sample mean".

Strain	glcP	gaP	2kgaP
CB (%)	94.40 ± 1.21	87.71 ± 5.23	105.34 ± 0.93
CE (%)	67.30 ± 2.03	123.20 ± 9.20	100.68 ± 12.66
Rate (mmol g_{CDW}^{-1} h^{-1})			
$r_{glucose}$	-0.020 ± 0.002	-0.111 ± 0.023	-0.079 ± 0.004
r_{GA}	0	0.077 ± 0.016	0.002 ± 0.002
r_{2KGA}	0	0	0.044 ± 0.011
$r_{acetate}$	0.006 ± 0.001	0.011 ± 0.002	0.011 ± 0.001
Yield ($mol_{product}$ $mol_{glucose}^{-1}$)			
Y_{GA}	0	0.693 ± 0.027	-0.022 ± 0.030
Y_{2KGA}	0	0	0.552 ± 0.139
$Y_{acetate}$	0.303 ± 0.061	0.098 ± 0.007	0.133 ± 0.010

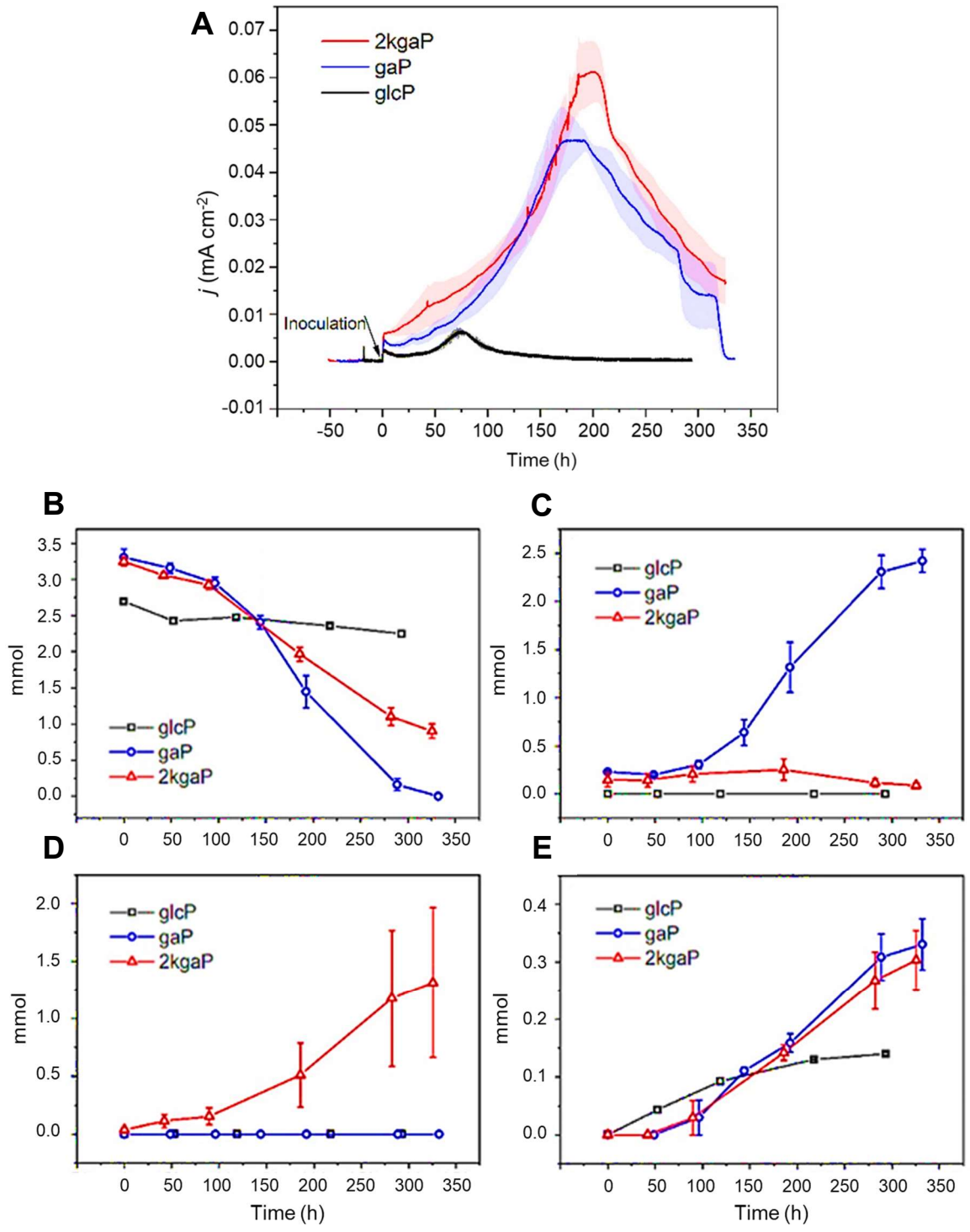

Figure 16. (**A**) Current density, (**B**) consumption of glucose, and production of (**C**) GA, (**D**) 2KGA, and (**E**) acetate of glcP (black line, black hollow square), gaP (blue line, blue hollow circle), and 2kgaP (red line, red hollow triangle) strains under BES condition. Data are averages of biological triplicates, the error bar on each data point represents the standard deviation of the sample mean (n=3).

5.1.2.2. Enrichment of ^{13}C-acetate using labeled glucose

To evaluate how much acetate was produced from catabolizing extracellular substrate instead of catabolizing intracellular carbon pools, the cells were cultivated aerobically with unlabeled glucose and then fed with fully-labeled glucose with ^{13}C isotope in BES. The obtained results were summarized in **Fig. 17**. Here, an additional set of experiments using unlabeled glucose as substrate (black circles) was used as the base line. The natural abundances of unlabeled, half-labeled, and fully labelled acetate were determined to be 97.2%, 2.6%, and 0.2%, respectively. As for the enrichment experiments, an increase in ^{13}C- acetate was observed in all strains, indicated by the decrease of [U-^{12}C]acetate and increase of [1,2-$^{13}C_2$]acetate over time. Enrichment of fully labeled acetate also showed a sharper increase than its half-labeled counterpart. The most noticeable enrichment of ^{13}C-acetate occurred in strain glcP, where up to 27% of total carbon in acetate were enriched. Meanwhile, strain gaP displayed only slight ^{13}C enrichment, mostly in the fully labeled form [1,2-$^{13}C_2$]acetate and seemingly no change in the abundance of [1-^{13}C]acetate. Finally, strain 2kgaP showed little to no enrichment, except for one reactor, where ^{13}C enrichment spiked at 290 hours and slowly decreased afterward, yet, only ~12% of total carbon in acetate were enriched.

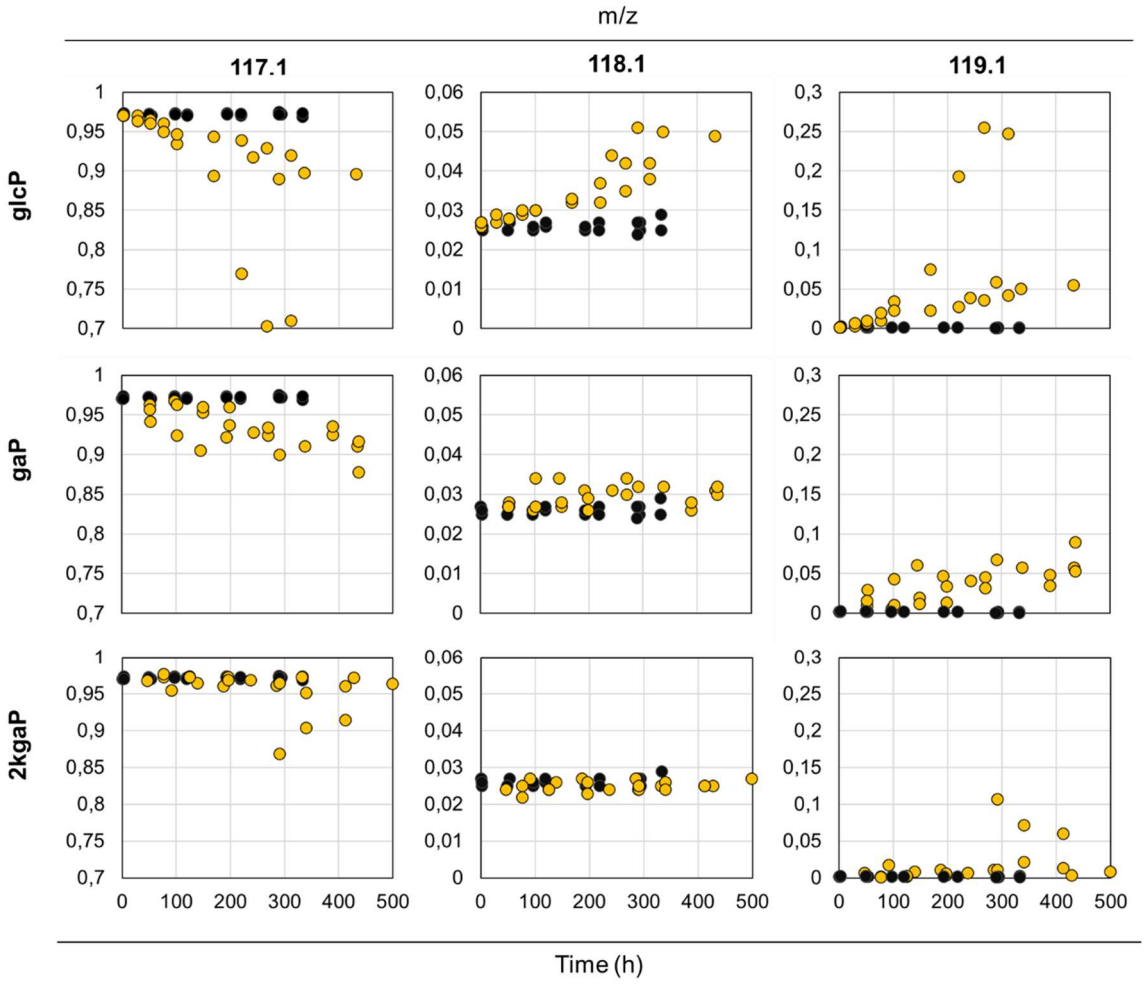

Figure 17. Enrichment of ^{13}C in extracellular acetate under BES condition by glcP, gaP, and 2kgaP strains. Peaks 117.1, 118.1, and 119.1 represent [U-^{12}C]acetate-, [1-^{13}C]acetate-, and [1,2-$^{13}C_2$]acetate-1TBDMS, respectively. Vertical axes represent peak abundance, i.e., occupancy of each type of labeled/unlabeled molecule in a sample. Black circle, peak abundance when unlabeled glucose was fed; yellow circle, peak abundance when fully labeled glucose was fed. Data were collected from at least two sets of independent experiments for each feeding condition.

5.1.3. Discussion

Several studies had been carried out to model the carbon flux within the POP of *P. putida* [30, 77, 81]; nevertheless, there has been little work done to evaluate how each pathway functioned individually. Here, the glcP, gaP, and 2kgaP strains, each representing a branch of cytoplasmic glucose uptake, were characterized in both aerobic and BES cultivation. Confluent with the aerobic flux models, the gaP branch might be favorable amongst other pathways, reflected by the similar performance in aerobic shake flask in comparison with WT strain without even producing 2KGA. Both of these strains also demonstrated a higher carbon influx toward downstream glycolysis and the TCA cycle, as seen in the accumulation of extracellular pyruvate, lactate, acetate, formate, and 2KG. It appears that 2KG was secreted toward the end of *P. putida*'s exponential phase in these cases, and its re-consumption rather correlated with the availability of extracellular GA; i.e., consumption of GA might have generated a transient overflow metabolism of 2KG, and extracellular 2KG is taken up when GA becomes depleted (**Fig. 15B, D**). Strain glcP, even though it had a comparable glucose consumption rate with the WT and gaP strain, grew nearly twice as slow (**Table 6**); this could be due to the fact that transport via the ABC system requires more ATP to energize translocation of glucose across the cytoplasmic membrane. Additionally, unlike the other three stains, carbon might have been diverted from the typical ED pathway in strain glcP, as indicated by the lower pyruvate production (**Fig. 15F**). On the other hand, biomass formation of strain 2kgaP was severely perturbed when the cell could only import 2KGA, despite having 2KGA yield three times higher than WT strain (**Table 6**). 2kgaP strain also had the lowest growth amongst the four strains, even though it was expected to have the highest net energy yield. This result seems to support the hypothesis that 2KGA uptake is limited by the redox pool, more specifically NADPH availability for the reduction of 6PKGA to 6PG (**Fig. 3**). Another possible explanation is that 2KGA might not be a strong effector in regulating the expression of the 2kgaP pathway. Further *-omics* analyses need to be conducted for confirmation of this hypothesis.

Under BES conditions, strain gaP and 2kgaP yield approximately 2 and 4 mol electron per mol glucose, respectively; this is not only in accordance with the stoichiometry of the POC

reactions (**Fig. 3-4**), but also similar to the result previously obtained by Lai, et al. [30] and Yu, et al. [31]. This shows once again that the POC is responsible for producing electrons during BES-mediated anaerobic respiration in *P. putida*. Interestingly, despite not having the same oxidation system to generate electrons, strain glcP also oxidized glucose and produced a small amount of current output at the beginning, but could not maintain it throughout the experiment (**Fig. 16A**, **Appendix C**). This implies that there might have been another pathway of catabolism, which did not dependent on the periplasmic glucose oxidizing enzymes, occurring during the cultivation. In addition, when comparing the performance parameters between aerobic and BES cultures, it is clear that under BES conditions, the sugar acid yields are up to one order of magnitude higher; however, the substrate consumption rate as well as production rate values are lowered by one to two orders of magnitude. Similar results can also be observed with other aldoses (see section **5.2.**), indicating that, despite that BES cultivation allows better mass yields, limitation on reaction rates is still needed to be overcome, for BES fermentation of *P. putida* to be able to compete with aerobic bioreaction.

The ^{13}C tracing experiment suggested that this might be another intracellular pathway that processed the labeled glucose molecule, as both fully-labeled and half-labeled acetate showed an increasing trend of enrichment in all three independent experiments with strain glcP. On the other hand, strain gaP displayed a similar behavior with a slight difference, as enrichment of half-labeled [1-^{13}C]acetate was not as pronounced in any of the repeats. In order to produce half-labeled acetate molecule from fully labeled glucose, the intermediate molecule must undergo C-chain elongation at one point using unlabeled carbon molecules stored inside the inoculum that had been previously grown on unlabeled glucose. In this scenario, it is possible that unlabeled carbon entered the ED-EMP cycle by catabolism of storage compounds – a behavior which has been previously observed in *P. putida* [22, 277]; this might explain the brief increase of current output at the beginning of the experiment with strain glcP. As for strain 2kgaP, two out of three reactors did not show significant enrichment of labeled acetate, although acetate production was comparable to that of strain gaP. This suggests that the acetate produced in this case might have come from carbon storage compounds instead of the external, labeled glucose.

After the initial results presented in this dissertation, Pause, et al. (2024) (**Fig. 18**) managed to achieve enrichment of ^{13}C in acetate up to more than 50% for strain gaP, ~36% for strain glcP, and ~26.5% for strain 2kgaP [278]. This result was obtained with (i) additional purification of acetate, and (ii) measurement by IC-MS. By comparison, the method used in this dissertation for ^{13}C-tracing of acetate showed some drawbacks: the lack of purification and irregular peak shape of acetate-1TBDMS (**Fig. 12A**) on the GC spectrum could result in some isobaric interferences. Nevertheless, these new data were still in accordance with our

hypothesis, that most of the carbon originated from biomass and carried-over carbon compounds instead of the ^{13}C-enriched substrate. Overall, the ^{13}C tracing experiment hints that, similar to aerobic conditions, the gaP-ED route is most favorable for intracellular carbon uptake during anodic respiration, yet only half of the carbon are exogenous, suggesting that energy shortage as well as possible downstream regulation could also contribute as limiting factors. The 2kgaP pathway is less likely to contribute to carbon uptake, but to generate proton gradient for energy production throughout BES cultivation, as well as during exponential growth of aerobic culture. While it is also possible for the cell to use the glcP route under anaerobic conditions, the lower glucose uptake rate could have caused starvation, and hence, leading to degradation of internal storage carbon in order to compensate.

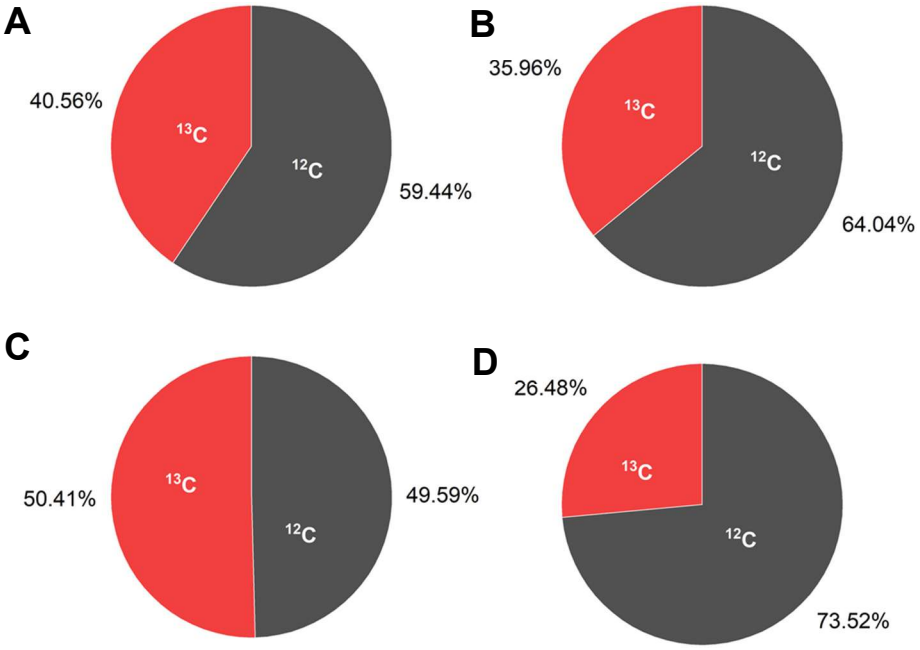

Figure 18. Summed fractional labelling of ^{12}C and ^{13}C of extracellular acetate under BES condition by (**A**) wild-type, (**B**) glcP, (**C**) gaP, and (**D**) 2kgaP strains. Figure was reproduced from a publication by Pause, et al. [278].

5.2. Periplasmic oxidation of aldoses by *Pseudomonas putida*

5.2.1. Aerobic oxidation of galactose and arabinose

P. putida KT2440 grew aerobically in neither D-galactose nor L-arabinose, as no increase in cell density was observed over 3 to 7 days of cultivation. However, measurement of D-galactose and L-arabinose concentration in the medium showed that both sugars had been consumed (**Fig. 19A-B**). The aerobic consumption rates of galactose and arabinose were -13.2 and -10.2 mmol g_{CDW}^{-1} h^{-1}, respectively. GC-MS analysis of the culture supernatant over

time showed that these sugars were oxidized to their corresponding aldonic acids, and while *P. putida* KT2440 only oxidized arabinose to one sugar acid product (i.e., arabinonic acid), both galactonic acid and 2-keto galactonic acid were found in the galactose cultures. No other sugars or sugar acids were detected (**Fig. 19C-D**).

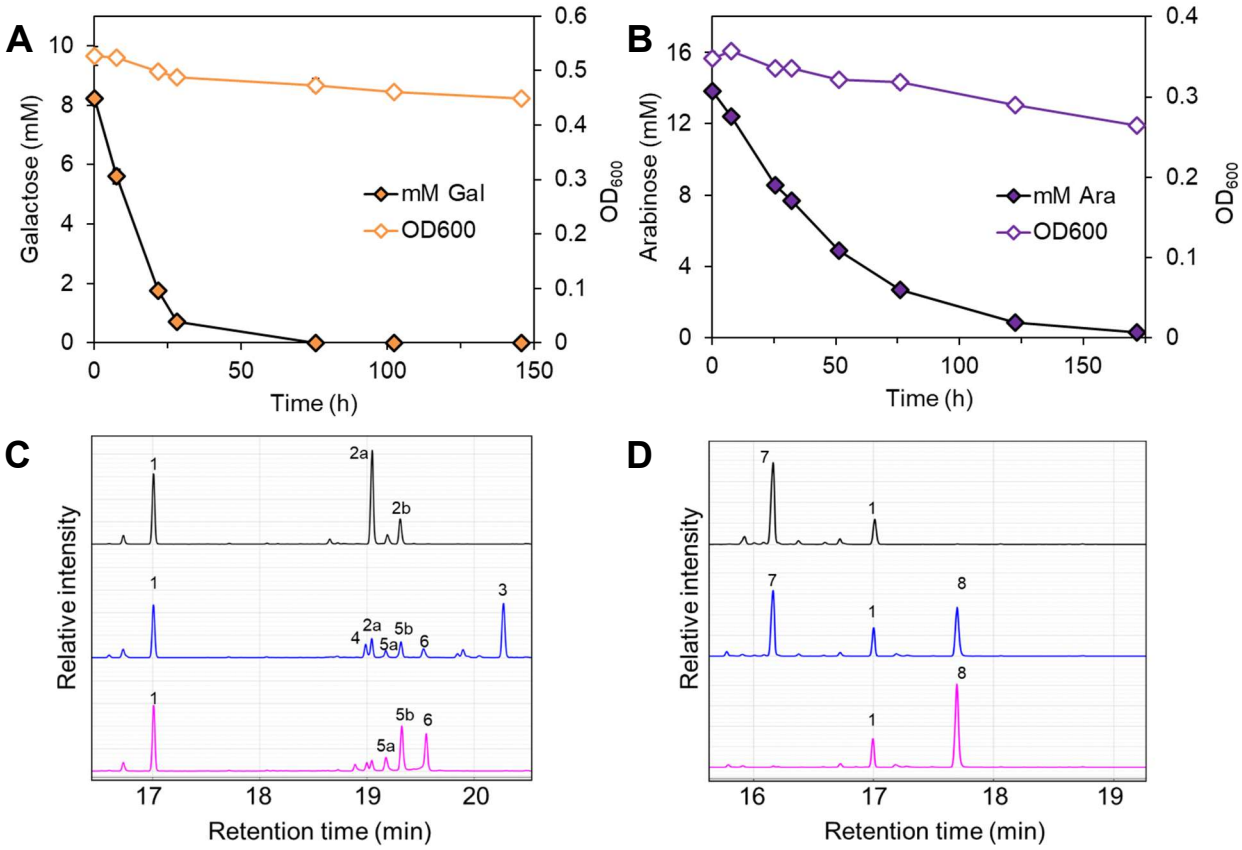

Figure 19. Aerobic oxidation of D-galactose and L-arabinose by *P. putida* KT2440. Sugar concentration and optical density of KT2440 when cultivated in (**A**) D-galactose and (**B**) L-arabinose; data are averages of biological triplicates, error bar on each data point represents the standard deviation of the sample mean (n=3). GC-MS analysis of extracellular metabolites at the beginning (black line), one day after inoculation (blue line) and at the end (magenta line) of the cultures in (**C**) D-galactose and (**D**) L-arabinose; peak **1**, adonitol-5TMS (internal standard), **2a,b**, galactose-1MOX-5TMS; **3**, galactonic acid-6TMS; **4**, galactono-1,4-lactone-4TMS; **5a,b**, 2-keto galactonic acid-1MOX-5TMS; **6**, 2-keto galactonic acid-5TMS; **7**, arabinose-1MOX-4TMS; **8**, arabinonic acid-5TMS.

5.2.2. Oxidation of aldohexoses and aldopentoses in BES

Under BES condition, in which the anode provided a surface to deposit electrons and where the electrode potential and current between the electrodes were continuously monitored, WT *P. putida* KT2440 cultures fed with D-glucose produced the highest peak current, followed by cultures with D-galactose, L-arabinose or D-ribose (**Fig. 20A**), yet no cell growth was detected

in any of the cultures (**Appendix D**). Concurrent with the current generation, sugars were consumed gradually over time (**Fig. 20C**), with glucose and galactose being oxidized at a similar rate, followed by arabinose and then ribose. The sugars' corresponding aldonates and 2-ketoaldonates were subsequently identified by GC-MS as the main end-products. Similar to the aerobic cultures, all tested sugars were also oxidized to their corresponding aldonic acids (all aldoses) and 2-keto aldonic acids (only aldohexoses, except for mannose, see section 5.3) (**Fig. 21**). Compared to the WT strain, the glucose dehydrogenase knockout mutant (Δ*gcd*) showed significantly lower current outputs in BES when either D-glucose, D-galactose or L-arabinose was fed (**Fig. 20B**). Sugar consumption rates were also significantly decreased (**Fig. 20D**), except for ribose. HPLC analyses of the respective samples also showed that in Δ*gcd* the UV absorption spectra corresponding to aldonates and 2-ketoaldonates were reduced or absent, compared to in WT strain.

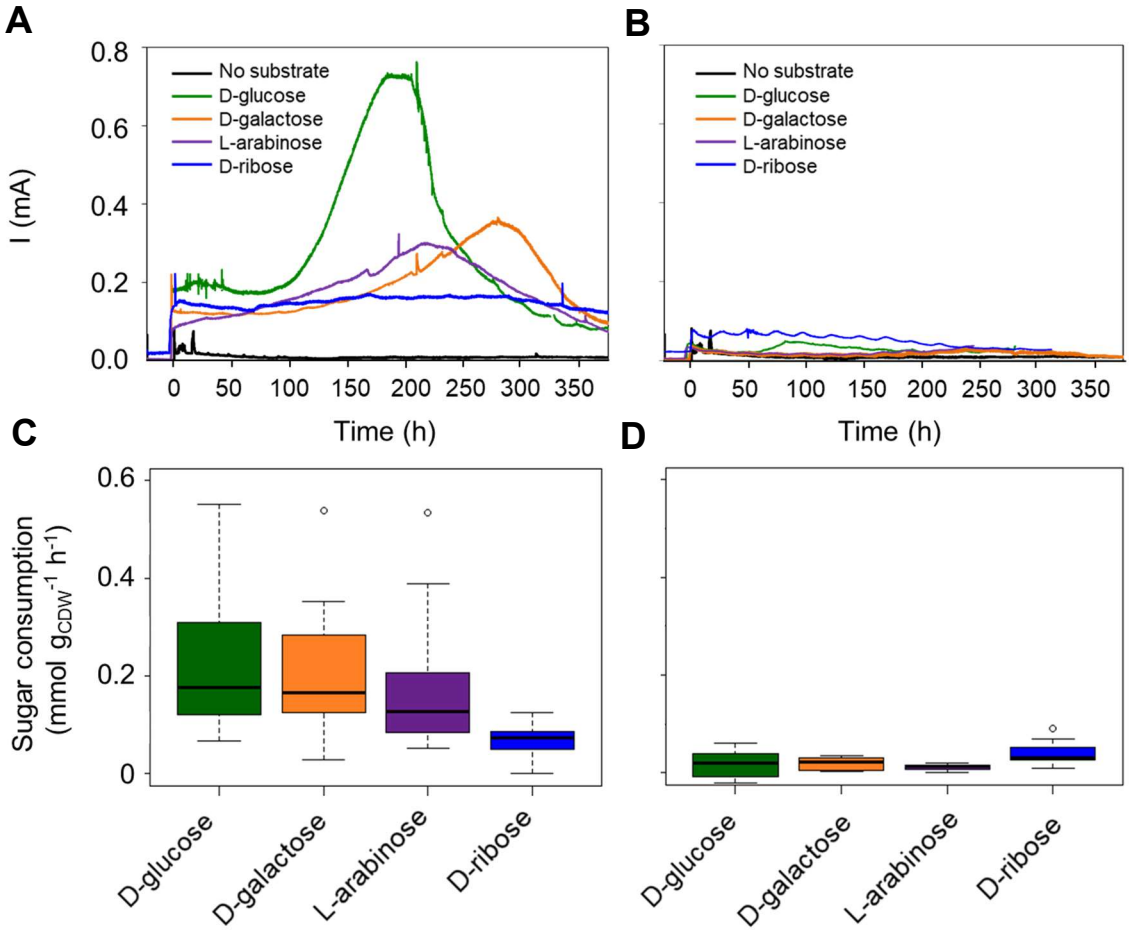

Figure 20. Comparative performance of *P. putida* KT2440 wild-type and Δ*gcd* in BES with different aldose substrates. Current densities of (**A**) KT2440 and (**B**) KT2440Δ*gcd* cultures in BES with various aldoses (n=1) versus no-substrate control (n=1), and box plots of the sugar consumption rate per g_{CDW} per hour of (**C**) wild-type and (**D**) Δ*gcd* between at least six sampling points during BES cultivation of each sugar (n ≥ 5). For each box plot, whiskers indicate values outside the upper and lower quartiles; outliers are plotted as individual points.

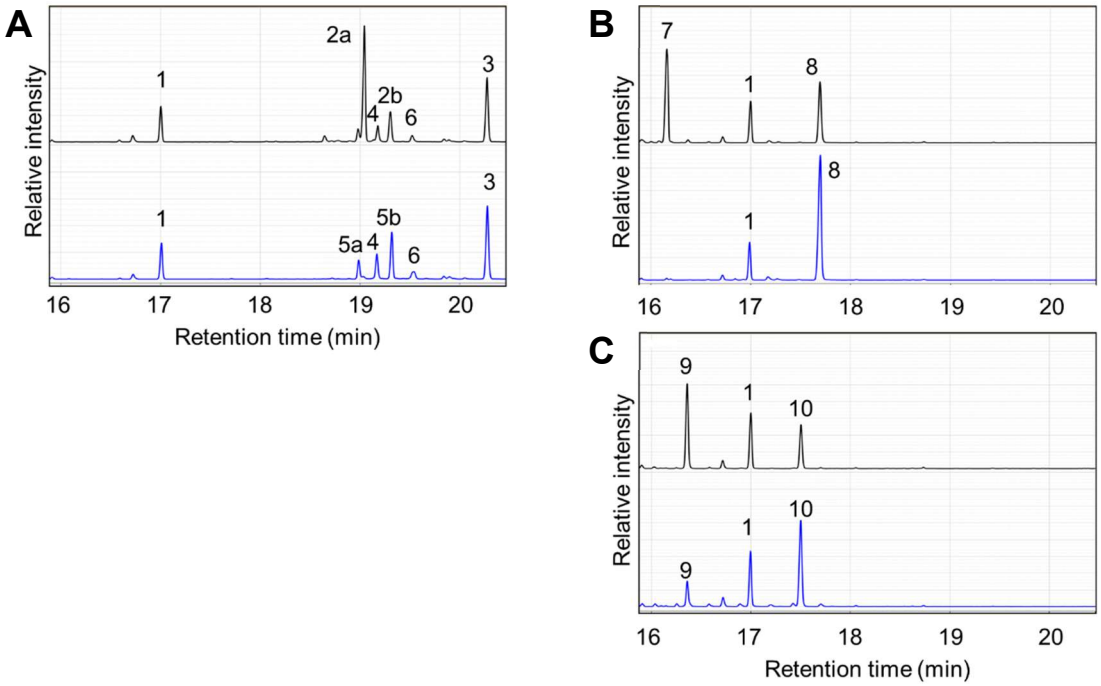

Figure 21. GC-MS analysis of extracellular metabolite composition of KT2440 culture in (**A**) D-galactose, (**B**) L-arabinose, and (**C**) D-ribose approximately 200 hours after inoculation (black line) and at the end (blue line) of the BES experiments. Peak **1**, adonitol-5TMS (internal standard); **2a,b**, D-galactose-1MOX-5TMS; **3**, D-galactonic acid-6TMS; **4**, D-galactono-1,4-lactone-4TMS; **5a**,**b**, 2-keto D-galactonic acid-1MOX-5TMS; **6**, 2-keto D-galactonic acid-5TMS; **7**, L-arabinose-1MOX-4TMS; **8**, L-arabinonic acid-5TMS; **9**, D-ribose-1MOX-4TMS; **10**, D-ribonic acid-5TMS.

5.2.3. Discussion

So far, our results suggested that *P. putida* was able to metabolize a wide range of monosaccharides, although not all of them were able to promote its growth. As a rhizosphere dweller, *P. putida* might encounter many different plant-based carbohydrates, including D-glucose, D-galactose and L-arabinose, which were found predominantly in cellulosic and hemicellulosic hydrolysates, and lignocellulosic biomasses [170, 279, 280]. In order to find a suitable substrate that could stir up intracellular carbon metabolism, several monosaccharides have been tested, including sugars that cannot be taken up and metabolized intracellularly in KT2440 such as D-galactose and L-arabinose, yet are consumed and generate current under both aerobic and BES condition (**Fig. 19, 20**). The extracellular metabolites measured by GC-MS demonstrated the production of aldonates, and, in some cases, 2-keto aldonates corresponding to each sugar (**Fig. 19C-D**, **21**): these were very similar to the case of glucose in BES, where gluconate (GA) and 2-ketogluconate (2KGA) were produced [30, 31]. Our evidences suggest that KT2440's Gcd is able to act widely on the C-1 position of aldose sugars, while Gad might have specificities toward 6-carbon aldonates. Similar results were found when KT2440 and other *P. putida* strains were fed with D-xylose, which was converted

to the dead-end D-xylonate [169, 281, 282]. It is possible that, in its natural habitats where various sugars are present, this feature benefits *P. putida* by generating additional energy from available resources when biomass-building sugars are absent. Hence, this offers a potential in bioproduction of different value-added sugar acids and their lactones, while employing a single catalytic system. In this particular work, however, it poses a challenge for unraveling intracellular metabolism of KT2440, since (i) it has been demonstrated that carbon flow was redirected toward POC, and so far, (ii) there is a lack of evidence suggesting that KT2440 cells can utilize sugar acids other than GA and 2KGA, or carbohydrates except glucose, fructose and ribose, as substrates without genetic engineering.

5.3. Metabolism of fructose by *Pseudomonas putida* under BES condition

In previous sections, it was demonstrated that utilizing aldose sugars poses a challenge for unraveling the cytoplasmic metabolism of KT2440 under the BES conditions, because the carbon flux was redirected toward POC in comparison with aerobic conditions, and so far, there is a lack of evidence of strain KT2440 utilizing sugar acids other than GA and 2KGA, or carbohydrates other than glucose/mannose, fructose and ribose, for growth. Nonetheless, achieving cytoplasmic metabolism is necessary to pinpoint the limitation in central carbon metabolism under BES conditions. For this reason, the following chapter focused on fructose as the substrate for the BES cultivation, for two reasons: (i) with fructose catabolism, more carbon is channeled toward NADPH-regenerating pathways, through which the hypothesized redox imbalance was anticipated to be overcome [109], (ii) this ketose has a completely different functional group compared to previously tested sugars, and (iii) KT2440 has a specialized PTS for its uptake [110]. The PTS system is not NAD(P)H-dependent, a metabolic constraint assumed previously for *P. putida* F1 on glucose under BES conditions [30]. Here, the bioelectrochemical performance of the WT strain was assessed alongside analysis of the metabolites in the medium, then compared with strain Δ*gcd* [283].

5.3.1. Bioelectrochemical performance

A similar decrease in planktonic biomass of WT and Δ*gcd* culture (Student's t-test yielded p-values > 0.05 at all sampling points) was accompanied by a respective consumption of 0.97 ± 0.13 and 0.62 ± 0.11 mmol of fructose (**Fig. 22A**). Interestingly, the WT strain produced in total 1.98 ± 0.46 mmol of electrons in comparison with only 0.34 ± 0.04 mmol of electrons for KT2440Δ*gcd*. At the same time, the observed pH drop in the medium was also steeper in the WT strain compared to Δ*gcd* (**Fig. 22D-F**). The Gcd, and hence POC, was involved in fructose metabolism, although the current output in *P. putida* Δ*gcd* mutant indicated a second metabolic pathway existing as well, as more electrons were produced during the first 244 h

compared to the background current. To clarify the nature of POC for fructose metabolism, the extracellular metabolites of the WT and Δ*gcd* cultures were analyzed with GC-MS (**Fig. 23**). In the WT cultures, mannonate – a stereoisomer at the C-2 position of GA – was found as the sole extracellular aldonate, while in the Δ*gcd* cultures, mannose was detected instead of mannonate. The WT strain produced 0.87 ± 0.09 mmol mannonate, and Δ*gcd* produced 0.51 ± 0.02 mmol of mannose. A constant mannose level in Δ*gcd* cultures after 244 h was observed, whereas mannonate continued to build up in WT cultures (**Fig. 22E-F**).

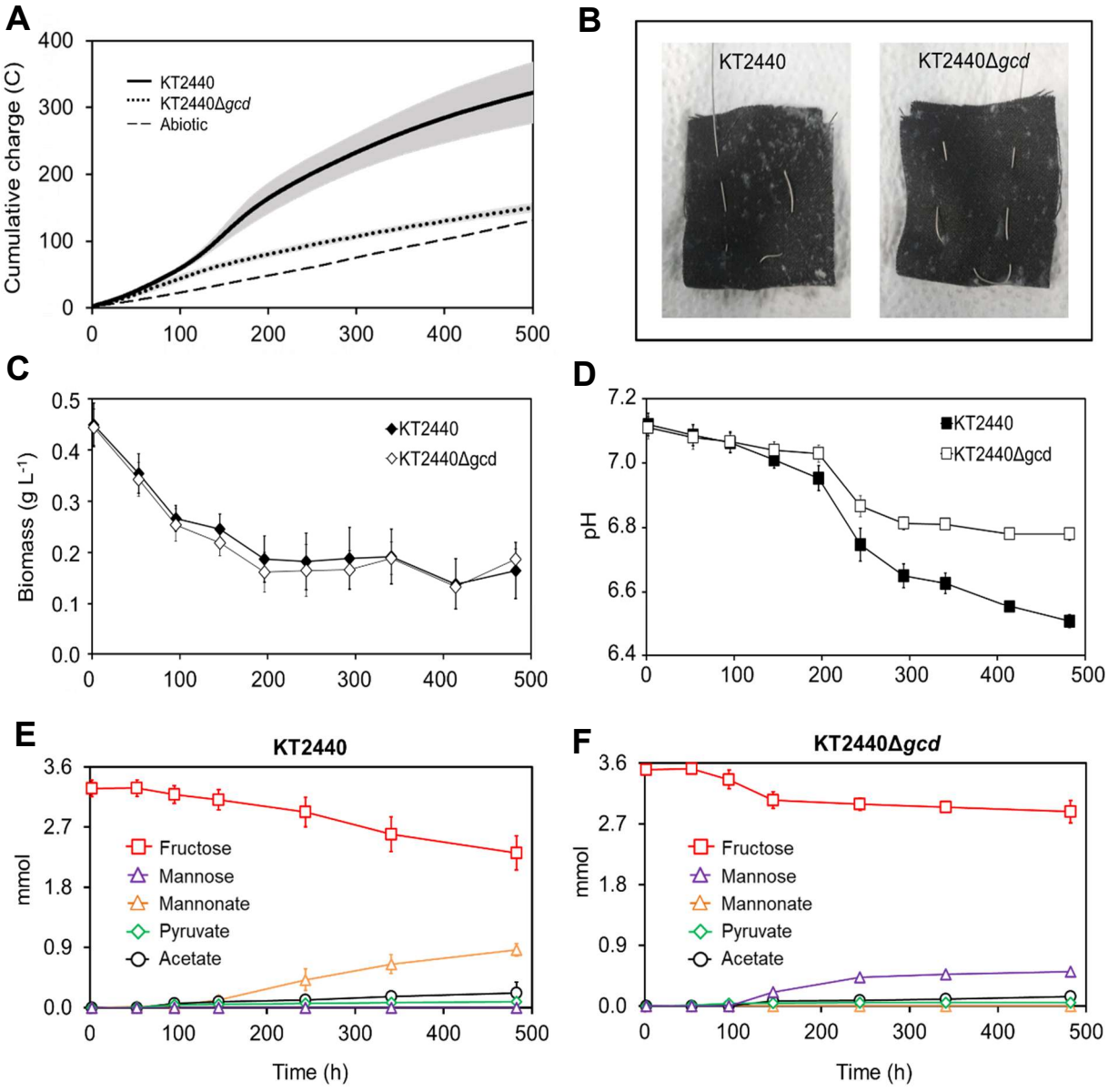

Figure 22. Comparative performance of *P. putida* KT2440 wild-type and Δ*gcd* in BES with fructose as substrate. (**A**) Cumulative charge (solid line) versus no-cell control (n=1, dot line); (**B**) adsorption of biomass on anode's surface; (**C**) planktonic biomass; (**D**) change in medium pH; absolute amount of fructose, mannose, mannonate (orange), pyruvate (black square), and acetate level of wild-type (**E**, n=3) and Δ*gcd* (**F**, n=3) during BES cultivation with fructose as substrate. Data are averages of biological triplicates; gray areas/error bars represent the standard deviation of the sample mean.

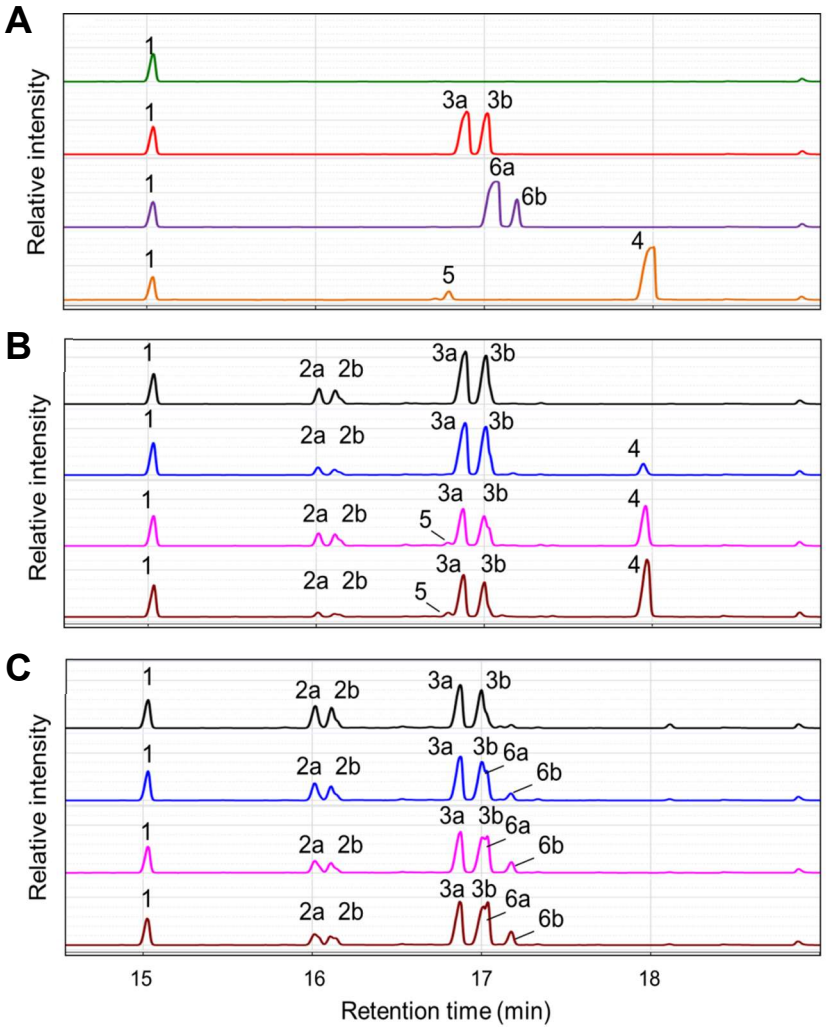

Figure 23. GC-MS analysis of *P. putida*'s extracellular sugars and sugar acids during BES cultivation with fructose. (**A**) Standard compound identification (green, adonitol; red, D-fructose; purple, D-mannose; orange, D-mannonate) and analysis of extracellular metabolite composition of (**B**) wild-type and (**C**) Δ*gcd* BES cultures at t=2 h (black line), t=146 h (blue line), t = 340 h (magenta line) and t = 480 h (brown line). Peak **1**, adonitol-5TMS (internal standard); **2a**,**b**, fructofuranose-5TMS; **3a**,**b**, D-fructose-1MOX-5TMS; **4**, D-mannonic acid-6TMS; **5**, D-mannono-1,4-lactone-4TMS; **6a**,**b**, D-mannose-1MOX-5TMS.

5.3.2. Extracellular metabolic profile

In addition to the POC discussed above, a second metabolic pathway might be present to catabolize fructose in BES, indicated by both the current output and the pH drop for the *P. putida* KT2440Δ*gcd*. The carbon balance was closed under the assumption that per mol acetate formed one mol of CO_2 was produced. This is an acceptable assumption for hexose metabolism to acetate in *P. putida* since decarboxylation is expected [30]. Because planktonic biomass decreased over time and no significant amount of biomass formation was observed on the electrode surface (**Fig. 22A**), biomass was omitted from the calculation. Product yields

and specific rates were calculated using the average planktonic biomass concentration throughout the processes. Interestingly, the WT strain consumed fructose twice as fast compared to its Δ*gcd* counterpart. $Y_{mannose}$ and $r_{mannose}$ were undetermined for the WT strain as mannose was not detectable in these cultures (**Table 8**). Regarding the electron fluxes, 87.6% of the measured electrons were associated with the POC activity for WT (with an estimation of 1.7 ± 0.2 mmol of electron released from fructose oxidation to mannonate, in comparison with 2.0 ± 0.5 mmol of captured electrons). On the other hand, the amounts of electrons produced by Δ*gcd* by an unidentified, pathway were 0.34 ± 0.04 mmol during the first 244 h, since the isomerization between fructose and mannose would not generate electrons.

Table 8. Process parameters of anoxic fructose conversion of *P. putida* KT2440 wild-type and Δ*gcd* in BES reactors. Data are average from biological triplicates (n=3); the values are depicted as "mean ± standard deviation of the sample mean".

	KT2440	KT2440Δ*gcd*
CB (%)	101.9 ± 1.7	102.4 ± 3.3
CE (%)	85.0 ± 5.4	93.5 ± 18.0 [a]
Yield ($mol_{product}$ $mol_{fructose}^{-1}$)		
$Y_{mannose}$	ND	0.820 ± 0.130
$Y_{mannonate}$	0.934 ± 0.127	0
$Y_{acetate}$	0.192 ± 0.102	0.204 ± 0.035
$Y_{pyruvate}$	0.079 ± 0.018	0.073 ± 0.028
Rate (μmol g_{CDW}^{-1} h^{-1})		
$r_{fructose}$	-24.05 ± 4.06	-11.95 ± 3.18
$r_{mannose}$	ND	9.69 ± 2.27
$r_{mannonate}$	22.77 ± 6.63	0
$r_{acetate}$	4.34 ± 1.48	2.46 ± 0.84
$r_{pyruvate}$	1.86 ± 0.29	0.86 ± 0.34

[a] Value determined at 244 h after inoculation; ND, not determined.

5.3.3. Impact of fructose metabolism on the energy and redox status of the cell

To investigate how fructose uptake and utilization affected the energy and redox status of the cell under BES conditions, the ATP/ADP and the NAD(P)H/$NAD(P)^+$ ratios were measured using protocol similar to Lai, et al. (2016) [30]. ATP/ADP ratio of KT2440 in BES was 3.6-times

lower compared to that of *P. putida* F1 in BES (**Table 9**). Furthermore, the ATP/ADP ratio of KT2440 was also more than twice as high as that of strain KT2440Δ*gcd*. Regarding the redox ratios, when KT2440 was cultivated in BES with fructose, NADPH/NADP$^+$ increased throughout the cultivation. The NADPH/NADP$^+$ value at around 170 hours after inoculation (which was approximately 24 h after peak current was reached) was around 8-fold higher compared to that of strain F1 cultivated on glucose at peak current. In contrast, the NAD pool was found to shift more toward the oxidized form when the cells were fed with fructose in BES, differing from a relatively stable NADH/NAD$^+$ ratio when glucose was fed (**Fig. 24**).

Table 9. Comparison of energy and redox ratios of *P. putida* cultivated in anoxic conditions. Data are average from biological triplicates (n=3); the values are depicted as "mean ± standard deviation of the sample mean".

Strain	Substrate	Condition	ATP/ADP (mol mol^{-1})	NADH/NAD$^+$ (mol mol^{-1})	NADPH/NADP$^+$ (mol mol^{-1})	Reference
F1	Glucose	Anaerobic [a]	2.37	0.22	0.09	[30]
		Anaerobic [b]	4.18	0.20	0.18	
		BES, peak current	3.73	0.22	0.08	
KT2440	Fructose	BES, peak current	1.04 ± 0.53	0.07 ± 0.01	0.49 ± 0.06	This study
KT2440 Δ*gcd*	Fructose	BES, peak current	0.50 ± 0.13	ND	ND	This study

[a] without ferricyanide, [b] with ferricyanide; ND, not determined.

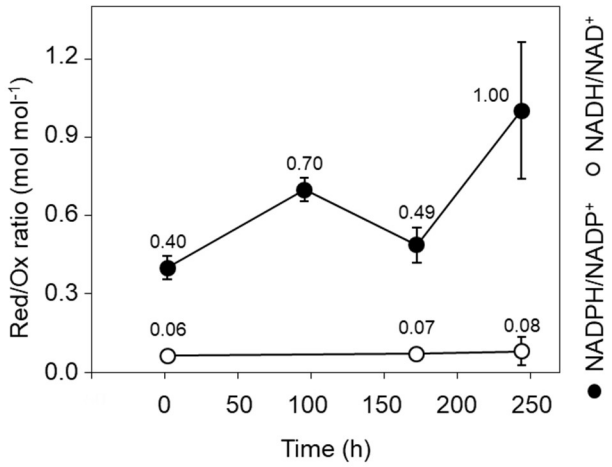

Figure 24. NADPH/NADP$^+$ and NADH/NAD$^+$ ratios of *P. putida* KT2440 cell extracts over the course of their BES cultivation. Data are the average of three biological replicates; error bars represent the standard deviation of the sample mean (n=3).

5.3.4. Proteomics of Pseudomonas putida under anaerobic cultivation

5.3.4.1. Overview

To explore the effect of anaerobic metabolism, protein expression of strain KT2440 during BES and open-circuit (OC) cultivation using fructose was investigated. In total, 2377 different proteins were detected across all samples, covering 43.5% of the predicted open reading frames in KT2440 [68, 69]. The threshold for expression fold change and p-value were 2 and 0.05, respectively, i.e., expressions increasing or decreasing by more than 2 times, in comparison with the reference point t_0, were considered significant. Normalized data from 146 h (peak current, t_1) and 414 h (t_2) after inoculation (**Fig. 25A**) showed that 479 and 212 proteins were significantly upregulated, and 56 and 95 proteins were significantly downregulated, respectively, compared to cultures at the time of inoculation (t_0) (**Fig. 25B-C**). Proteins that could not be quantified at all time points were excluded from the volcano plots as their normalized-to-t_0 log fold change could not be calculated. This affected on the one hand 200 and 393 proteins at t_1 and t_2, respectively, which could not be quantified for t_0, and on the other hand 348 and 276 t_0 proteins which could not be quantified at t_1 and t_2, respectively. Similarly, an OC experiment (i.e., no potential applied on the anode) with two biological replicates were conducted as control, resulting in 1753 different proteins detected across all samples; only 7 and 15 proteins were upregulated, and 90 and 62 proteins were downregulated at the respective sampling points of the BES experiment (**Fig. 25D-E**).

To further differentiate proteins with highly significant change during the cultivations, arbitrary lines were drawn between the points $\log_2(FC) = \pm 3.0$ (or $FC = \pm 8$) and $-\log_{10}(\text{p-value}) = 3.0$ (or p-value = 0.001) to highlight the extreme dots on the volcano plots. The proteins with the expression change outside of this area in the upper left and upper right areas of the graph (i.e., with very significant changes, which is defined here as having very high fold change and/or very high statistical significance) are listed in the **Appendices E** and **F**. 17 and 13 proteins with highly significant upregulation at t_1 and t_2, respectively, were found during BES cultivation, against only two proteins during OC mode; 16 of which involved in compound or macromolecule catabolism/biosynthesis. Other functions include cellular structure (1), membrane transport (7), signaling/regulating (2), and electron transfer (4). On the other hand, 48 and 31 proteins were found with highly significant downregulation during BES and OC cultivation, respectively; many structural proteins from these lists were ribosomal proteins, and 5 enzymes were involved in the central carbon metabolism during OC mode.

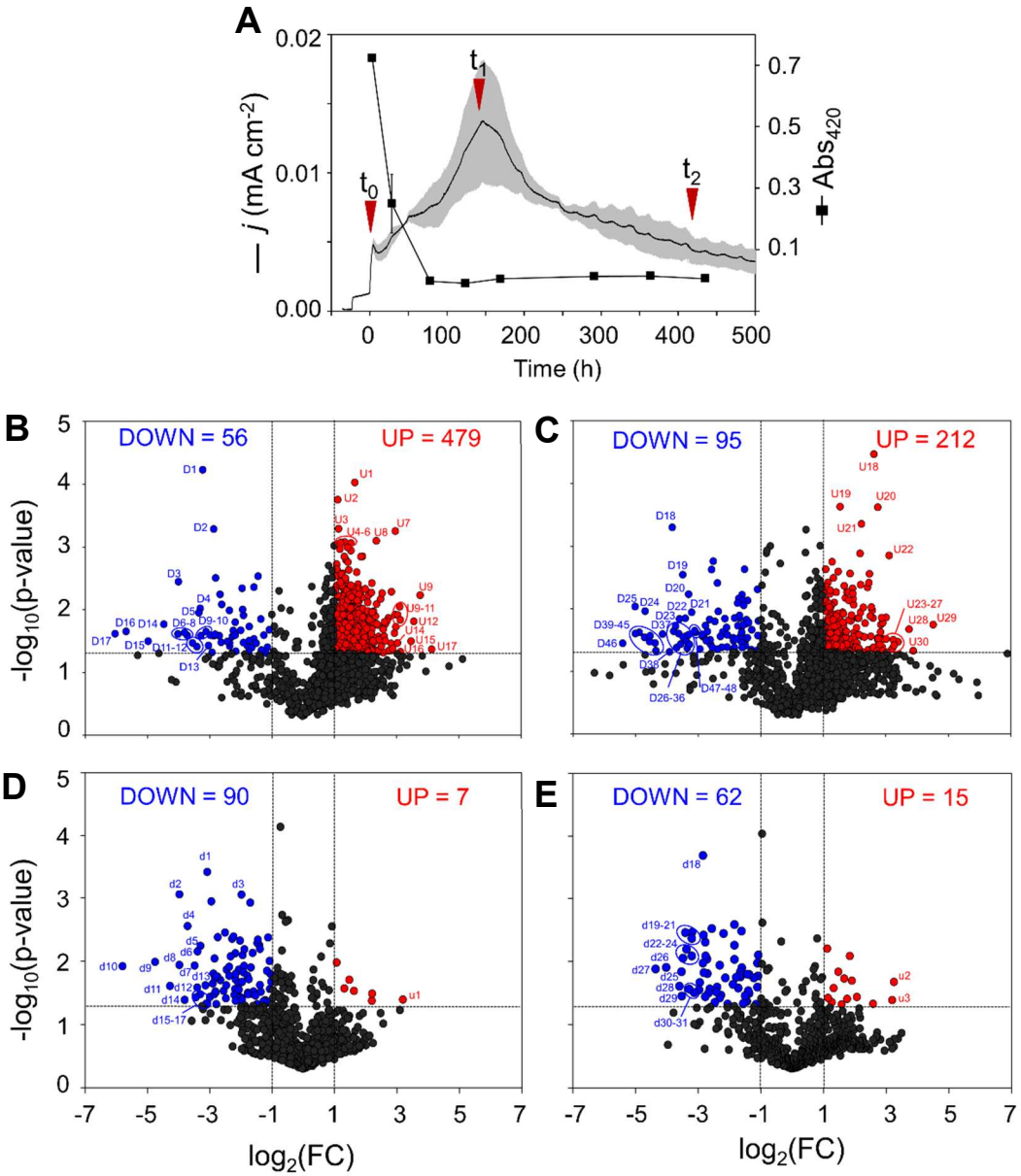

Figure 25. Relative differences in abundances of detected proteins in *P. putida* under different anaerobic cultivation setups. (**A**) The current density of KT2440 cultures (n=3) observed during BES cultivation with 2 g L^{-1} fructose and three sampling points for proteomics; KT2440 cultures (n=2) with OC setting were simultaneously sampled at the same time points, using the absorbance (Abs_{420}) of ferricyanide as an indicator of substrate oxidation. Data are averages of biological replicates; gray area and error bars represent the standard deviations of the sample mean. Volcano plots of KT2440's proteome during BES cultivation with fructose at t_1 versus t_0 (**B**) and t_2 versus t_0 (**C**), and volcano plots of KT2440's proteome during OC cultivation with fructose at t_1 versus t_0 (**D**) and t_2 versus t_0 (**E**), were constructed. Blue, significantly downregulated; red, significantly upregulated; black dots, no significant change. Protein with highly significant change (i.e., $log_2(FC) = \pm 3.0$ (or FC = ± 8) and/or $-log_{10}$(p-value) = 3.0 (or p-value = 0.001) are highlighted; during BES cultivation: U1-30, highly significantly upregulated, D1-48, highly significantly downregulated; during OC cultivation: u1-3, highly significantly upregulated, d1-31, highly significantly downregulated.

In relation to the second objective this dissertation, which concerns the physiological changes of the cell (e.g., carbon metabolism and respiration) during electrochemically mediated oxidation of sugar, the proteins of the central carbon metabolism and electron transport chain are further investigated in depth. Moreover, as the transport of redox mediator across the outer membrane is hypothesized to be linked to the cell's ability to import of iron and iron-based compound, TonB complex and TBDTs are also evaluated (Objective 3).

5.3.4.2. Central carbon metabolism

The expression of proteins from the peripheral oxidation pathway, glycolytic pathways of the ED-EMP cycle, substrate-level phosphorylation, pyruvate dehydrogenase complex, TCA cycle, glyoxylate shunt, and several anaplerotic reactions associated with the central carbon metabolism in KT2440 were analyzed in detail (**Table 10**). Overall, protein expression tended to decrease overtime; however, upregulation of protein in the central carbon metabolism was found mostly during the BES experiment (especially at peak current) in contrary to the OC experiment, where the majority of the proteins from the central carbon metabolism did not show a significant increase in expression, with the exception of glucose 6-phosphate isomerase (Pgi-1) and the acetyltransferase component of pyruvate dehydrogenase complex (AceF).

While many enzymes of glycolysis were downregulated during BES cultivation, the majority of the proteins from the lower central carbon metabolism (i.e., pathways that follow the metabolite glyceraldehyde 3-phosphate) were increased in expression level. More specifically, the TCA cycle was mostly either upregulated or made no significant change during the BES cultivation, especially at peak current, with a few exceptions such as phosphoglycerate kinase (Pgk), isocitrate dehydrogenase (Idh), malate synthase (GlcB), and malic enzyme B (MaeB), which were downregulated. Proteins responsible for fructose metabolism were also found to be either upregulated or have no significant change in expression over time. Surprisingly, the Gcd was the only protein from the peripheral oxidation pathway that was found to be upregulated at both t_1 and t_2 and was one of the only two peripheral oxidation pathway proteins detected in all of the samples; the other was the cytoplasmic gluconate kinase, GnuK, which did show significant change at neither t_1 nor t_2

.

Table 10. Changes in protein expression of the central carbon metabolism in *P. putida* KT2440 during bioelectrochemical (BES, n=3) and open-circuit (OC, n=2) cultivation in fructose. t_1, at peak current; t_2, 414 h after inoculation. Red, upregulated; blue, downregulated, black, not significantly changed; blank box, undefined ratio due to insufficient data; the number in each box indicates the $\log_2$(FC) value.

Pathway	Protein	Locus tag	BES		OC	
			t_1	t_2	t_1	t_2
Fructose uptake	Fructose PTS permease	FruA	0.765	0.252	-0.234	0.067
	Phosphocarrier protein HPr	FruB	1.116	1.700	0.048	-0.655
	1-phosphofructokinase	FruK	0.896	0.283	-0.874	
Fructose/ mannose interconversion	Aldose-ketose isomerase	YihS	0.860	-0.451		
	Mannose-6-phosphate isomerase/mannose-1-phosphate guanylyltransferase	AlgA				
		PP_1776	0.994	-1.042		
		PP_4860				
Glucose/ mannose transport	Periplasmic binding protein	GtsA	-1.994	-4.133	-1.630	-1.730
	Permease	GtsBC				
	ATP-binding subunit	GtsD	2.280	1.358	0.211	-0.364
Peripheral oxidation	Glucose dehydrogenase	Gcd	1.334	1.075	-0.989	-1.881
	Gluconate transporter	GntT				
		PP_0625				
	Gluconate kinase	GnuK	0.674	1.156		
	Gluconate dehydrogenase complex (Gad)	PP_3382				
		PP_3383				
		PP_3384				
	2KGA transporter	KguT				
	2KGA kinase	KguK				
	2KGA 6-phosphate reductase	KguD				
Embden-Meyerhof-Parnas	Glucokinase	Glk	0.131	0.854	-1.361	-0.954
	G6P isomerase	Pgi-1			1.366	1.907
		Pgi-2	1.202	0.924	-0.513	
	F16Pase	Fbp		3.267		
	F16P aldolase	Fba	0.207	-1.579	-1.128	-1.646
	Triose phosphate isomerase	TpiA		-4.528	-0.852	
Pentose phosphate	6PG dehydrogenase	GntZ	0.174	-1.417	-1.064	
	RL5P 3-epimerase	Rpe				
	R5P isomerase A	RpiA		0.121		
	Transketolase	TktA	1.106	0.137	-0.626	-2.388
	Transaldolase	Tal	-1.594	-1.291	-1.735	
Entner-Doudoroff	G6P 1-dehydrogenase	Zwf1	1.009	0.126	-0.380	
		Zwf2	1.681	-0.093		
		Zwf3				
	6-phosphogluconolactonase	Pgl	-2.233	-3.078	-2.376	-1.833
	6PG dehydratase	Edd	0.982	1.015	-0.965	
	KDPG aldolase	Eda	-1.410	-1.833	-1.028	-3.366
Substrate-level phosphorylation	GA3P dehydrogenases	GapA	0.148	0.362	-0.702	-3.191
		GapB	1.080	1.090	0.289	0.732
		PP_0665				
		PP_3443	1.185	0.498	-0.055	-0.825
	Phosphoglycerate kinase	Pgk	-3.297	-2.350	-2.114	-3.087
	Phosphoglycerate mutase	Pgm	-0.432		-1.824	
		PP_2243				
		PP_3923				
		PP_4450				

	Enolase	Eno	-0.902	-0.745	-1.516	-4.357
	Pyruvate kinase	PykA	1.271	0.632	-0.776	-2.107
		Pyk				
Link reaction	Pyruvate dehydrogenase complex	AceE	1.020	1.432	0.001	0.871
		AceF	1.050	0.533	3.195	3.248
		AcoA				
		BkdB	1.677	0.764	0.369	0.924
		Lpd	-0.052	2.261	-1.800	
		LpdV	-0.620	0.493	-0.281	
Tricarboxylic acid cycle	Citrate synthase	GltA	0.959	0.676	0.332	-1.005
	Aconitate hydratase	AcnA-I	0.488	1.200	-0.960	
		AcnA-II	0.981	1.560	0.058	0.891
		AcnB	0.882	0.740	-0.635	-1.163
	Isocitrate dehydrogenase	Icd	-0.553	0.104	-0.815	-0.488
		Idh	-0.724	-1.863	2.279	-2.462
	2-ketoglutarate dehydrogenase complex	SucA	1.323	1.007	0.429	-0.414
		SucB	1.376	0.538	0.872	0.131
		PP_2652				
		PP_3662	1.955	2.250	1.710	0.974
		LpdG	1.160	0.631	-0.706	-0.828
	Succinyl coenzyme A synthetase	SucD	1.274	0.783	-0.016	-2.782
		SucC	1.137	0.670	-0.560	-2.188
	Succinate dehydrogenase complex	SdhB	1.374	1.982	0.579	-0.994
		SdhA	0.734	0.705	0.112	0.100
		SdhCD			0.112	
	Fumarate hydratase	FumC-I	1.120	0.567	0.146	-1.681
		FumC-II	1.025	-0.706	0.130	-0.502
		PP_0897	1.183	0.576	-0.298	0.222
	Malate dehydrogenase	Mdh	0.434			
		Mqo-1	1.720			
		Mqo-2				
		Mqo-3		-4.053		
Glyoxylate shunt	Isocitrate lyase	AceA	1.445	1.730	-0.167	0.810
	Malate synthase	GlcB	-3.040	-1.486		
Anaplerosis (Pyruvate shunt)	Malic enzyme B	MaeB	-0.634	-2.758	-1.206	-2.769
	PEP carboxylase	Ppc	1.048	0.240	-1.105	-0.208
	Oxaloacetate decarboxylase	PP_1389	0.704		-0.832	
	Pyruvate carboxylase	PycA	1.192	1.413	0.123	-1.462
		PycB	1.100	0.354	0.458	-0.883
Anaplerosis (Amino acid catabolism)	Glutamate synthase complex	GltB	1.454	1.572	0.647	0.408
		GltD	1.785	1.248	0.680	
		PP_1060				
	Glutamate dehydrogenase	GdhA				
		GdhB	1.321	1.608	0.560	1.612
	Aspartate ammonia-lyase	AspA	2.254	1.306		
	Aspartate aminotranferase	AspC				

2KGA, 2-ketogluconate; G6P, glucose 6-phosphate; F16P, fructose 1,6-bisphosphate; 6PG, 6-phospho-gluconate; KDPG, 2-keto-3-deoxy-6-phosphogluconate; RL5P, ribulose 5-phosphate; R5P, ribose 5-phosphate; GA3P, glyceraldehyde 3-phosphate; PEP, phosphoenolpyruvate

5.3.4.3. Electron transport chain

Similarly, comparative quantification of proteins of the electron transport chain was also carried out for the cells in both BES and OC cultivations (**Table 11**). Overall, a clear difference in the expression of complex I (NADH dehydrogenase/ubiquinone reductase), complex III (cytochrome c reductase), and complex V (ATP synthase) between the two conditions were observed. Whereas in OC mode protein expression of these complexes showed no significant change, complex I and III in BES cultivation showed significant upregulation throughout the experiment, and complex V exhibited high expression, especially at peak current in the BES reactor, then decreased as the current generation dropped. Complex II, as a part of the central carbon metabolism, was increased in expression only in BES as observed above (**Table 10**). Interestingly, in both experimental setups, complex IV (cytochrome c oxidases) and alternative oxidases (i.e., cytochrome bd ubiquinol oxidase, cytochrome o ubiquinol oxidase) were mostly not detected, or showed no change.

Table 11. Changes in protein expression of the electron transport chain in *P. putida* KT2440 during bioelectrochemical (BES, n=3) and open-circuit (OC, n=2) cultivation in fructose. t_1, at peak current; t_2, 414 h after inoculation. Red, upregulated; blue, downregulated, black, not significantly changed; blank box, undefined ratio due to insufficient data; the number in each box indicates the $\log_2$(FC) value.

Protein	Subunit	Locus tag	BES		OC	
			t_1	t_2	t_1	t_2
Complex I						
NADH dehydrogenase		Ndh		1.302		
Pyridine nucleotide-disulphide oxidoreductase family protein		PP_2867	1.955	2.150		
NADH-quinone oxidoreductase	Subunit A	NuoA				
	Subunit B	NuoB	1.330	0.220	1.284	2.014
	Subunit C/D	NuoCD	1.410	1.410	0.736	1.046
	Subunit E	NuoE				
	Subunit F	NuoF	1.797	1.739	-0.827	-0.976
	Subunit G	NuoG	1.468	0.840	0.851	1.408
	Subunit H	NuoH				
	Subunit I	NuoI	1.356	0.586	-0.044	1.897
	Subunit J	NuoJ				
	Subunit K	NuoK				
	Subunit L	NuoL				
	Subunit M	NuoM				
	Subunit N	NuoN				
Complex II						
Succinate dehydrogenase complex	Flavoprotein subunit	SdhA	0.734	0.705	0.579	-0.994
	Iron-sulfur subunit	SdhB	1.374	1.982	0.112	0.100
	Membrane subunit	SdhCD			0.112	
Complex III						
Ubiquinol-cytochrome c reductase	Iron-sulfur subunit	PetA	1.756	1.329	0.486	1.330
	Cytochrome b subunit	PetB			-0.866	0.244
	Cytochrome c1 subunit	PetC	1.600	1.844	0.673	1.911

		Complex IV				
Cytochrome c	Cytochrome c4	Cc		3.092		
	Putative cytochrome c5	PP_5267	0.392	-1.033	-1.454	
Cytochrome c oxidase	CyoE-like protoheme IX farnesyltransferase	PP_0110				
	Assembly protein subunit 11	PP_0105				
	Heme a synthase	PP_0109				
	Subunit 1	CtaD				
	Subunit 2	PP_0103	0.291	0.308	1.629	3.466
	Subunit 3	PP_0106				
Cytochrome c oxidase, cbb3-type	Subunit I	CcoN-I	1.412	2.052	-0.914	
		CcoN-II	0.691	0.939	-1.153	0.175
	Subunit II	CcoO-I				
		CcoO-II				
	Subunit IV	CcoQ-I				
		CcoQ-II				
	Subunit III	CcoP-I				
		CcoP-II	0.929	-0.084	-0.166	0.904
Cytochrome bd ubiquinol oxidase	Subunit I	CioA				
	Subunit II	CioB				
Cytochrome o ubiquinol oxidase	Subunit II	CyoA				
	Subunit I	CyoB				
	Subunit III	CyoC				
	Subunit IV	CyoD				
	Protoheme IX farnesyl-transferase 2	CyoE				
		Complex V				
ATP synthase	Subunit α	AtpA	1.102	0.588	0.489	1.528
	Subunit β	AtpD	1.078	0.770	0.142	0.063
	Subunit γ	AtpG	1.186	0.767	-0.357	-0.486
	Subunit δ	AtpH	0.824	0.147	-0.234	
	Subunit ε	AtpC	1.219	-0.150	-0.348	-1.645
	Subunit a	AtpB				
	Subunit b	AtpF	1.044	0.959	0.294	0.759
	Subunit c	AtpE				

5.3.5. Discussion

In the context of anodic respiration, organic acids are generally not favorable substrates, as more reducing power is required for *P. putida*'s cellular function with oxidized carbon compounds [284]. Furthermore, as we found out earlier, all aldoses were somewhat affected by the POC due to the broad specificity of its enzymes. Therefore, a non-aldose, reducing carbon source should be used. In the end, fructose was chosen as the carbon source. Fructose is a hexose with a keto-function at the C-2 position, which was thought to make it inaccessible for oxidation by Gcd. Instead, fructose is imported into the cytoplasm via PTS. This PTS transporter is encoded by the *fruBKA* operon in *P. putida* KT2440 [108-110]. It is also worth noting that, under aerobic conditions, the cells channel around 48% of the carbon through EMP and PP pathways when fed with fructose, compared to only ~4% with glucose. For this study, it was anticipated that this could help overcome the previously observed

decrease in NADPH/NADP$^+$ ratio in anaerobic *P. putida* culture by improving NADPH fluxes [82].

Proteomic analysis suggests that intracellular uptake of fructose was taking place, as demonstrated by the expression of the *fruBKA* operon and the putative GapDH PP_3443 in the BES experiment (**Table 10**, **Fig. 26**). Both loci are expressed under the modulation of fructose 1-phosphate – a cytoplasmic metabolite that can only be produced via the fructose PTS activity [108, 111]. At the same time, periplasmic oxidation activity was observed occurring during BES cultivation: fructose was unexpectedly metabolized to mannose, which then could be oxidized by Gcd. Since abiotic control experiments indicated that fructose was not abiotically converted to other sugars, in addition to the analysis of extracellular metabolites, fructose was hypothesized to be isomerized into mannose by the enzyme aldose-ketose isomerase (YihS), whose encoding gene locates next to (i.e., 110 base pairs upstream of) the glucose/mannose ABC transporter operon *gtsABCD* [68, 69]. YihS is found widely distributed in bacteria and possibly shares a similar mechanism of action as YihS in *Escherichia coli* and *Salmonella enterica* [285]. While YihS was not specifically upregulated, this protein was found in almost all replicates under BES conditions. It readily interconverts fructose and mannose, which can be further taken up by either PTS or ABC transporter system (**Fig. 3**). Mannose, as an aldose, could also be subjected to POC activity, in which an aldonate (i.e., mannonate) was subsequently produced (**Fig. 22E-F**). A significant increase in Gcd expression was observed throughout the BES cultivation of KT2440 (**Table 10**), which might have helped to maintain mannonate production. The reason behind its upregulation, nonetheless, remains unknown; as Gcd expression and its activity depend on several factors, such as the availability of sugar, oxygen, cAMP, soluble phosphate, and co-factor pyrroloquinoline quinone [100, 105], the explanation for this behavior, hence, might not be straight forward. No protein from the Gad complex and 2-ketogluconate uptake pathway was detected from the proteome analysis in either BES or OC control experiments, explaining the lack of the corresponding 2-ketoaldonate production in strain KT2440. Even if the Gad complex was present, it still might not be able to further oxidize mannonate due to the incorrect stereogenic center at the C-2 position compared to gluconate. This is unlike the case of galactose where both galactonate and 2-ketogalactonate were detected (**Fig. 19C, 21A**). It is possible that the cells of the galactose culture only expressed Gad-like behavior as a result of pre-culturing in glucose.

Multiple enzymes involving in the anaplerotic pyruvate shunt, which are responsible for the replenishment and interconversion of PEP and pyruvate, were found upregulated (**Fig. 26**). This could be another indication of fructose uptake, as the fructose PTS uses PEP as phosphoryl source (**Fig. 3**). The change in metabolism was indicated more clearly in the shift in NADPH/NADP$^+$ ratio not only at the peak current, but also throughout the BES cultivation.

In previous observations with BES cultivation of *P. putida* F1 with glucose, the NADP pool was found to be more oxidized, pointing at a limitation in NADPH-generating pathways [286]. This study with fructose, however, revealed the complete opposite phenomenon as NADPH/ $NADP^+$ ratio increased during the first 250 hours of the BES experiment, including at peak current (**Fig. 24**). One possible contributing factor was that 2-ketogluconate 6-phosphate reductase (KguD), which reduced 2-ketogluconate 6-phosphate to 6-phosphogluconate by consuming NADPH, might not be expressed, or, if so, inactive as a result of having fructose as substrate. The influence of this reaction on the overall NADP pool of the cell, nonetheless, remains to be elucidated.

Meanwhile, expression analysis of proteins involved in NADPH regeneration in the central carbon metabolism (Zwf, GntZ, GapDH, Icd, and Idh) and anaplerotic pathways (MaeB, GltBD) revealed that these proteins were either upregulated or remained the same when peak current was reached. On the other hand, even though many proteins involved in NADH regeneration in the central carbon metabolism (GapDH, 2-keto glutarate dehydrogenase complex, Mdh, Mqo, GdhB) were also found to be upregulated, the NADH pool became much more oxidized, in contrast to a higher NADH/NAD^+ ratio across different anaerobic cultivations of strain F1 on glucose (**Table 9**). As the expression of many of these enzymes is controlled by the global regulators modulated by intracellular redox state in strictly aerobic and facultatively anaerobic bacteria [287], the changes in protein expression of the TCA cycle enzymes might have been the result of cell response to the shifts in NAD(P)H/$NAD(P)^+$ ratios. Conversely, the proteomic data did not reflect enzymatic activities; thus, the full extent of protein expression's impact on internal redox ratios remained to be investigated. Interestingly, many anaplerotic, amino-acid-catabolizing enzymes were also found upregulated, resembling KT2440 cells under glucose starvation [277], suggesting that the cytoplasmic carbon flux from upstream fructose metabolism might still be insufficient to functionalize the TCA cycle (**Fig. 26**). This result implied that it would take more than just changing substrate in order to achieve cell growth under anaerobic conditions. Nonetheless, the systematic upregulation of proteins of the central carbon metabolism pathways proved that the combination of an available pool of electron acceptor (in this case, ferricyanide) and a substrate that the cell could take up (fructose) would be sufficient to recover some cellular activities for a period of time, at least at the protein expression level.

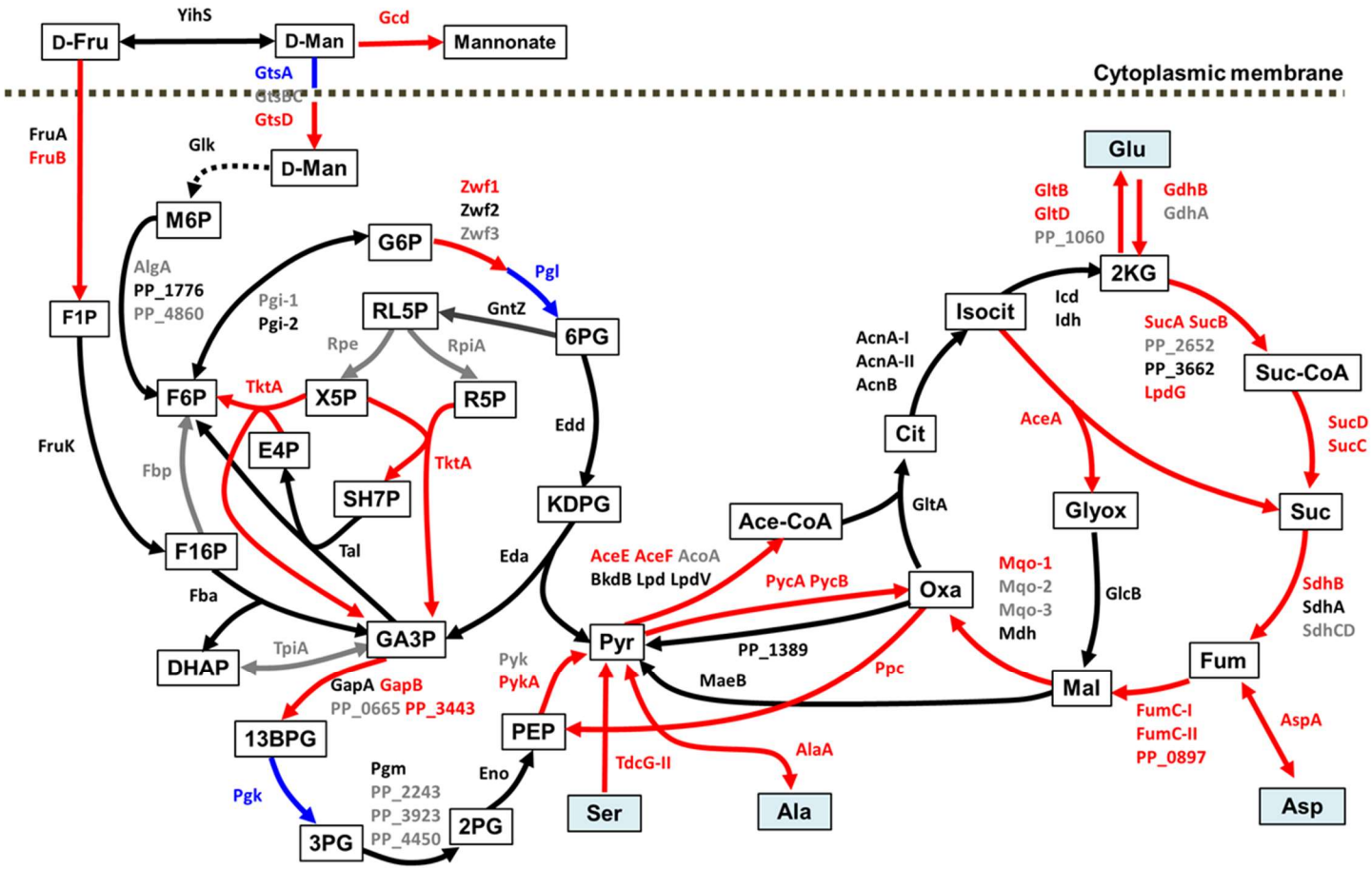

Figure 26. Changes in protein expression of the central carbon metabolism in *P. putida* KT2440 during bioelectrochemical cultivation in fructose at peak current (t_1/t_0). Red, upregulated; blue, downregulated, black, not significantly changed; gray, undetermined. D-Fru, fructose; F1P, fructose 1-phosphate; D-Man, mannose; M6P, mannose 6-phosphate; G6P, glucose 6-phosphate; F6P, fructose 6-phosphate; F16P, fructose 1,6-bisphosphate; DHAP, dihydroxyacetone phosphate; RL5P, ribulose 5-phosphate; 6PG, 6-phosphogluconate; KDPG, 2-dehydro-3-deoxy-phosphogluconate; GA3P, glyceraldehyde 3-phosphate; 13BPG, 1,3-bisphosphoglycerate; 3PG, 3-phosphoglycerate; 2PG, 2-phosphoglycerate; PEP, phosphoenolpyruvate; Pyr, pyruvate; Ace-CoA, acetyl coenzyme A; Cit, citrate; Isocit, isocitrate; 2KG, 2-ketoglutarate; Suc-CoA, Succinyl coenzyme A; Suc, succinate; Fum, fumarate; Mal, (L-)malate; Oxa, oxaloacetate; Glyox, glyoxylate; Ala, alanine; Asp, aspartate; Glu: glutamate; Ser, serine.

This was also further supported by comparing the expression of the electron transport chain between the polarized and unpolarized BES settings, as many proteins of complex I, complex II, complex III, and complex V, especially at the peak current of the BES reactor, showed significant upregulation (**Table 12**, **Fig. 27**). This result once again implies that *P. putida* could utilize ferricyanide as a substitute for an electron acceptor when oxygen is absent, and the provided electrode potential improved cellular respiration by maintaining the pool of oxidized mediators. More so, it is also in accordance with the prediction of Lai, et al. (2016) through flux balance analysis, that under BES cultivation the cell generates energy mainly via oxidative phosphorylation [30]. Interestingly, most of the protein subunits from cytochrome c oxidase, cytochrome bd ubiquinol oxidase, and cytochrome o ubiquinol oxidase were not detected, hinting that these complexes might not be as important to the respiration of *P. putida* under BES condition. This hypothesis is also supported by the hypothesis of Lai, et al. (2020), where ferricyanide interacted and harvested electrons from cytochrome c reductase and inhibition of complex IV does not affect the cell's anoxic respiration [45]. In any case, the absence of these proteins, or any other protein, in the dataset, should not be construed as a non-expression due to the inherent limitation of the dynamic exclusion filtering used with shotgun proteomics, as well as data-dependent acquisition (DDA) mode [288, 289]. Hence, further investigation will still be required to explain this change more thoroughly.

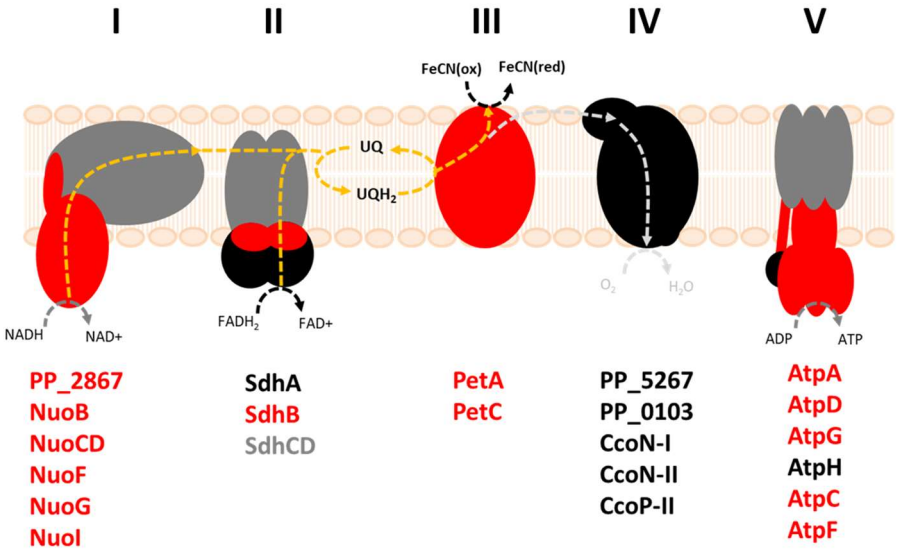

Figure 27. Changes in protein expression of the electron transport chain in *P. putida* KT2440 during bioelectrochemical cultivation in fructose at peak current (t_1/t_0). Red, upregulated; blue, downregulated, black, not significantly changed; gray, undetermined.

5.4. Inhibition of TonB decreases the bioelectrochemical activity of *Pseudomonas putida*

The third question to be tackled in this thesis is how the cells remove excess electrons from catabolic reactions in the absence of oxygen. Answering this question is important, as the limited mediator turnover in the periplasm could lead to a slower respiratory rate and a decrease in energy output. This includes: (i) from which respiratory complex the mediator removes the electrons, and (ii) how it crosses the outer membrane barrier to interact with said complex on the cytoplasmic membrane. A recent study conducted by Lai, et al. [45] showed that the artificial mediator ferricyanide might interact with cytochrome c reductase (complex III) in the electron transport chain of *P. putida*. To achieve this result, the authors employed an inhibitory study to examine which respiratory complex inhibition would lead to a decrease in current output. By adopting the rationale of this work, the following experiments were conducted, providing a proof-of-concept for the role of the TonB protein complex in ferricyanide uptake into the periplasm, and afterward, the first attempt to improve mediator flux via homologous overexpression of TonB in *P. putida*.

5.4.1. Effect of TonB inhibitors on P. putida's sugar catabolism under aerobic conditions

In this study, two putative TonB inhibitors found for *E. coli* CFT073 via high throughput screening [116] were acquired and tested on *P. putida* KT2440. The compounds were 2-(((3-chloro-4-methoxyphenyl)amino)methyl)-8-quinolinol (CMPAMQ) and 3-hydroxy-2-(4-isopropylphenyl)-6-methyl-4H-chromen-4-one (HIPPMC). The half-maximal inhibitory concentration for CMPAMQ in *E. coli* was 8 ± 2 µM and for HIPPMC 11 ± 2 µM [116]. However, since no value had been identified for *P. putida*, the compounds were examined at various concentrations in aerobically cultivated *P. putida* before the BES experiment.

The inhibitors were solubilized in pure dimethyl sulfoxide (DMSO); therefore, for the control experiments, *P. putida* was cultivated with 0.25% (v/v) filtered DMSO, similarly to the amount of DMSO added when the highest inhibitor concentration of each inhibitor was tested. Inhibitors were added at the beginning of the cultivation and up to a concentration five times that of *E. coli*'s half-maximal inhibitory concentrations. After nearly 7 hours, no inhibitory effect on bacterial growth was observed for both compounds when the cells were cultivated in DM9 medium supplemented with 5 g L^{-1} glucose, as the cells had similar growth curves at different concentrations (**Fig. 28**), showing that both inhibitors showed no systematic inhibitory effect on KT2440 under aerobic condition.

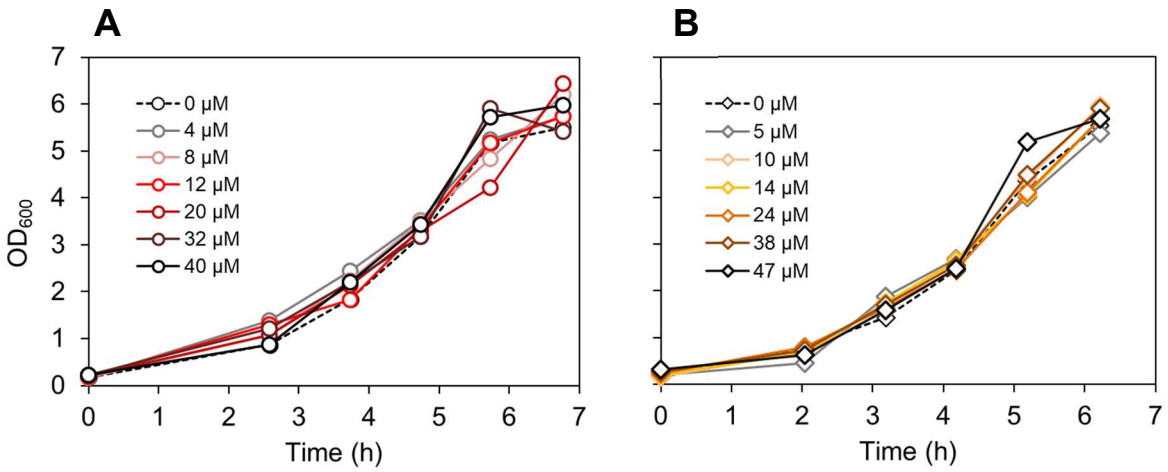

Figure 28. Aerobic growth of *P. putida* KT2440 with the addition of (**A**) 2-(((3-chloro-4-methoxy-phenyl)amino)methyl)-8-quinolinol and (**B**) 3-hydroxy-2-(4-isopropylphenyl)-6-methyl-4H-chromen-4-one at different concentrations. At 0 mM of inhibitor, a final concentration of 0.25% DMSO (v/v) was used instead.

To determine if the addition of TonB inhibitors affects aerobic ferricyanide reduction, the cells were tested again, now with L-arabinose, which had been previously shown to not promote growth in *P. putida* KT2440. In this experiment, 1 mM of ferricyanide was added to simulate the same mediator availability in BES setups, as well as 40-48 µM of inhibitor of each type, since it was demonstrated previously that no significant effect on cell's survival was to be expected at these concentrations. A cell-free control with the addition of HIPPMC, and a control with only DMSO added were conducted simultaneously. Over the course of 5 days, the optical density, the medium absorbance at λ=420 nm, and pH were monitored. Upon additional of HIPPMC to the medium, the liquid turned slightly cloudy at the beginning and the compound slowly dissolved overtime; this was not observed, or at least not visually distinguishable in comparison with the other cultures. Otherwise, no-to-very-little growth (which might have been due to pre-culture carryover) was observed for all cell cultures as expected (**Fig. 29A**). Nonetheless, the decrease in pH and absorbance at 420 nm, which could be quantitatively translated to the reduction of ferricyanide to ferrocyanide in the medium, indicating that the cells had been oxidizing the substrate and releasing electrons. The mediators were found to be reduced abiotically over time, but the drop in Abs_{420} was much slower in comparison with the cell cultures (**Fig. 26B**). Interestingly, the pH drop and reduction of ferricyanide were slightly slower with the addition of CMPAMQ, compared to when HIPPMC or pure DMSO was added (**Fig. 29C**).

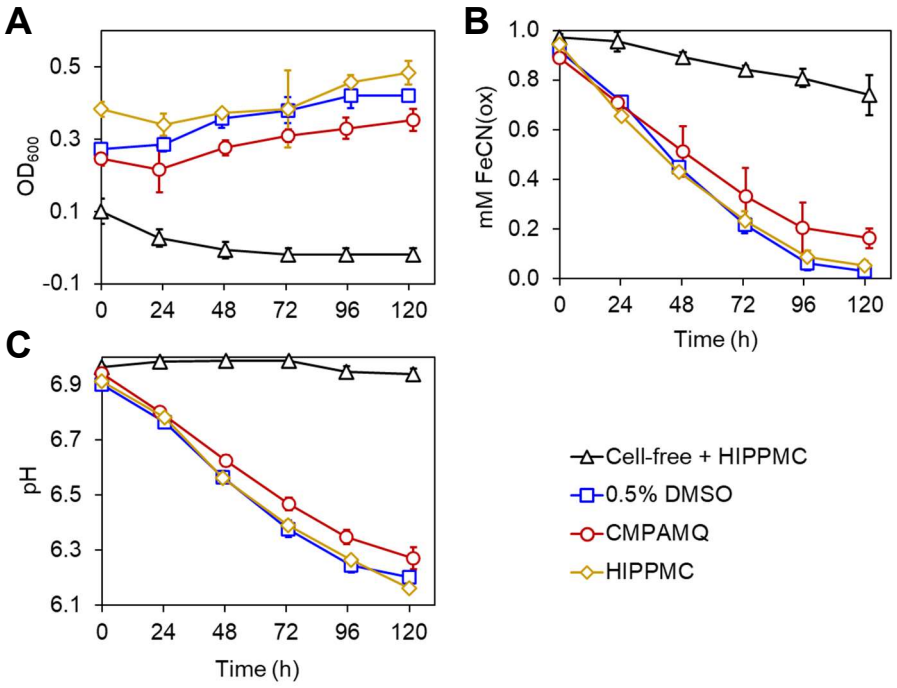

Figure 29. (**A**) Optical densities, (**B**) absorbances of ferricyanide at λ=420 nm, and (**C**) pH values of aerobic cultures of *P. putida* KT2440 with and without TonB inhibitors, using L-arabinose as substrate and $K_3[FeCN]_6$ as an additional electron sink. The conversion coefficient from absorbance to a concentration of $K_3[FeCN]_6$ was 0.99 mM per absorbance unit [30].

5.4.2. Effect of TonB inhibitors on the bioelectrochemical activity of P. putida

Next, the inhibitory effect of TonB inhibitors was evaluated in the BES setup. *P. putida* KT2440 was cultivated in BES (with 2 g L^{-1} glucose as substrate) for 200-250 h before either CMPAMQ or HIPPMC (both were prepared in pure DMSO) was added. For the first injection, a final concentration of 28.6 µM of CMPAMQ and 34.3 µM of HIPPMC was achieved. A second administration of HIPPMC was made at approximately 360 h, bringing the concentration of HIPPMC in the reactor to 72.2 µM. The addition of the solubilized inhibitors resulted in 0.34% and 0.72% v/v DMSO in the first (for both inhibitors) and the second injection of the inhibitor (for HIPPMC only), respectively. Simultaneously to the experiment with HIPPMC, a control using pure DMSO was carried out in case of possible toxicity to the cells. In addition to the current density recorded during the cultivation, Abs_{420} of ferricyanide and the pH value of the medium were monitored as an indication of glucose oxidation, similar to the previous experiment in aerobic conditions.

After two injections, both the control reactor and the reactor with HIPPMC showed no to little difference from each other, in terms of electron discharge and oxidation of the substrate, as indicated by the similar current density curves and pH drop. Moreover, the presence of both DMSO and HIPPMC did not show an inhibitory effect on the activity of the cells, as pH continued to decrease as a result of continuous glucose oxidation, and no immediate change

in the concentration of oxidized ferricyanide was observed (**Fig. 30**). Meanwhile, the addition of 28.6 μM of CMPAMQ immediately caused the current to drop significantly, as well as medium pH to stop decreasing, and the mediator to nearly completely return to the oxidized form. On the other hand, HIPPMC showed no to possibly little inhibitory effect, at least at the concentration used in this experiment.

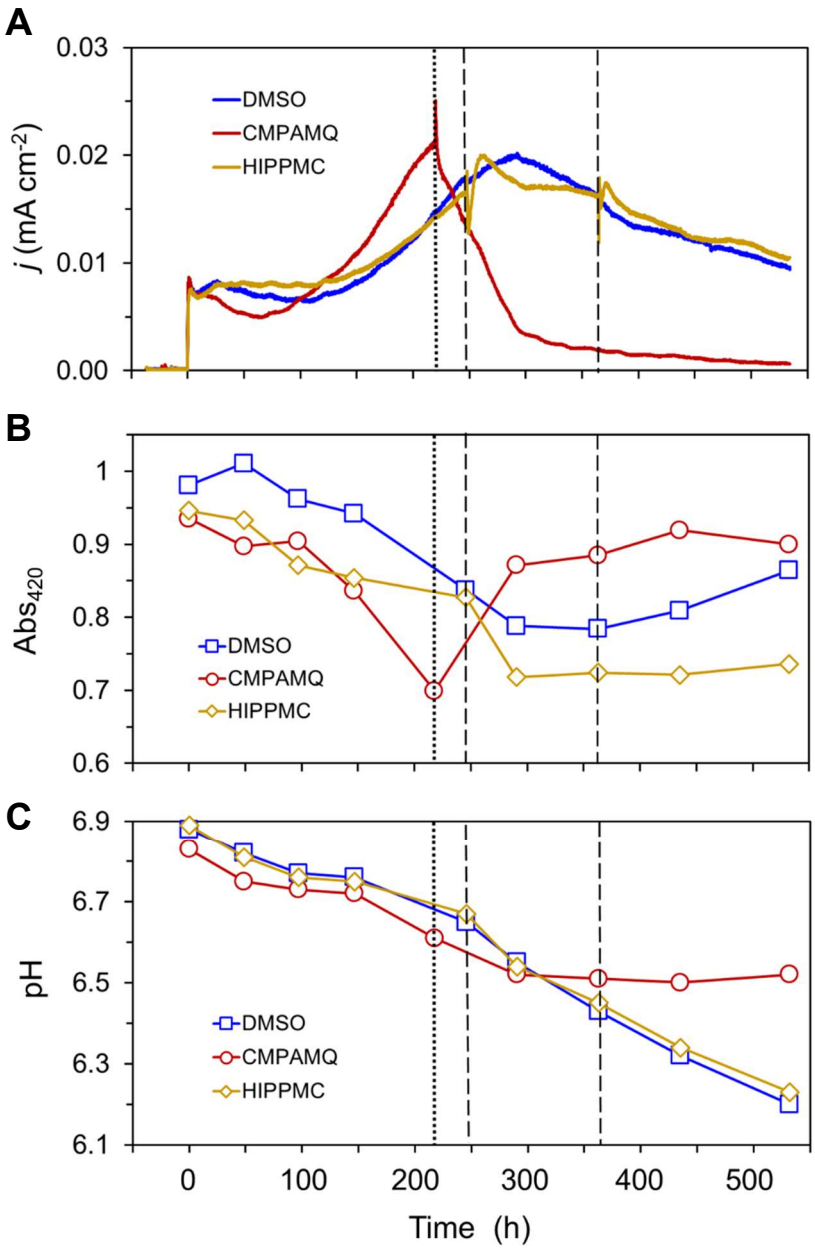

Figure 30. Effect of TonB inhibitors and DMSO on glucose oxidation of *P. putida* under BES condition. (**A**) Current densities, (**B**) absorbances of ferricyanide at λ=420 nm, and (**C**) pH values were recorded during the cultivation with the addition of either CMPAMQ at 220 h (dotted line), HIPPMC, and only DMSO as control at 250 and 360 h (dashed lines) after inoculation.

5.4.3. Discussion

In the other experiments, most of the hypotheses were developed based on observation of the bacteria's performance and physiological changes, while very little information on the underlying molecular mechanism to these adaptive traits has been unraveled. Without this, it is very difficult to have a clear direction for strain engineering strategy. In this section, nevertheless, a proof of concept to elucidate the probable role of a key protein complex in electron exchange between the bacterial cell and the electrode is provided. To demonstrate the role of this protein complex in transporting iron-based redox mediator across the outer membrane, a general approach is to conduct knockout mutation of TonB; however, due to its functional plethora, this could be lethal to the cell. Mutant *P. putida* that completely lacked TonB complex were found to be unable to grow in a minimal medium with an iron concentration of less than 10 µM [290]. Therefore, direct manipulation of the TonB protein alone or any other proteins of the inner membrane-binding complex would also not provide solid proof of its function as a mediator transporter. Moreover, manipulation of outer membrane transporters could also potentially be detrimental for the cell owing to the disruption of iron uptake. Adopting the work of Lai, et al. [45], compounds that inhibit TonB activity were first tested to examine the effect of TonB inhibition on the electron discharge from the cell to the electrode.

The first concern within the inhibitory study was the effect of DMSO. It was unknown if the addition of DMSO as a solvent for the inhibitors would cause any additional toxic effect to the cells, especially under more stressful conditions for the cells like in the BES reactor. However, published results showed that DMSO only displayed a significant inhibitory effect on various bacterial species at concentrations above 2% [291], and some species could tolerate up to 25% of DMSO [292]. Furthermore, unperturbed growth and/or activity of *P. putida* in our previous aerobic experiments indicated that the concentration of DMSO used in this case might as well be non-lethal.

Both inhibitors used in this study showed no effect on the growth of *P. putida* KT2440 under aerobic conditions. This was initially expected, because both inhibitors were screened as TonB inhibitors for *E. coli*, and no published work has been done so far to assess their effect on the TonB protein of *P. putida*; moreover, the TonB protein homologs of the two species are not interchangeable, even though their functions are similar [293]. In addition, *E. coli* only possesses one copy of the *tonB-exbBD* genes, whereas *P. putida* has multiple TonB-ExbBD homologs [294]; some of which, nonetheless, are related to the Tol-Pal family. The Tol-Pal complex highly resembles TonB in terms of structure and location on the membrane, but differs in functions and to which outer membrane proteins it interacts with [295, 296].

Thus, the compounds were predicted to have very low affinity and effectiveness toward *P. putida* in term of inhibiting mediator transport. This could be the case for HIPPMC, as no significant difference compared to the DMSO control was observed in any of the experiments with this inhibitor. Meanwhile, the addition of CMPAMQ caused a slight decrease in ferricyanide reduction and oxidation of sugar (**Fig. 29**), although, under aerobic conditions, ferricyanide does not contribute much to the respiration of the cell unlike in the BES setup. Also, it is unknown if iron and iron complexes could be taken up via TonB-independent transporters or not. While experimental data in this study suggest the possible inhibitory effect of CMPAMQ under BES condition, it remains inconclusive that this was (solely) coming from the inhibition of TonB, and further investigations are needed for the characterization of the process. Nevertheless, as ferricyanide concentration, reflected by the Abs_{420} value, immediately increased back to the original value following the addition of CMPAMQ (**Fig. 30B**), it implied that inhibition by CMPAMQ on oxidation activity of *P. putida* was perhaps not by interacting with the electrode nor by depleting the mediator, but by interaction with a cellular component. HIPPMC, on the other hand, was found to deplete ferricyanide under aerobic conditions (**Fig. 29B**). In a similar manner, the compound might have reduced mediator availability in the reactor, as the absorbance of the medium did not rise as electron discharge ceased, unlike with the control experiment with DMSO (**Fig. 30B**). This, however, did not seem to have any observable effect on the respiration of the cell during BES cultivation, as the current output was unaffected by the presence of HIPPMC in comparison with the control reactor (**Fig. 30A**)

.

Chapter 6.
Final remarks and future prospects

6.1. Summary

The overall objective of this dissertation was to investigate the obligate aerobe *P. putida* in the bioelectrochemical system, providing further understanding of its metabolism to support current and future engineering works to generate new bacterial strains capable of anaerobic biotransformation. In summary, the results obtained have shed light on some of the previously unanswered questions, including how the carbon substrate enters the central carbon metabolism through the cell membrane, and how respiration under anoxic cultivation facilitated by an electrode affects cellular physiology and phenotype. Once again, this work has highlighted the versatility of *P. putida*'s metabolism, especially toward different carbon sources.

First, regarding the uptake of carbon under anoxic conditions, *P. putida* might also prefer the gaP-ED route to overcome energy and internal redox constraints, reflected by the enrichment of [1,2-$^{13}C_2$]acetate with gaP mutant. Strain glcP also showed enrichment of acetate, yet the more noticeable increase in half-labeled [1-^{13}C]acetate over time indicated that this pathway might have required internal carbon storage to compensate for low net energy yield. In contrast, the 2kgaP pathway might not be favorable for carbon uptake at all, despite being the main route in the periplasm used for substrate oxidation.

BES, as well as aerobic, cultivation experiments, highlighted the versatility of *P. putida* in metabolizing carbohydrates, especially aldoses. Through the POC, the cell could extract energy from substrates that usually do not promote growth; additionally, it also revealed that the Gcd of *P. putida* is capable of oxidizing a broad range of aldoses to their corresponding aldonates, which could be a potential source of an enzyme catalyst for the production of sugar acids. When fructose was fed, the cell was also able to extract energy extracellularly by converting fructose to mannonate through the POC – a never-before-seen reaction under anoxic conditions. While achieving anaerobic growth remained unsuccessful, this study described the physiological alterations, including changes in protein expression as well as internal redox pool toward a more reduced state, during anaerobic fructose metabolism and points to possible future optimization strategies.

Last but not least, the inhibitory study of TonB protein provided a proof-of-concept that this protein complex, alongside some TonB-dependent iron transporters, might be responsible for the crossing of iron-based redox mediator through the outer membrane into the periplasmic space for the cell's respiration under BES setup. Nevertheless, more experiments are required

to elucidate the mechanisms as well as to improve the respiratory rate of the cell, so that anoxic catabolism of carbon substrate could be improved.

6.2. Future prospects

6.2.1. New protein targets for strain engineering

Based on the analyses above, it is anticipated that targeting transcriptional regulators of central carbon metabolism is one possible engineering strategy for improving cultivation under BES conditions in the future, as the intracellular uptake of sugars remained rather low due to the shift of carbon flux toward energy-generating pathway in the periplasm. In this scenario, one promising protein is the global transcriptional regulator HexR, which negatively regulates the expression of *gap-1* gene, the *edd-glk-gltR-2* and *zwf-pgl-eda* operons under modulation of KDPG [91, 93, 95]. The protein expression pattern of the ED-EMP cycle in this study suggested that repression by HexR might have been taking place. A similar approach, which included a HexR knockout mutation, has been previously attempted to boost a highly NADPH-demanding *para*-hydroxybenzoate production in strain KT2440 [297]. Additional mutation of negative regulators, such as PtxS, which regulates 2KGA metabolism [91, 94, 97], or Cra, might also add to the alleviation of limited intracellular carbon flux of KT2440 in the case of anoxic catabolism of glucose and fructose, respectively.

Since non-essential genes represent a considerable fraction of the core-genome of *P. putida*, a different strategy involving the reduction of the bacterium's genome could be considered [298]; it was found not only to help relieve the internal redox burden, but also increase ATP yield, biomass yield, and overall viability of the cell, even under glucose-limited cultivation [299-301]. Nevertheless, improving the carbon flux or NADPH pool would only be a part of the puzzle: an *in silico* approach by Kampers et al. [25, 71] revealed that genetic and metabolic engineering to enable a facultatively anaerobic lifestyle in KT2440 was a much more elaborate process than previously thought. Hence, the substitution of oxygen-dependent reactions to acclimate the cell to the anoxic environment of the BES should consequently be taken into consideration. Implementing the recently published oxygen-independent anabolic reactions [25] and further works on de-regulation of the central carbon metabolism might be able to finally allow anaerobic metabolism and growth in *P. putida*.

In order to develop commercially viable bioelectrochemical technologies, high current densities are required [302]. One of the aims of investigating the membrane transport systems that are responsible for the translocation of redox mediators across the membrane is to identify the key proteins, which could help improve the system performance by avoiding any potential mass transfer limits. As *P. putida* KT2440 possesses over 30 different (possible) TBDTs with only a few with known substrate, direct manipulation of a specific TBDT could end up futile.

Meanwhile, any knockout mutation on the inner membrane complex could be lethal to the cell, since the TonB complex control a broad range of membrane transport functions [116]. One possible approach to strain engineering that involves TonB is overexpressing *tonB-exbBD* complex. Since both ExbB and ExbD are required for TonB to associate with the cytoplasmic membrane, as well as for TonB to conformationally respond to proton motive force [121], overexpression of the entire operon might yield a better result compared to TonB overexpression alone. In fact, Létoffé, et al. (2004) found that expression of TonB was 50% lower in a bacterial strain overexpressing single TonB protein than in those overexpressing all three proteins of the complex [113]. Another possible target for engineering is the iron uptake regulation system of the cell. *P. putida* KT2440 possesses two ferric uptake regulators (Fur): PP_0119 and PP_4730. Fur protein is one of the most important regulators of iron homeostasis in prokaryotes, as it negatively regulates the expression of all iron uptake systems in *E. coli* and many different genes of *P. aeruginosa* [303-305]. Nevertheless, the Fur-knockout in a *P. aeruginosa* mutant was found to only affect certain features like biofilm formation, whereas it did not cause oxidative stress and the toxicity caused by the mutation was not common amongst *Pseudomonas* spp. [306]. Therefore, by knocking out these co-repressors in *P. putida* in the future, we hope to achieve an increase of expression in the iron uptake systems, regardless if they are TonB-dependent or not, and hence, improve iron-based mediator transport across the membrane.

Parallel to the mystery of the translocation of redox mediators from the outside into the periplasm, another question remains: how do the mediators cross the membrane back to the outside of the cell? So far, there has been no concrete evidence or proposed hypothesis. Nonetheless, there might have been a hint of what could be responsible for this from previous studies. As observed by Yu, et al. (2018), recombinant *P. putida* carrying an empty vector as a control also had improved bioelectrochemical performance; the authors hypothesized that the antibiotics used for selection induce biosynthesis of PQQ and that PQQ is also a limiting factor in BES [31]. However, another possibility is that the cell might have triggered overexpression of different efflux pump systems in response to the presence of antibiotics in the selection medium [307], which could have also improved mass transfer across the membrane. In fact, it was known that some Gram-negative bacteria, such as *E. coli* and *P. aeruginosa*, use these transport systems to secrete their siderophores [308, 309]. Proteomic works on the recombinant cells with antibiotic-resisting vectors could be the next step in answering this question.

6.2.2. Additional analytical approaches

For the first objective, investigating carbon uptake using *P. putida* mutants in combination with ^{13}C enrichment in acetate was demonstrated to be a feasible approach. However, in this work,

no flux model was generated due to the limited information gained from acetate analysis. By looking at only acetate, it is possible to have a glimpse at most of the cell's glycolytic process, but not an overview of the entire central carbon metabolism, as the compound is only one of the many products of substrate-level oxidation and rather a by-product of glucose electro-fermentation and not an important intermediate metabolite for the cell to build biomass. In order to have a more in-depth evaluation of the effect of different carbon uptake routes, the metabolic profile for the ^{13}C isotope tracing should be broadened, not only to glycolytic intermediates, but organic acids that are generated through the TCA cycle, or amino acids as well. Therefore, other analytical methods might be required for such a feat; one of the possibilities is to use IC- or LC-MS/MS. So far, liquid chromatography has been a useful tool for quantifying secreted metabolites produced by *P. putida* during BES cultivation. However, it relies heavily on the sensitivity of the equipment and separability of the compounds under certain analytical conditions; thus, only a limited range of molecules could be analyzed with the currently used method [44]. Additional tandem mass spectrometry (MS/MS), which involves multiple steps of mass spectrometry with fragmentations occurring in between the stages, could vastly improve the quality of the analysis [310]. With a solid metabolic profile, a complete flux model could be therefore constructed.

Another possible method improvement lies within the proteomic studies. Our study utilized shotgun proteomics with DDA mode. In DDA mode, the mass spectrometer selects the most intense peptide ions in the first stage of tandem MS, which are further fragmented and analyzed in the second stage, offering cleaner spectra compared to other modes [311]. A major disadvantage, however, is the limited time for fragmentation, which is caused by the peak width and MS scan time [312]; hence, proteins with lower abundances usually suffer from under-sampling. Additionally, in a shotgun proteomic experiment, a peptide is usually triggered for fragmentation only once (or limited times) due to the dynamic exclusion function, to improve the depth of identification. The reporter ions used for quantification ultimately reflect only the peptide abundances at that given time and substantially decrease the reproducibility of second MS spectra acquisition among runs [269, 289]. An alternative option to DDA is data-independent acquisition (DIA); a common DIA method is the sequential windowed acquisition of all theoretical fragment ion mass spectra (or SWATH-MS), in which the mass spectrometer divides the mass range into small mass windows, resulting in the co-fragmentation of many co-eluting peptides selected in the precursor ion window, and thus, generating highly complex fragmentation spectra. As a consequence, proteome characterization from SWATH-MS data sets is usually exhaustive [313, 314]. Nonetheless, the DIA approach might help improve qualitative and quantitative analysis of low-abundance proteins, e.g., regulatory proteins, which could give a better picture of *P. putida*'s adaptation strategies to the anoxic and electrifying condition of BES

Bibliography

1. United Nations: *World Population Prospects 2022.* United Nations; 2022.
2. United Nations Department of Economic Social Affairs: *The Sustainable Development Goals Report 2022.* United Nations; 2022.
3. European Chemical Industry Council: **The European Chemical industry Facts and Figures 2023.** In *A Pillar Of The European Economy*2023.
4. European Commission: **Chemicals.** In *Internal Market, Industry, Entrepreneurship and Small and Medium-sized Enterprises (SMEs)*.
5. Committee on Industrialization of Biology, Board on Chemical Sciences and Technology, Board on Life Sciences, Division on Earth and Life Studies, Council NR: **Industrial Biotechnology: Past and Present.** In *Industrialization of Biology: A Roadmap to Accelerate the Advanced Manufacturing of Chemicals.* Washington (DC): National Academies Press (US); 2015: 25-52.
6. European Commission: **Bio-based products.** In *Internal Market, Industry, Entrepreneurship and Small and Medium-sized Enterprises (SMEs)*.
7. Taneja P, Biresaw SS, KumraTaneja N, Jha SK, Zeleke B, Srivastava S, Taneja M, Prasad S, Juneja V: **Chapter 15 - Advances in fermented foods and therapeutics.** In *Innovations in Fermentation and Phytopharmaceutical Technologies.* Edited by Thatoi H, Mohapatra S, Das SK: Elsevier; 2022: 341-358.
8. Nielsen J, Tillegreen CB, Petranovic D: **Innovation trends in industrial biotechnology.** *Trends Biotechnol* 2022, **40:**1160-1172.
9. Glittenberg D: **10.07 - Starch-Based Biopolymers in Paper, Corrugating, and Other Industrial Applications.** In *Polymer Science: A Comprehensive Reference.* Edited by Matyjaszewski K, Möller M. Amsterdam: Elsevier; 2012: 165-193.
10. Nielsen J: **Production of biopharmaceutical proteins by yeast.** *Bioengineered* 2013, **4:**207-211.
11. Ghangrekar MM, Behera M: **3.5 - Suspended Growth Treatment Processes.** In *Comprehensive Water Quality and Purification.* Edited by Ahuja S. Waltham: Elsevier; 2014: 74-89.
12. Huang W-C, Tang I-C: **Chapter 8 - Bacterial and Yeast Cultures – Process Characteristics, Products, and Applications.** In *Bioprocessing for Value-Added Products from Renewable Resources.* Edited by Yang S-T. Amsterdam: Elsevier; 2007: 185-223.
13. Stephanopoulos GN, Aristidou AA, Nielsen J: **Chapter 6 - Examples of Pathway Manipulations: Metabolic Engineering in Practice.** In *Metabolic Engineering.* Edited by Stephanopoulos GN, Aristidou AA, Nielsen J. San Diego: Academic Press; 1998: 203-283.
14. Garcia-Ochoa F, Gomez E: **Bioreactor scale-up and oxygen transfer rate in microbial processes: an overview.** *Biotechnol Adv* 2009, **27:**153-176.
15. Pinhal S, Ropers D, Geiselmann J, de Jong H: **Acetate Metabolism and the Inhibition of Bacterial Growth by Acetate.** *J Bacteriol* 2019, **201:**e00147-00119.
16. Takahashi CM, Takahashi DF, Carvalhal ML, Alterthum F: **Effects of acetate on the growth and fermentation performance of *Escherichia coli* KO11.** *Appl Biochem Biotechnol* 1999, **81:**193-203.

17. De Mey M, De Maeseneire S, Soetaert W, Vandamme E: **Minimizing acetate formation in *E. coli* fermentations.** *J Ind Microbiol Biotechnol* 2007, **34:**689-700.
18. Wackett LP: ***Pseudomonas putida*—a versatile biocatalyst.** *Nat Biotechnol* 2003, **21:**136-138.
19. Nikel PI, Martinez-Garcia E, de Lorenzo V: **Biotechnological domestication of pseudomonads using synthetic biology.** *Nat Rev Microbiol* 2014, **12:**368-379.
20. Loeschcke A, Thies S: ***Pseudomonas putida* - a versatile host for the production of natural products.** *Appl Microbiol Biot* 2015, **99:**6197-6214.
21. Poblete-Castro I, Becker J, Dohnt K, dos Santos VM, Wittmann C: **Industrial biotechnology of *Pseudomonas putida* and related species.** *Appl Microbiol Biot* 2012, **93:**2279-2290.
22. Molina L, Rosa R, Nogales J, Rojo F: ***Pseudomonas putida* KT2440 metabolism undergoes sequential modifications during exponential growth in a complete medium as compounds are gradually consumed.** *Environ Microbiol* 2019, **21:**2375-2390.
23. La Rosa R, Behrends V, Williams HD, Bundy JG, Rojo F: **Influence of the Crc regulator on the hierarchical use of carbon sources from a complete medium in *Pseudomonas*.** *Environ Microbiol* 2016, **18:**807-818.
24. Nikel PI, Chavarría M, Danchin A, de Lorenzo V: **From dirt to industrial applications: *Pseudomonas putida* as a Synthetic Biology chassis for hosting harsh biochemical reactions.** *Curr Opin Chem Biol* 2016, **34:**20-29.
25. Kampers LFC, van Heck RGA, Donati S, Saccenti E, Volkers RJM, Schaap PJ, Suarez-Diez M, Nikel PI, Martins Dos Santos VAP: **In silico-guided engineering of *Pseudomonas putida* towards growth under micro-oxic conditions.** *Microb Cell Fact* 2019, **18:**179.
26. Sohn SB, Kim TY, Park JM, Lee SY: ***In silico* genome-scale metabolic analysis of *Pseudomonas putida* KT2440 for polyhydroxyalkanoate synthesis, degradation of aromatics and anaerobic survival.** *Biotechnol J* 2010, **5:**739-750.
27. Nikel PI, de Lorenzo V: **Engineering an anaerobic metabolic regime in *Pseudomonas putida* KT2440 for the anoxic biodegradation of 1,3-dichloroprop-1-ene.** *Metab Eng* 2013, **15:**98-112.
28. Steen A, Utkur FO, Borrero-de Acuna JM, Bunk B, Roselius L, Buhler B, Jahn D, Schobert M: **Construction and characterization of nitrate and nitrite respiring *Pseudomonas putida* KT2440 strains for anoxic biotechnical applications.** *J Biotechnol* 2013, **163:**155-165.
29. Hintermayer S, Yu S, Krömer JO, Weuster-Botz D: **Anodic respiration of *Pseudomonas putida* KT2440 in a stirred-tank bioreactor.** *Biochem Eng J* 2016, **115:**1-13.
30. Lai B, Yu S, Bernhardt PV, Rabaey K, Virdis B, Kromer JO: **Anoxic metabolism and biochemical production in Pseudomonas putida F1 driven by a bioelectrochemical system.** *Biotechnol Biofuels* 2016, **9:**39.
31. Yu S, Lai B, Plan MR, Hodson MP, Lestari EA, Song H, Krömer JO: **Improved performance of *Pseudomonas putida* in a bioelectrochemical system through overexpression of periplasmic glucose dehydrogenase.** *Biotechnol Bioeng* 2018, **115:**145-155.
32. Schmitz S, Nies S, Wierckx N, Blank LM, Rosenbaum MA: **Engineering mediator-based electroactivity in the obligate aerobic bacterium *Pseudomonas putida* KT2440.** *Front Microbiol* 2015, **6:**284.

33. Askitosari TD, Boto ST, Blank LM, Rosenbaum MA: **Boosting Heterologous Phenazine Production in *Pseudomonas putida* KT2440 Through the Exploration of the Natural Sequence Space.** *Front Microbiol* 2019, **10:**1990.
34. Askitosari TD, Berger C, Tiso T, Harnisch F, Blank LM, Rosenbaum MA: **Coupling an Electroactive *Pseudomonas putida* KT2440 with Bioelectrochemical Rhamnolipid Production.** *Microorganisms* 2020, **8**.
35. Logan BE: **Scaling up microbial fuel cells and other bioelectrochemical systems.** *Appl Microbiol Biotechnol* 2010, **85:**1665-1671.
36. Pant D, Singh A, Van Bogaert G, Olsen SI, Singh Nigam P, Diels L, Vanbroekhoven K: **Bioelectrochemical systems (BES) for sustainable energy production and product recovery from organic wastes and industrial wastewaters.** *RSC Advances* 2012, **2:**1248-1263.
37. Jadhav DA, Chendake AD, Vinayak V, Atabani A, Ali Abdelkareem M, Chae K-J: **Scale-up of the bioelectrochemical system: Strategic perspectives and normalization of performance indices.** *Bioresour Technol* 2022, **363:**127935.
38. Leicester D, Amezaga J, Heidrich E: **Is bioelectrochemical energy production from wastewater a reality? Identifying and standardising the progress made in scaling up microbial electrolysis cells.** *Renew Sust Energ Rev* 2020, **133:**110279.
39. Xie X, Criddle C, Cui Y: **Design and fabrication of bioelectrodes for microbial bioelectrochemical systems.** *Energy Environ Sci* 2015, **8:**3418-3441.
40. Babauta J, Renslow R, Lewandowski Z, Beyenal H: **Electrochemically active biofilms: facts and fiction. A review.** *Biofouling* 2012, **28:**789-812.
41. Angelaalincy MJ, Navanietha Krishnaraj R, Shakambari G, Ashokkumar B, Kathiresan S, Varalakshmi P: **Biofilm Engineering Approaches for Improving the Performance of Microbial Fuel Cells and Bioelectrochemical Systems.** *Front Energy Res* 2018, **6**.
42. Zheng T, Li J, Ji Y, Zhang W, Fang Y, Xin F, Dong W, Wei P, Ma J, Jiang M: **Progress and Prospects of Bioelectrochemical Systems: Electron Transfer and Its Applications in the Microbial Metabolism.** *Front Bioeng Biotechnol* 2020, **8**.
43. **STROMER - Nachhaltige Transformation durch elektrochemische Reaktionen: Das Doktorandenkolleg des Themenbereiches Umwelt- und Biotechnologie.** Helmholtz-Zentrum für Umweltforschung UFZ.
44. Lai B, Plan M, Hodson M, Krömer J: **Simultaneous Determination of Sugars, Carboxylates, Alcohols and Aldehydes from Fermentations by High Performance Liquid Chromatography.** *Fermentation* 2016, **2**.
45. Lai B, Bernhardt PV, Krömer JO: **Cytochrome c Reductase is a Key Enzyme Involved in the Extracellular Electron Transfer Pathway towards Transition Metal Complexes in Pseudomonas Putida.** *ChemSusChem* 2020, **13:**5308-5317.
46. Parte AC, Sarda Carbasse J, Meier-Kolthoff JP, Reimer LC, Goker M: **List of Prokaryotic names with Standing in Nomenclature (LPSN) moves to the DSMZ.** *Int J Syst Evol Microbiol* 2020, **70:**5607-5612.
47. Lalucat J, Mulet M, Gomila M, Garcia-Valdes E: **Genomics in Bacterial Taxonomy: Impact on the Genus *Pseudomonas*.** *Genes (Basel)* 2020, **11**.

48. Palleroni NJ: **The *Pseudomonas* story.** *Environ Microbiol* 2010, **12:**1377-1383.
49. Meyer JM, Geoffroy VA, Baida N, Gardan L, Izard D, Lemanceau P, Achouak W, Palleroni NJ: **Siderophore typing, a powerful tool for the identification of fluorescent and nonfluorescent pseudomonads.** *Appl Environ Microbiol* 2002, **68:**2745-2753.
50. Matthijs S, Tehrani KA, Laus G, Jackson RW, Cooper RM, Cornelis P: **Thioquinolobactin, a Pseudomonas siderophore with antifungal and anti-Pythium activity.** *Environ Microbiol* 2007, **9:**425-434.
51. Lau GW, Hassett DJ, Ran H, Kong F: **The role of pyocyanin in *Pseudomonas aeruginosa* infection.** *Trends Mol Med* 2004, **10:**599-606.
52. Harwood CS, Fosnaugh K, Dispensa M: **Flagellation of Pseudomonas putida and analysis of its motile behavior.** *J Bacteriol* 1989, **171:**4063-4066.
53. Silby MW, Winstanley C, Godfrey SA, Levy SB, Jackson RW: ***Pseudomonas* genomes: diverse and adaptable.** *FEMS Microbiol Rev* 2011, **35:**652-680.
54. Moradali MF, Ghods S, Rehm BH: ***Pseudomonas aeruginosa* Lifestyle: A Paradigm for Adaptation, Survival, and Persistence.** *Front Cell Infect Microbiol* 2017, **7:**39.
55. Xin XF, Kvitko B, He SY: ***Pseudomonas syringae*: what it takes to be a pathogen.** *Nat Rev Microbiol* 2018, **16:**316-328.
56. Scales BS, Dickson RP, LiPuma JJ, Huffnagle GB: **Microbiology, genomics, and clinical significance of the *Pseudomonas fluorescens* species complex, an unappreciated colonizer of humans.** *Clin Microbiol Rev* 2014, **27:**927-948.
57. Ganeshan G, Manoj Kumar A: ***Pseudomonas fluorescens*, a potential bacterial antagonist to control plant diseases.** *J Plant Interact* 2005, **1:**123-134.
58. Kim J, Park W: **Oxidative stress response in *Pseudomonas putida*.** *Appl Microbiol Biotechnol* 2014, **98:**6933-6946.
59. Inoue A, Horikoshi K: **A *Pseudomonas* thrives in high concentrations of toluene.** *Nature* 1989, **338:**264-266.
60. Rühl J, Schmid A, Blank LM: **Selected *Pseudomonas putida* strains able to grow in the presence of high butanol concentrations.** *Appl Environ Microbiol* 2009, **75:**4653-4656.
61. Ramos JL, Sol Cuenca M, Molina-Santiago C, Segura A, Duque E, Gomez-Garcia MR, Udaondo Z, Roca A: **Mechanisms of solvent resistance mediated by interplay of cellular factors in *Pseudomonas putida*.** *FEMS Microbiol Rev* 2015, **39:**555-566.
62. Jimenez JI, Minambres B, Garcia JL, Diaz E: **Genomic analysis of the aromatic catabolic pathways from *Pseudomonas putida* KT2440.** *Environ Microbiol* 2002, **4:**824-841.
63. Nikel PI, de Lorenzo V: **Robustness of *Pseudomonas putida* KT2440 as a host for ethanol biosynthesis.** *N Biotechnol* 2014, **31:**562-571.
64. Elmore JR, Dexter GN, Salvachua D, Martinez-Baird J, Hatmaker EA, Huenemann JD, Klingeman DM, Peabody GLt, Peterson DJ, Singer C, et al: **Production of itaconic acid from alkali pretreated lignin by dynamic two stage bioconversion.** *Nat Commun* 2021, **12:**2261.
65. Nitschel R, Ankenbauer A, Welsch I, Wirth NT, Massner C, Ahmad N, McColm S, Borges F, Fotheringham I, Takors R, Blombach B: **Engineering *Pseudomonas putida* KT2440 for the production of isobutanol.** *Eng Life Sci* 2020, **20:**148-159.

66. Bagdasarian M, Lurz R, Rückert B, Franklin FC, Bagdasarian MM, Frey J, Timmis KN: **Specific-purpose plasmid cloning vectors. II. Broad host range, high copy number, RSF1010-derived vectors, and a host-vector system for gene cloning in *Pseudomonas*.** *Gene* 1981, **16:**237-247.
67. Regenhardt D, Heuer H, Heim S, Fernandez DU, Strömpl C, Moore ERB, Timmis KN: **Pedigree and taxonomic credentials of *Pseudomonas putida* strain KT2440.** *Environ Microbiol* 2002, **4:**912-915.
68. Nelson KE, Weinel C, Paulsen IT, Dodson RJ, Hilbert H, Martins dos Santos VAP, Fouts DE, Gill SR, Pop M, Holmes M, et al: **Complete genome sequence and comparative analysis of the metabolically versatile *Pseudomonas putida* KT2440.** *Environ Microbiol* 2002, **4:**799-808.
69. Belda E, van Heck RGA, José Lopez-Sanchez M, Cruveiller S, Barbe V, Fraser C, Klenk H-P, Petersen J, Morgat A, Nikel PI, et al: **The revisited genome of *Pseudomonas putida* KT2440 enlightens its value as a robust metabolic chassis.** *Environ Microbiol* 2016, **18:**3403-3424.
70. Martins dos Santos VAP, Timmis KN, Tümmler B, Weinel C: **Genomic Features of *Pseudomonas putida* Strain KT2440.** In *Pseudomonas: Volume 1 Genomics, Life Style and Molecular Architecture.* Edited by Ramos J-L. Boston, MA: Springer US; 2004: 77-112.
71. Kampers LFC, Koehorst JJ, van Heck RJA, Suarez-Diez M, Stams AJM, Schaap PJ: **A metabolic and physiological design study of *Pseudomonas putida* KT2440 capable of anaerobic respiration.** *BMC Microbiol* 2021, **21:**9.
72. Sudarsan S, Blank LM, Dietrich A, Vielhauer O, Takors R, Schmid A, Reuss M: **Dynamics of benzoate metabolism in *Pseudomonas putida* KT2440.** *Metab Eng Commun* 2016, **3:**97-110.
73. Dinamarca MA, Ruiz-Manzano A, Rojo F: **Inactivation of Cytochrome o Ubiquinol Oxidase Relieves Catabolic Repression of the Pseudomonas putida GPo1 Alkane Degradation Pathway.** *J Bacteriol* 2002, **184:**3785-3793.
74. Yuan Q, Huang T, Li P, Hao T, Li F, Ma H, Wang Z, Zhao X, Chen T, Goryanin I: **Pathway-Consensus Approach to Metabolic Network Reconstruction for *Pseudomonas putida* KT2440 by Systematic Comparison of Published Models.** *PLoS One* 2017, **12:**e0169437.
75. Wang Q, Nomura CT: **Monitoring differences in gene expression levels and polyhydroxyalkanoate (PHA) production in *Pseudomonas putida* KT2440 grown on different carbon sources.** *J Biosci Bioeng* 2010, **110:**653-659.
76. Rojo F: **Carbon catabolite repression in *Pseudomonas*: optimizing metabolic versatility and interactions with the environment.** *FEMS Microbiol Rev* 2010, **34:**658-684.
77. Nikel PI, Chavarría M, Fuhrer T, Sauer U, de Lorenzo V: ***Pseudomonas putida* KT2440 Strain Metabolizes Glucose through a Cycle Formed by Enzymes of the Entner-Doudoroff, Embden-Meyerhof-Parnas, and Pentose Phosphate Pathways.** *J Biol Chem* 2015, **290:**25920-25932.
78. Valentini M, Garcia-Maurino SM, Perez-Martinez I, Santero E, Canosa I, Lapouge K: **Hierarchical management of carbon sources is regulated similarly by the CbrA/B systems in *Pseudomonas aeruginosa* and *Pseudomonas putida*.** *Microbiology* 2014, **160:**2243-2252.
79. Mendonca CM, Yoshitake S, Wei H, Werner A, Sasnow SS, Thannhauser TW, Aristilde L: **Hierarchical routing in carbon metabolism favors iron-scavenging strategy in iron-deficient soil *Pseudomonas* species.** *Proc Natl Acad Sci U S A* 2020, **117:**32358-32369.

80. Sasnow SS, Wei H, Aristilde L: **Bypasses in intracellular glucose metabolism in iron-limited *Pseudomonas putida*.** *Microbiologyopen* 2016, **5:**3-20.
81. Kohlstedt M, Wittmann C: **GC-MS-based (13)C metabolic flux analysis resolves the parallel and cyclic glucose metabolism of *Pseudomonas putida* KT2440 and *Pseudomonas aeruginosa* PAO1.** *Metab Eng* 2019, **54:**35-53.
82. Nikel PI, Fuhrer T, Chavarría M, Sánchez-Pascuala A, Sauer U, de Lorenzo V: **Redox stress reshapes carbon fluxes of *Pseudomonas putida* for cytosolic glucose oxidation and NADPH generation.** *bioRxiv* 2020**:**2020.2006.2013.149542.
83. Chavarría M, Nikel PI, Perez-Pantoja D, de Lorenzo V: **The Entner-Doudoroff pathway empowers *Pseudomonas putida* KT2440 with a high tolerance to oxidative stress.** *Environ Microbiol* 2013, **15:**1772-1785.
84. del Castillo T, Ramos JL, Rodriguez-Herva JJ, Fuhrer T, Sauer U, Duque E: **Convergent peripheral pathways catalyze initial glucose catabolism in *Pseudomonas putida*: genomic and flux analysis.** *J Bacteriol* 2007, **189:**5142-5152.
85. Peekhaus N, Conway T: **What's for Dinner?: Entner-Doudoroff Metabolism in *Escherichia coli*.** *J Bacteriol* 1998, **180:**3495-3502.
86. Lessie TG, Phibbs PV: **Alternative pathways of carbohydrate utilization in pseudomonads.** *Annu Rev Microbiol* 1984, **38:**359-388.
87. Kobayashi K, Mustafa G, Tagawa S, Yamada M: **Transient Formation of a Neutral Ubisemiquinone Radical and Subsequent Intramolecular Electron Transfer to Pyrroloquinoline Quinone in the *Escherichia coli* Membrane-Integrated Glucose Dehydrogenase.** *Biochemistry* 2005, **44:**13567-13572.
88. Matsushita K, Ohno Y, Shinagawa E, Adachi O, Ameyama M: **Membrane-bound, Electron Transport-linked, d-Glucose Dehydrogenase of *Pseudomonas fluorescens*. Interaction of the Purified Enzyme with Ubiquinone or Phospholipid.** *Agric Biol Chem* 1982, **46:**1007-1011.
89. Matsushita K, Shinagawa E, Adachi O, Ameyama M: **Membrane-bound D-gluconate dehydrogenase from *Pseudomonas aeruginosa*. Purification and structure of cytochrome-binding form.** *J Biochem* 1979, **85:**1173-1181.
90. Matsushita K, Shinagawa E, Adachi O, Ameyama M: **Membrane-bound D-gluconate dehydrogenase from *Pseudomonas aeruginosa*. Its kinetic properties and a reconstitution of gluconate oxidase.** *J Biochem* 1979, **86:**249-256.
91. del Castillo T, Duque E, Ramos JL: **A set of activators and repressors control peripheral glucose pathways in *Pseudomonas putida* to yield a common central intermediate.** *J Bacteriol* 2008, **190:**2331-2339.
92. Nikel PI, Kim J, de Lorenzo V: **Metabolic and regulatory rearrangements underlying glycerol metabolism in *Pseudomonas putida* KT2440.** *Environ Microbiol* 2014, **16:**239-254.
93. Daddaoua A, Krell T, Ramos JL: **Regulation of glucose metabolism in *Pseudomonas*: the phosphorylative branch and Entner-Doudoroff enzymes are regulated by a repressor containing a sugar isomerase domain.** *J Biol Chem* 2009, **284:**21360-21368.
94. Udaondo Z, Ramos JL, Segura A, Krell T, Daddaoua A: **Regulation of carbohydrate degradation pathways in *Pseudomonas* involves a versatile set of transcriptional regulators.** *Microb Biotechnol* 2018, **11:**442-454.

95. Campilongo R, Fung RKY, Little RH, Grenga L, Trampari E, Pepe S, Chandra G, Stevenson CEM, Roncarati D, Malone JG: **One ligand, two regulators and three binding sites: How KDPG controls primary carbon metabolism in *Pseudomonas*.** *PLoS Genet* 2017, **13:**e1006839.
96. Daddaoua A, Corral-Lugo A, Ramos JL, Krell T: **Identification of GntR as regulator of the glucose metabolism in *Pseudomonas aeruginosa*.** *Environ Microbiol* 2017, **19:**3721-3733.
97. Daddaoua A, Krell T, Alfonso C, Morel B, Ramos JL: **Compartmentalized glucose metabolism in *Pseudomonas putida* is controlled by the PtxS repressor.** *J Bacteriol* 2010, **192:**4357-4366.
98. Tribelli PM, Lujan AM, Pardo A, Ibarra JG, Fernandez Do Porto D, Smania A, Lopez NI: **Core regulon of the global anaerobic regulator Anr targets central metabolism functions in *Pseudomonas* species.** *Sci Rep* 2019, **9:**9065.
99. Kaur R, Macleod J, Foley W, Nayudu M: **Gluconic acid: an antifungal agent produced by *Pseudomonas* species in biological control of take-all.** *Phytochemistry* 2006, **67:**595-604.
100. An R, Moe LA: **Regulation of Pyrroloquinoline Quinone-Dependent Glucose Dehydrogenase Activity in the Model Rhizosphere-Dwelling Bacterium *Pseudomonas putida* KT2440.** *Appl Environ Microbiol* 2016, **82:**4955-4964.
101. Oteino N, Lally RD, Kiwanuka S, Lloyd A, Ryan D, Germaine KJ, Dowling DN: **Plant growth promotion induced by phosphate solubilizing endophytic *Pseudomonas* isolates.** *Front Microbiol* 2015, **6**.
102. Sashidhar B, Podile AR: **Mineral phosphate solubilization by rhizosphere bacteria and scope for manipulation of the direct oxidation pathway involving glucose dehydrogenase.** *J App Microbiol* 2010, **109:**1-12.
103. Rasul M, Yasmin S, Suleman M, Zaheer A, Reitz T, Tarkka MT, Islam E, Mirza MS: **Glucose dehydrogenase gene containing phosphobacteria for biofortification of Phosphorus with growth promotion of rice.** *Microbiol Res* 2019, **223-225:**1-12.
104. Kumar C, Yadav K, Archana G, Naresh Kumar G: **2-ketogluconic acid secretion by incorporation of *Pseudomonas putida* KT2440 gluconate dehydrogenase (gad) operon in *Enterobacter asburiae* PSI3 improves mineral phosphate solubilization.** *Curr Microbiol* 2013, **67:**388-394.
105. Zeng Q, Wu X, Wen X: **Effects of Soluble Phosphate on Phosphate-Solubilizing Characteristics and Expression of *gcd* Gene in *Pseudomonas frederiksbergensis* JW-SD2.** *Curr Microbiol* 2016, **72:**198-206.
106. Naveed M, Sohail Y, Khalid N, Ahmed I, Mumtaz AS: **Evaluation of Glucose Dehydrogenase and Pyrroloquinoline Quinine (*pqq*) Mutagenesis that Renders Functional Inadequacies in Host Plants.** *J Microbiol Biotechnol* 2015, **25:**1349-1360.
107. Yu K, Liu Y, Tichelaar R, Savant N, Lagendijk E, van Kuijk SJL, Stringlis IA, van Dijken AJH, Pieterse CMJ, Bakker P, et al: **Rhizosphere-Associated *Pseudomonas* Suppress Local Root Immune Responses by Gluconic Acid-Mediated Lowering of Environmental pH.** *Curr Biol* 2019, **29:**3913-3920 e3914.

108. Chavarría M, Goni-Moreno A, de Lorenzo V, Nikel PI: **A Metabolic Widget Adjusts the Phosphoenolpyruvate-Dependent Fructose Influx in *Pseudomonas putida*.** *mSystems* 2016, **1**.
109. Chavarría M, Kleijn RJ, Sauer U, Pfluger-Grau K, de Lorenzo V: **Regulatory tasks of the phosphoenolpyruvate-phosphotransferase system of *Pseudomonas putida* in central carbon metabolism.** *mBio* 2012, **3**.
110. Sawyer MH, Baumann P, Baumann L, Berman SM, Cánovas JL, Berman RH: **Pathways of D-fructose catabolism in species of *Pseudomonas*.** *Arch Microbiol* 1977, **112:**49-55.
111. Chavarría M, Durante-Rodriguez G, Krell T, Santiago C, Brezovsky J, Damborsky J, de Lorenzo V: **Fructose 1-phosphate is the one and only physiological effector of the Cra (FruR) regulator of *Pseudomonas putida*.** *FEBS Open Bio* 2014, **4:**377-386.
112. Ogierman M, Braun V: **Interactions between the outer membrane ferric citrate transporter FecA and TonB: studies of the FecA TonB box.** *J Bacteriol* 2003, **185:**1870-1885.
113. Létoffé S, Delepelaire P, Wandersman C: **Free and hemophore-bound heme acquisitions through the outer membrane receptor HasR have different requirements for the TonB-ExbB-ExbD complex.** *J Bacteriol* 2004, **186:**4067-4074.
114. Schauer K, Rodionov DA, de Reuse H: **New substrates for TonB-dependent transport: do we only see the 'tip of the iceberg'?** *Trends Biochem Sci* 2008, **33:**330-338.
115. Tang K, Jiao N, Liu K, Zhang Y, Li S: **Distribution and functions of TonB-dependent transporters in marine bacteria and environments: implications for dissolved organic matter utilization.** *PLoS One* 2012, **7:**e41204.
116. Yep A, McQuade T, Kirchhoff P, Larsen M, Mobley HL: **Inhibitors of TonB function identified by a high-throughput screen for inhibitors of iron acquisition in uropathogenic *Escherichia coli* CFT073.** *mBio* 2014, **5:**e01089-01013.
117. Noinaj N, Guillier M, Barnard TJ, Buchanan SK: **TonB-dependent transporters: regulation, structure, and function.** *Annu Rev Microbiol* 2010, **64:**43-60.
118. Hickman SJ, Cooper REM, Bellucci L, Paci E, Brockwell DJ: **Gating of TonB-dependent transporters by substrate-specific forced remodelling.** *Nat Commun* 2017, **8:**14804.
119. Krewulak KD, Vogel HJ: **Structural biology of bacterial iron uptake.** *Biochim Biophys Acta* 2008, **1778:**1781-1804.
120. Ciragan A, Backlund SM, Mikula KM, Beyer HM, Samuli Ollila OH, Iwaï H: **NMR Structure and Dynamics of TonB Investigated by Scar-Less Segmental Isotopic Labeling Using a Salt-Inducible Split Intein.** *Front Chem* 2020, **8**.
121. Held KG, Postle K: **ExbB and ExbD do not function independently in TonB-dependent energy transduction.** *J Bacteriol* 2002, **184:**5170-5173.
122. Maki-Yonekura S, Matsuoka R, Yamashita Y, Shimizu H, Tanaka M, Iwabuki F, Yonekura K: **Hexameric and pentameric complexes of the ExbBD energizer in the Ton system.** *Elife* 2018, **7**.
123. Molina L, Geoffroy VA, Segura A, Udaondo Z, Ramos JL: **Iron Uptake Analysis in a Set of Clinical Isolates of *Pseudomonas putida*.** *Front Microbiol* 2016, **7:**2100.

124. Perraud Q, Cantero P, Roche B, Gasser V, Normant VP, Kuhn L, Hammann P, Mislin GLA, Ehret-Sabatier L, Schalk IJ: **Phenotypic Adaption of *Pseudomonas aeruginosa* by Hacking Siderophores Produced by Other Microorganisms.** *Mol Cell Proteomics* 2020, **19:**589-607.
125. Crowley DE, Wang YC, Reid CPP, Szaniszlo PJ: **Mechanisms of iron acquisition from siderophores by microorganisms and plants.** *Plant Soil* 1991, **130:**179-198.
126. Mehtio T, Toivari M, Wiebe MG, Harlin A, Penttila M, Koivula A: **Production and applications of carbohydrate-derived sugar acids as generic biobased chemicals.** *Crit Rev Biotechnol* 2016, **36:**904-916.
127. de Lederkremer RM, Marino C: **Acids and other products of oxidation of sugars.** *Adv Carbohydr Chem Biochem* 2003, **58:**199-306.
128. Takashi T, Tomoki A, Isao N, Tadahiro F, Mitsutaka O, Kazuyuki O, Jiahui H, Tamao I, Masatake H: **Chapter One - Heterogeneous Catalysis by Gold.** *Adv Catal* 2012, **55:**1-126.
129. Jin D, Ma J, Li Y, Jiao G, Liu K, Sun S, Zhou J, Sun R: **Development of the synthesis and applications of xylonic acid: A mini-review.** *Fuel* 2022, **314:**122773.
130. Chubukov V, Mukhopadhyay A, Petzold CJ, Keasling JD, Martín HG: **Synthetic and systems biology for microbial production of commodity chemicals.** *NPJ Syst Biol Appl* 2016, **2:**16009.
131. Shinagawa E, Chiyonobu T, Matsushita K, Adachi O, Amhyama M: **Distribution of Gluconate Dehydrogenase and Ketogluconate Reductases in Aerobic Bacteria.** *Agric Biol Chem* 1978, **42:**1055-1057.
132. Ramachandran S, Fontanille P, Pandey A, Larroche C: **Gluconic Acid: Properties, Applications and Microbial Production.** *Food Technol Biotechnol* 2006, **44:**185-195.
133. Ma Y, Li B, Zhang X, Wang C, Chen W: **Production of Gluconic Acid and Its Derivatives by Microbial Fermentation: Process Improvement Based on Integrated Routes.** *Front Bioeng Biotechnol* 2022, **10**.
134. Pezzotti F, Therisod M: **Enzymatic synthesis of aldonic acids.** *Carbohydr Res* 2006, **341:**2290-2292.
135. Hancock RD, Viola R: **The use of micro-organisms for L-ascorbic acid production: current status and future perspectives.** *Appl Microbiol Biotechnol* 2001, **56:**567-576.
136. Tucaliuc A, Cîșlaru A, Kloetzer L, Blaga AC: **Strain Development, Substrate Utilization, and Downstream Purification of Vitamin C.** *Processes* 2022, **10:**1595.
137. Singh OV, Kumar R: **Biotechnological production of gluconic acid: future implications.** *Appl Microbiol Biotechnol* 2007, **75:**713-722.
138. Kornecki JF, Carballares D, Tardioli PW, Rodrigues RC, Berenguer-Murcia Á, Alcántara AR, Fernandez-Lafuente R: **Enzyme production of D-gluconic acid and glucose oxidase: successful tales of cascade reactions.** *Catal Sci Technol* 2020, **10:**5740-5771.
139. Pfeifer VF, Vojnovich C, Heger EN, Nelson GEN, Haynes WC: **Production of Calcium 2-Ketogluconate by Fermentation with Species of *Pseudomonas*.** *Ind Eng Chem Res* 1958, **50:**1009-1012.
140. Bremus C, Herrmann U, Bringer-Meyer S, Sahm H: **The use of microorganisms in L-ascorbic acid production.** *J Biotech* 2006, **124:**196-205.

141. Li K, Mao X, Liu L, Lin J, Sun M, Wei D, Yang S: **Overexpression of membrane-bound gluconate-2-dehydrogenase to enhance the production of 2-keto-D-gluconic acid by *Gluconobacter oxydan*s.** *Microb Cell Fact* 2016, **15:**121.
142. Zeng W, Cai W, Liu L, Du G, Chen J, Zhou J: **Efficient biosynthesis of 2-keto-D-gluconic acid by fed-batch culture of metabolically engineered *Gluconobacter japonicus*.** *Synth Syst Biotechnol* 2019, **4:**134-141.
143. Sun L, Wang DM, Sun WJ, Cui FJ, Gong JS, Zhang XM, Shi JS, Xu ZH: **Two-Stage Semi-Continuous 2-Keto-Gluconic Acid (2KGA) Production by *Pseudomonas plecoglossicida* JUIM01 From Rice Starch Hydrolyzate.** *Front Bioeng Biotechnol* 2020, **8:**120.
144. Sun W, Alexander T, Man Z, Xiao F, Cui F, Qi X: **Enhancing 2-Ketogluconate Production of Pseudomonas plecoglossicida JUIM01 by Maintaining the Carbon Catabolite Repression of 2-Ketogluconate Metabolism.** *Molecules* 2018, **23:**2629.
145. Anderson S, Marks CB, Lazarus R, Miller J, Stafford K, Seymour J, Light D, Rastetter W, Estell D: **Production of 2-Keto-L-Gulonate, an Intermediate in L-Ascorbate Synthesis, by a Genetically Modified *Erwinia herbicola*.** *Science* 1985, **230:**144-149.
146. Yang W, Xu H: **Industrial Fermentation of Vitamin C.** In *Industrial Biotechnology of Vitamins, Biopigments, and Antioxidants.* Edited by Vandamme EJ, Revuelta JL2016: 161-192.
147. Lim SM, Lau MSL, Tiong EIJ, Goon MM, Lau RJC, Yeo WS, Lau SY, Mubarak NM: **Process design and economic studies of two-step fermentation for production of ascorbic acid.** *SN Appl Sci* 2020, **2**.
148. Gao L, Liu Y, Zhang X, Zhang H: **Efficient Optimization of *Gluconobacter oxydans* Based on Protein Scaffold-Trimeric CutA to Enhance the Chemical Structure Stability of Enzymes for the Direct Production of 2-Keto-L-gulonic Acid.** *J Chem* 2020, **2020:**1-8.
149. Mao S, Liu Y, Hou Y, Ma X, Yang JH, Han H, Wu J, Jia L, Qin H, Lu F: **Efficient production of sugar-derived aldonic acids by *Pseudomonas fragi* TCCC11892.** *RSC Adv* 2018, **8:**39897-39901.
150. Liu H, Valdehuesa KN, Ramos KR, Nisola GM, Lee WK, Chung WJ: **L-arabonate and D-galactonate production by expressing a versatile sugar dehydrogenase in metabolically engineer*ed Escherichia* coli.** *Bioresour Technol* 2014, **159:**455-459.
151. Dongnv J, Jiliang M, Yancong L, Gaojie J, Kangning L, Shaolong S, Jinghui Z, Runcang S: **Development of the synthesis and applications of xylonic acid: A mini-review.** *Fuel* 2022, **314:**122773.
152. Toivari MH, Nygard Y, Penttila M, Ruohonen L, Wiebe MG: **Microbial D-xylonate production.** *Appl Microbiol Biotechnol* 2012, **96:**1-8.
153. Trichez D, Carneiro C, Braga M, Almeida JRM: **Recent progress in the microbial production of xylonic acid.** *World J Microbiol Biotechnol* 2022, **38:**127.
154. Fricke PM, Hartmann R, Wirtz A, Bott M, Polen T: **Production of L-arabinonic acid from L-arabinose by the acetic acid bacteri*um Gluconobacter oxyd*ans.** *Bioresour Technol Rep* 2022, **17**.
155. Nasir SS, Wilken LO, Jr., Akhtar B: **Application of gluconolactone in direct tablet compression.** *J Pharm Sci* 1977, **66:**370-379.

156. Moreaux M, Bonneau G, Peru A, Brunissen F, Janvier M, Haudrechy A, Allais F: **High-Yielding Diastereoselective syn-Dihydroxylation of Protected HBO: An Access to D-(+)-Ribono-1,4-lactone and 5-O-Protected Analogues.** *Eur J Org Chem* 2019, **2019:**1600-1604.
157. Cardozo HM, Ribeiro TF, Sá MM, Sebrão D, Nascimento MG, Silveira GP: **Molecular Sieves Mediated Green Per-O-Acetylation of Carbohydrate Templates and Lipase Catalyzed Regioselective Alcoholysis of 2,3,5-Tri-O-Acetyl-D-Ribonolactone.** *J Braz Chem Soc* 2015.
158. Sarenkova I, Sáez-Orviz S, Ciprovica I, Rendueles M, Díaz M: **Lactobionic acid production by *Pseudomonas taetrolens* in a fed-batch bioreactor using acid whey as substrate.** *Int J Dairy Technol* 2022, **75:**361-371.
159. Alonso S, Rendueles M, Díaz M: **Bio-production of lactobionic acid: Current status, applications and future prospects.** *Biotechnol Adv* 2013, **31:**1275-1291.
160. Kuusisto J, Tokarev AV, Murzina EV, Roslund MU, Mikkola J-P, Murzin DY, Salmi T: **From renewable raw materials to high value-added fine chemicals—Catalytic hydrogenation and oxidation of d-lactose.** *Catal Today* 2007, **121:**92-99.
161. Oh YR, Jang YA, Hong SH, Eom GT: **High-level production of maltobionic acid from high-maltose corn syrup by genetically engineered *Pseudomonas taetrolens*.** *Biotechnol Rep (Amst)* 2020, **28:**e00558.
162. Hancock RD, Viola R: **Biotechnological approaches for l-ascorbic acid production.** *Trends Biotechnol* 2002, **20:**299-305.
163. Wang P, Zeng W, Xu S, Du G, Zhou J, Chen J: **Current challenges facing one-step production of l-ascorbic acid.** *Biotechnol Adv* 2018, **36:**1882-1899.
164. Kirimura K, Yoshioka I: **3.14 - Gluconic and Itaconic Acids.** In *Comprehensive Biotechnology (Third Edition).* Third Edition edition. Edited by Murray M-Y. Oxford: Pergamon; 2019: 166-171.
165. Mussatto SI, Teixeira JAC: *Lignocellulose as raw material in fermentation processes.*2010.
166. Brodeur G, Yau E, Badal K, Collier J, Ramachandran KB, Ramakrishnan S: **Chemical and physicochemical pretreatment of lignocellulosic biomass: a review.** *Enzyme Res* 2011, **2011:**787532.
167. Gírio FM, Fonseca C, Carvalheiro F, Duarte LC, Marques S, Bogel-Łukasik R: **Hemicelluloses for fuel ethanol: A review.** *Bioresour Technol* 2010, **101:**4775-4800.
168. Silveira GP, Cardozo HM, Rossa TA, Sá MM: **D‐Ribonolactone, a Versatile Synthetic Precursor of Biologically Relevant Scaffolds.** *ChemInform* 2015, **47**.
169. Meijnen JP, de Winde JH, Ruijssenaars HJ: **Engineering *Pseudomonas putida* S12 for efficient utilization of D-xylose and L-arabinose.** *Appl Environ Microbiol* 2008, **74:**5031-5037.
170. Wang Y, Horlamus F, Henkel M, Kovacic F, Schläfle S, Hausmann R, Wittgens A, Rosenau F: **Growth of engineered *Pseudomonas putida* KT2440 on glucose, xylose, and arabinose: Hemicellulose hydrolysates and their major sugars as sustainable carbon sources.** *GCB Bioenergy* 2019, **11:**249-259.
171. Blom RH, Pfeifer VF, Moyer AJ, TraufRer DH, Conway HF, Crocker CK, Farison RE, Hannibal DV: **Sodium gluconate production. Fermentation with *Aspergillus niger*.** *Ind Eng Chem* 1952, **44:**435-440.
172. Show PL, Oladele KO, Siew QY, Aziz Zakry FA, Lan JC-W, Ling TC: **Overview of citric acid production from *Aspergillus niger*.** *Front Life Sci* 2015, **8:**271-283.

173. Papagianni M, Mattey M: **Morphological development of *Aspergillus niger* in submerged citric acid fermentation as a function of the spore inoculum level. Application of neural network and cluster analysis for characterization of mycelial morphology.** *Microb Cell Factories* 2006, **5:**3.
174. Ramachandran S, Nair S, Larroche C, Pandey A: **26 - Gluconic Acid.** In *Current Developments in Biotechnology and Bioengineering.* Edited by Ashok P, Sangeeta N, Carlos Ricardo S: Elsevier; 2017: 577-599.
175. Lu F, Ping K, Wen L, Zhao W, Wang Z, Chu J, Zhuang Y: **Enhancing gluconic acid production by controlling the morphology of *Aspergillus niger* in submerged fermentation.** *Process Biochem* 2015, **50:**1342-1348.
176. Muir M, Williams L, Ferenci T: **Influence of transport energization on the growth yield of *Escherichia coli*.** *J Bacteriol* 1985, **163:**1237-1242.
177. Tran QH, Unden G: **Changes in the proton potential and the cellular energetics of *Escherichia coli* during growth by aerobic and anaerobic respiration or by fermentation.** *Eur J Biochem* 1998, **251:**538-543.
178. Baez A, Shiloach J: **Effect of elevated oxygen concentration on bacteria, yeasts, and cells propagated for production of biological compounds.** *Microb Cell Fact* 2014, **13:**181.
179. Hannon JR, Bakker A, Lynd LR, Wyman CE: **Comparing the Scale-Up of Anaerobic and Aerobic Processes.** In *Annual Meeting of the American Institute of Chemical Engineers* Salt Lake City, Utah2007.
180. Hernandez CA, Osma JF: **Microbial Electrochemical Systems: Deriving Future Trends From Historical Perspectives and Characterization Strategies.** *Front Environ Sci* 2020, **8**.
181. Rosenbaum MA, Franks AE: **Microbial catalysis in bioelectrochemical technologies: status quo, challenges and perspectives.** *Appl Microbiol Biotechnol* 2014, **98:**509-518.
182. Sisler FD: **Electrical Energy from Microbiological Processes.** *J Wash Acad Sci* 1962, **52:**181-187.
183. Davis JB: **Generation of Electricity by Microbial Action.** *Volume* 5. Edited by Wayne WU: Academic Press; 1963: 51-64.
184. Liu H, Grot S, Logan BE: **Electrochemically Assisted Microbial Production of Hydrogen from Acetate.** *Environ Sci Technol* 2005, **39:**4317-4320.
185. Rabaey K, Rozendal RA: **Microbial electrosynthesis - revisiting the electrical route for microbial production.** *Nat Rev Microbiol* 2010, **8:**706-716.
186. Hassan RYA, Febbraio F, Andreescu S: **Microbial Electrochemical Systems: Principles, Construction and Biosensing Applications.** *Sensors (Basel)* 2021, **21**.
187. Edel M, Philipp L-A, Lapp J, Reiner J, Gescher J: **Electron transfer of extremophiles in bioelectrochemical systems.** *Extremophiles* 2022, **26:**31.
188. Hernandez ME, Newman DK: **Extracellular electron transfer.** *Cell Mol Life Sci CMLS* 2001, **58:**1562-1571.
189. Shi L, Richardson DJ, Wang Z, Kerisit SN, Rosso KM, Zachara JM, Fredrickson JK: **The roles of outer membrane cytochromes of Shewanella and Geobacter in extracellular electron transfer.** *Environ Microbiol Rep* 2009, **1:**220-227.

190. Ueki T: **Cytochromes in Extracellular Electron Transfer in *Geobacter*.** *Appl Environ Microbiol* 2021, **87**.
191. Bonanni PS, Schrott GD, Busalmen JP: **A long way to the electrode: how do *Geobacter* cells transport their electrons?** *Biochem Soc Trans* 2012, **40:**1274-1279.
192. Pirbadian S, Barchinger SE, Leung KM, Byun HS, Jangir Y, Bouhenni RA, Reed SB, Romine MF, Saffarini DA, Shi L, et al: ***Shewanella oneidensis* MR-1 nanowires are outer membrane and periplasmic extensions of the extracellular electron transport components.** *Proc Natl Acad Sci U S A* 2014, **111:**12883-12888.
193. von Canstein H, Ogawa J, Shimizu S, Lloyd JR: **Secretion of flavins by *Shewanella* species and their role in extracellular electron transfer.** *Appl Environ Microbiol* 2008, **74:**615-623.
194. Pierson LS, 3rd, Pierson EA: **Metabolism and function of phenazines in bacteria: impacts on the behavior of bacteria in the environment and biotechnological processes.** *Appl Microbiol Biotechnol* 2010, **86:**1659-1670.
195. El-Fouly MZ, Sharaf AM, Shahin AAM, El-Bialy HA, Omara AMA: **Biosynthesis of pyocyanin pigment by *Pseudomonas aeruginosa*.** *J Radiat Res Appl Sci* 2015, **8:**36-48.
196. Hall S, McDermott C, Anoopkumar-Dukie S, McFarland AJ, Forbes A, Perkins AV, Davey AK, Chess-Williams R, Kiefel MJ, Arora D, Grant GD: **Cellular Effects of Pyocyanin, a Secreted Virulence Factor of *Pseudomonas aeruginosa*.** *Toxins (Basel)* 2016, **8**.
197. Bosire EM, Rosenbaum MA: **Electrochemical Potential Influences Phenazine Production, Electron Transfer and Consequently Electric Current Generation by *Pseudomonas aeruginosa*.** *Front Microbiol* 2017, **8:**892.
198. Chukwubuikem A, Berger C, Mady A, Rosenbaum MA: **Role of phenazine-enzyme physiology for current generation in a bioelectrochemical system.** *Microb Biotechnol* 2021, **14:**1613-1626.
199. Cheng KY, Karthikeyan R, Wong JWC: **Chapter 4.2 - Microbial Electrochemical Remediation of Organic Contaminants: Possibilities and Perspective.** In *Microbial Electrochemical Technology: Sustainable Platform for Fuels, Chemicals and Remediation.* Edited by Mohan SV, Varjani S, Pandey A: Elsevier; 2019: 613-640.
200. Zhang C, Zhang D, Xiao Z: **Application of Redox Mediators in Bioelectrochemical System.** In *Bioelectrochemistry Stimulated Environmental Remediation: From Bioelectrorespiration to Bioelectrodegradation.* Edited by Wang A, Liang B, Li Z, Cheng H. Singapore: Springer Singapore; 2019: 205-226.
201. Gemünde A, Lai B, Pause L, Krömer JO, Holtmann D: **Redox Mediators in Microbial Electrochemical Systems.** *ChemElectroChem* 2022, **9**.
202. O'Reilly JE: **Oxidation-reduction potential of the ferro-ferricyanide system in buffer solutions.** *Biochim Biophys Acta Bioenerg* 1973, **292:**509-515.
203. Chandrasekhar K, Kumar AN, Raj T, Kumar G, Kim S-H: **Bioelectrochemical system-mediated waste valorization.** *Syst Microbiol Biomanuf* 2021, **1:**432-443.
204. Reddy MV, Sun X: **Chapter 5.3 - Bioelectrosynthesis of Various Chemicals and Evaluation of Their Microbiological Aspects.** In *Biomass, Biofuels and Biochemicals.* 2019: 757-776.

205. Gong Z, Yu H, Zhang J, Li F, Song H: **Microbial electro-fermentation for synthesis of chemicals and biofuels driven by bi-directional extracellular electron transfer.** *Synth Syst Biotechnol* 2020, **5:**304-313.
206. Alvarez Chavez B, Raghavan V, Tartakovsky B: **A comparative analysis of biopolymer production by microbial and bioelectrochemical technologies.** *RSC Adv* 2022, **12:**16105-16118.
207. Wu R, Yu YY, Wang Y, Wang YZ, Song H, Ma C, Qu G, You C, Sun Z, Zhang W, et al: **Wastewater-powered high-value chemical synthesis in a hybrid bioelectrochemical system.** *iScience* 2021, **24:**103401.
208. Phour M, Danish MS, Sabory NR, Ahmadi M, Senjyu T: **Electro-Microbiology: A Green Approach for Energy and Environment Sustainability.** In *Sustainability*, vol. 142022.
209. Zhang S, Jiang J, Wang H, Li F, Hua T, Wang W: **A review of microbial electrosynthesis applied to carbon dioxide capture and conversion: The basic principles, electrode materials, and bioproducts.** *J CO_2 Util* 2021, **51:**101640.
210. Hengsbach J-N, Sabel-Becker B, Ulber R, Holtmann D: **Microbial electrosynthesis of methane and acetate—comparison of pure and mixed cultures.** *Appl Microbiol Biotechnol* 2022, **106:**4427-4443.
211. Jourdin L, Burdyny T: **Microbial Electrosynthesis: Where Do We Go from Here?** *Trends Biotechnol* 2021, **39:**359-369.
212. Quraishi M, Wani K, Pandit S, Gupta PK, Rai AK, Lahiri D, Jadhav DA, Ray RR, Jung SP, Thakur VK, Prasad R: **Valorisation of CO_2 into Value-Added Products via Microbial Electrosynthesis (MES) and Electro-Fermentation Technology.** *Fermentation* 2021, **7:**291.
213. Christodoulou X, Velasquez-Orta SB: **Microbial Electrosynthesis and Anaerobic Fermentation: An Economic Evaluation for Acetic Acid Production from CO(2) and CO.** *Environ Sci Technol* 2016, **50:**11234-11242.
214. Coma M, Vilchez-Vargas R, Roume H, Jauregui R, Pieper DH, Rabaey K: **Product Diversity Linked to Substrate Usage in Chain Elongation by Mixed-Culture Fermentation.** *Environ Sci Technol* 2016, **50:**6467-6476.
215. Kracke F, Lai B, Yu S, Kromer JO: **Balancing cellular redox metabolism in microbial electrosynthesis and electro fermentation - A chance for metabolic engineering.** *Metab Eng* 2018, **45:**109-120.
216. Reiner JE, Jung T, Lapp CJ, Siedler M, Bunk B, Overmann J, Gescher J: ***Kyrpidia spormannii* sp. nov., a thermophilic, hydrogen-oxidizing, facultative autotroph, isolated from hydrothermal systems at São Miguel Island, and emended description of the genus *Kyrpidia*.** *Int J Syst Evol Microbiol* 2018, **68:**3735-3740.
217. Reiner JE, Geiger K, Hackbarth M, Fink M, Lapp CJ, Jung T, Dötsch A, Hügler M, Wagner M, Hille-Reichel A, et al: **From an extremophilic community to an electroautotrophic production strain: identifying a novel Knallgas bacterium as cathodic biofilm biocatalyst.** *ISME J* 2020, **14:**1125-1140.
218. Jung T, Hackbarth M, Horn H, Gescher J: **Improving the Cathodic Biofilm Growth Capabilities of *Kyrpidia spormannii* EA-1 by Undirected Mutagenesis.** *Microorganisms* 2020, **9**.

219. Pillot G, Sunny S, Comes V, Kerzenmacher S: **Optimization of growth and electrosynthesis of PolyHydroxyAlkanoates by the thermophilic bacterium *Kyrpidia spormannii*.** *Bioresour Technol Reports* 2022, **17:**100949.
220. Zhang X, McIlroy SJ, Vassilev I, Rabiee H, Plan M, Cai C, Virdis B, Tyson GW, Yuan Z, Hu S: **Polyhydroxyalkanoate-driven current generation via acetate by an anaerobic methanotrophic consortium.** *Water Res* 2022, **221:**118743.
221. Choi O, Kim T, Woo HM, Um Y: **Electricity-driven metabolic shift through direct electron uptake by electroactive heterotroph *Clostridium pasteurianum*.** *Sci Rep* 2014, **4:**6961.
222. Alberto García Mogollón C, Carlos Quintero Díaz J, Omar Gil Posada J: **Production of acetone, butanol, and ethanol by electro-fermentation with *Clostridium saccharoperbutylacetonicum* N1-4.** *Bioelectrochemistry* 2023, **152:**108414.
223. Wu Z, Wang J, Liu J, Wang Y, Bi C, Zhang X: **Engineering an electroactive *Escherichia coli* for the microbial electrosynthesis of succinate from glucose and CO_2.** *Microb Cell Factories* 2019, **18:**15.
224. Isipato M, Dessì P, Sánchez C, Mills S, Ijaz UZ, Asunis F, Spiga D, De Gioannis G, Mascia M, Collins G, et al: **Propionate Production by Bioelectrochemically-Assisted Lactate Fermentation and Simultaneous CO_2 Recycling.** *Front Microbiol* 2020, **11**.
225. Mayer F, Enzmann F, Lopez AM, Holtmann D: **Performance of different methanogenic species for the microbial electrosynthesis of methane from carbon dioxide.** *Bioresour Technol* 2019, **289:**121706.
226. Villano M, Aulenta F, Ciucci C, Ferri T, Giuliano A, Majone M: **Bioelectrochemical reduction of CO_2 to CH_4 via direct and indirect extracellular electron transfer by a hydrogenophilic methanogenic culture.** *Bioresour Technol* 2010, **101:**3085-3090.
227. LaBelle EV, May HD: **Energy Efficiency and Productivity Enhancement of Microbial Electrosynthesis of Acetate.** *Front Microbiol* 2017, **8**.
228. Yu L, Yuan Y, Tang J, Zhou S: **Thermophilic Moorella thermoautotrophica-immobilized cathode enhanced microbial electrosynthesis of acetate and formate from CO_2.** *Bioelectrochemistry* 2017, **117:**23-28.
229. Marshall CW, Ross DE, Fichot EB, Norman RS, May HD: **Electrosynthesis of commodity chemicals by an autotrophic microbial community.** *Appl Environ Microbiol* 2012, **78:**8412-8420.
230. Nevin KP, Woodard TL, Franks AE, Summers ZM, Lovley DR: **Microbial electrosynthesis: feeding microbes electricity to convert carbon dioxide and water to multicarbon extracellular organic compounds.** *mBio* 2010, **1**.
231. Vassilev I, Hernandez PA, Batlle-Vilanova P, Freguia S, Krömer JO, Keller J, Ledezma P, Virdis B: **Microbial Electrosynthesis of Isobutyric, Butyric, Caproic Acids, and Corresponding Alcohols from Carbon Dioxide.** *ACS Sustain Chem Eng* 2018, **6:**8485-8493.
232. Torella JP, Gagliardi CJ, Chen JS, Bediako DK, Colón B, Way JC, Silver PA, Nocera DG: **Efficient solar-to-fuels production from a hybrid microbial–water-splitting catalyst system.** *PNAS* 2015, **112:**2337-2342.

233. Stöckl M, Harms S, Dinges I, Dimitrova S, Holtmann D: **From CO_2 to Bioplastic – Coupling the Electrochemical CO_2 Reduction with a Microbial Product Generation by Drop-in Electrolysis.** *ChemSusChem* 2020, **13:**4086-4093.
234. Chaturvedi V, Verma P: **Microbial fuel cell: a green approach for the utilization of waste for the generation of bioelectricity.** *Bioresour Bioprocess* 2016, **3:**38.
235. Nawaz A, ul Haq I, Qaisar K, Gunes B, Raja SI, Mohyuddin K, Amin H: **Microbial fuel cells: Insight into simultaneous wastewater treatment and bioelectricity generation.** *Process Saf Environ Prot* 2022, **161:**357-373.
236. Vishwanathan AS: **Microbial fuel cells: a comprehensive review for beginners.** *3 Biotech* 2021, **11:**248.
237. Ibrahim M, Raajaraam L, Raman K: **Modelling microbial communities: Harnessing consortia for biotechnological applications.** *Comput Struct Biotechnol J* 2021, **19:**3892-3907.
238. Sydow A, Krieg T, Mayer F, Schrader J, Holtmann D: **Electroactive bacteria--molecular mechanisms and genetic tools.** *Appl Microbiol Biotechnol* 2014, **98:**8481-8495.
239. Kracke F, Vassilev I, Kromer JO: **Microbial electron transport and energy conservation - the foundation for optimizing bioelectrochemical systems.** *Front Microbiol* 2015, **6:**575.
240. Nikel PI, de Lorenzo V: ***Pseudomonas putida* as a functional chassis for industrial biocatalysis: From native biochemistry to trans-metabolism.** *Metab Eng* 2018.
241. Sathesh-Prabu C, Lee SK: **Genome Editing Tools for *Escherichia coli* and Their Application in Metabolic Engineering and Synthetic Biology.** In *Emerging Areas in Bioengineering.* 2018: 307-319.
242. Chen X, Zhou L, Tian K, Kumar A, Singh S, Prior BA, Wang Z: **Metabolic engineering of *Escherichia coli*: a sustainable industrial platform for bio-based chemical production.** *Biotechnol Adv* 2013, **31:**1200-1223.
243. Adams BL: **The Next Generation of Synthetic Biology Chassis: Moving Synthetic Biology from the Laboratory to the Field.** *ACS Synth Biol* 2016, **5:**1328-1330.
244. Vassilev I, Averesch NJH, Ledezma P, Kokko M: **Anodic electro-fermentation: Empowering anaerobic production processes via anodic respiration.** *Biotechnol Adv* 2021, **48:**107728.
245. Santos-Merino M, Singh AK, Ducat DC: **New Applications of Synthetic Biology Tools for Cyanobacterial Metabolic Engineering.** *Front Bioeng Biotechnol* 2019, **7**.
246. Flynn JM, Ross DE, Hunt KA, Bond DR, Gralnick JA: **Enabling unbalanced fermentations by using engineered electrode-interfaced bacteria.** *mBio* 2010, **1**.
247. Speers AM, Young JM, Reguera G: **Fermentation of Glycerol into Ethanol in a Microbial Electrolysis Cell Driven by a Customized Consortium.** *Environ Sci Technol* 2014, **48:**6350-6358.
248. Sturm-Richter K, Golitsch F, Sturm G, Kipf E, Dittrich A, Beblawy S, Kerzenmacher S, Gescher J: **Unbalanced fermentation of glycerol in *Escherichia coli* via heterologous production of an electron transport chain and electrode interaction in microbial electrochemical cells.** *Bioresour Technol* 2015, **186:**89-96.
249. Förster AH, Beblawy S, Golitsch F, Gescher J: **Electrode-assisted acetoin production in a metabolically engineered *Escherichia coli* strain.** *Biotechnol Biofuels* 2017, **10:**65.

250. Bursac T, Gralnick JA, Gescher J: **Acetoin production via unbalanced fermentation in *Shewanella oneidensis*.** *Biotechnol Bioeng* 2017, **114:**1283-1289.
251. Sun Y, Kokko M, Vassilev I: **Anode-assisted electro-fermentation with *Bacillus subtilis* under oxygen-limited conditions.** *Biotechnol Biofuels Bioprod* 2023, **16:**6.
252. Kim C, Kim MY, Michie I, Jeon B-H, Premier GC, Park S, Kim JR: **Anodic electro-fermentation of 3-hydroxypropionic acid from glycerol by recombinant *Klebsiella pneumoniae* L17 in a bioelectrochemical system.** *Biotechnol Biofuels* 2017, **10:**199.
253. Nguyen AV, Lai B, Adrian L, Krömer JO: **The anoxic electrode-driven fructose catabolism of *Pseudomonas putida* KT2440.** *Microb Biotechnol* 2021, **14:**1784-1796.
254. Vassilev I, Giesselmann G, Schwechheimer SK, Wittmann C, Virdis B, Kromer JO: **Anodic electro-fermentation: Anaerobic production of L-Lysine by recombinant Corynebacterium glutamicum.** *Biotechnol Bioeng* 2018, **115:**1499-1508.
255. Aderem A: **Systems Biology: Its Practice and Challenges.** *Cell* 2005, **121:**511-513.
256. Clarke CJ, Haselden JN: **Metabolic Profiling as a Tool for Understanding Mechanisms of Toxicity.** *Toxicol Pathol* 2008, **36:**140-147.
257. Shah SH, Kraus WE, Newgard CB: **Metabolomic profiling for the identification of novel biomarkers and mechanisms related to common cardiovascular diseases: form and function.** *Circ* 2012, **126:**1110-1120.
258. Shockcor JP: **HPLC–NMR, Pharmaceutical Applications.** In *Encyclopedia of Spectroscopy and Spectrometry (Third Edition).* Edited by Lindon JC, Tranter GE, Koppenaal DW. Oxford: Academic Press; 2017: 141-151.
259. Wang JH, Byun J, Pennathur S: **Analytical approaches to metabolomics and applications to systems biology.** *Semin Nephrol* 2010, **30:**500-511.
260. Lempp M, Lubrano P, Bange G, Link H: **Metabolism of non-growing bacteria.** *Biol Chem* 2020, **401:**1479-1485.
261. Lowe R, Shirley N, Bleackley M, Dolan S, Shafee T: **Transcriptomics technologies.** *PLoS Comput Biol* 2017, **13:**e1005457.
262. Chen H, Shiroguchi K, Ge H, Xie XS: **Genome-wide study of mRNA degradation and transcript elongation in *Escherichia coli*.** *Mol Syst Biol* 2015, **11:**781.
263. Takano S, Takahashi H, Yama Y, Miyazaki R, Furusawa C, Tsuru S: **Inference of transcriptome signatures of *Escherichia coli* in long-term stationary phase.** *Sci Rep* 2023, **13:**5647.
264. Moran MA, Satinsky B, Gifford SM, Luo H, Rivers A, Chan LK, Meng J, Durham BP, Shen C, Varaljay VA, et al: **Sizing up metatranscriptomics.** *ISME J* 2013, **7:**237-243.
265. Gygi SP, Rochon Y, Franza BR, Aebersold R: **Correlation between protein and mRNA abundance in yeast.** *Mol Cell Biol* 1999, **19:**1720-1730.
266. Finehout EJ, Lee KH: **An introduction to mass spectrometry applications in biological research.** *Biochem Mol Biol Educ* 2004, **32:**93-100.
267. Graham RLJ, Graham C, McMullan G: **Microbial proteomics: a mass spectrometry primer for biologists.** *Microb Cell Factories* 2007, **6:**26.
268. Han X, Aslanian A, Yates JR, 3rd: **Mass spectrometry for proteomics.** *Curr Opin Chem Biol* 2008, **12:**483-490.

269. Zhang Y, Fonslow BR, Shan B, Baek MC, Yates JR, 3rd: **Protein analysis by shotgun/bottom-up proteomics.** *Chem Rev* 2013, **113:**2343-2394.
270. Jurtshuk P, Jr.: **Chapter 4: Bacterial Metabolism.** In *Medical Microbiology.* Edited by Baron S. Galveston (TX): University of Texas Medical Branch at Galveston; 1996.
271. Diard S, Carlier JP, Ageron E, Grimont PA, Langlois V, Guerin P, Bouvet OM: **Accumulation of poly(3-hydroxybutyrate) from octanoate in different *Pseudomonas* belonging to the rRNA homology group I.** *Syst Appl Microbiol* 2002, **25:**183-188.
272. Rozendal RA, Sleutels THJA, Hamelers HVM, Buisman CJN: **Effect of the type of ion exchange membrane on performance, ion transport, and pH in biocatalyzed electrolysis of wastewater.** *Water Sci Technol* 2008, **57:**1757-1762.
273. Guo K, Prévoteau A, Patil SA, Rabaey K: **Engineering electrodes for microbial electrocatalysis.** *Curr Opin Biotechnol* 2015, **33:**149-156.
274. Lai B, Nguyen AV, Krömer JO: **Characterizing the Anoxic Phenotype of *Pseudomonas putida* Using a Bioelectrochemical System.** *Methods Protoc* 2019, **2**.
275. Rosman KJR, Taylor PDP: **Isotopic compositions of the elements 1997 (Technical Report).** *Pure Appl Chem* 1998, **70:**217-235.
276. Millard P, Letisse F, Sokol S, Portais J-C: **Correction of MS Data for Naturally Occurring Isotopes in Isotope Labelling Experiments.** In *Metabolic Flux Analysis: Methods and Protocols.* Edited by Krömer JO, Nielsen LK, Blank LM. New York, NY: Springer New York; 2014: 197-207.
277. Ankenbauer A, Schafer RA, Viegas SC, Pobre V, Voss B, Arraiano CM, Takors R: ***Pseudomonas putida* KT2440 is naturally endowed to withstand industrial-scale stress conditions.** *Microb Biotechnol* 2020, **13:**1145-1161.
278. Pause L, Weimer A, Wirth NT, Nguyen AV, Lenz C, Kohlstedt M, Wittmann C, Nikel PI, Lai B, Krömer JO: **Anaerobic glucose uptake in Pseudomonas putida KT2440 in a bioelectrochemical system.** *Microb Biotechnol* 2024, **17:**e14375.
279. Peabody GL, Elmore JR, Martinez-Baird J, Guss AM: **Engineered *Pseudomonas putida* KT2440 co-utilizes galactose and glucose.** *Biotechnol Biofuels* 2019, **12:**295.
280. Derrien D, Marol C, Balesdent J: **The dynamics of neutral sugars in the rhizosphere of wheat. An approach by ^{13}C pulse-labelling and GC/C/IRMS.** *Plant Soil* 2004, **267:**243-253.
281. Bator I, Wittgens A, Rosenau F, Tiso T, Blank LM: **Comparison of Three Xylose Pathways in *Pseudomonas putida* KT2440 for the Synthesis of Valuable Products.** *Front Bioeng Biotechnol* 2019, **7:**480.
282. Meijnen JP, de Winde JH, Ruijssenaars HJ: **Establishment of oxidative D-xylose metabolism in *Pseudomonas putida* S12.** *Appl Environ Microbiol* 2009, **75:**2784-2791.
283. Sánchez-Pascuala A, Fernández-Cabezón L, de Lorenzo V, Nikel PI: **Functional implementation of a linear glycolysis for sugar catabolism in *Pseudomonas putida*.** *Metab Eng* 2019, **54:**200-211.
284. Sanchez-Clemente R, Guijo MI, Nogales J, Blasco R: **Carbon Source Influence on Extracellular pH Changes along Bacterial Cell-Growth.** *Genes (Basel)* 2020, **11**.

285. Itoh T, Mikami B, Hashimoto W, Murata K: **Crystal structure of YihS in complex with D-mannose: structural annotation of *Escherichia coli* and *Salmonella enterica yihS*-encoded proteins to an aldose-ketose isomerase.** *J Mol Biol* 2008, **377:**1443-1459.
286. Lai B, Yu S, Bernhardt PV, Rabaey K, Virdis B, Krömer JO: **Anoxic metabolism and biochemical production in *Pseudomonas putida* F1 driven by a bioelectrochemical system.** *Biotechnol Biofuels* 2016b, **9:**39.
287. Vemuri GN, Altman E, Sangurdekar DP, Khodursky AB, Eiteman MA: **Overflow metabolism in *Escherichia coli* during steady-state growth: transcriptional regulation and effect of the redox ratio.** *Appl Environ Microbiol* 2006, **72:**3653-3661.
288. Michalski A, Cox J, Mann M: **More than 100,000 detectable peptide species elute in single shotgun proteomics runs but the majority is inaccessible to data-dependent LC-MS/MS.** *J Proteome Res* 2011, **10:**1785-1793.
289. Wang X, Shen S, Rasam SS, Qu J: **MS1 ion current-based quantitative proteomics: A promising solution for reliable analysis of large biological cohorts.** *Mass Spectrom Rev* 2019, **38:**461-482.
290. Molina MA, Godoy P, Ramos-González MI, Muñoz N, Ramos JL, Espinosa-Urgel M: **Role of iron and the TonB system in colonization of corn seeds and roots by *Pseudomonas putida* KT2440.** *Environ Microbiol* 2005, **7:**443-449.
291. Wadhwani T, Desai K, Patel DT, Lawani D, Bahaley P, Joshi P, Kothari V: **Effect of various solvents on bacterial growth in context of determining MIC of various antimicrobials.** *Int J Microbiol* 2008, **7**.
292. Ilieva Y, Dimitrova L, Zaharieva MM, Kaleva M, Alov P, Tsakovska I, Pencheva T, Pencheva-El Tibi I, Najdenski H, Pajeva I: **Cytotoxicity and Microbicidal Activity of Commonly Used Organic Solvents: A Comparative Study and Application to a Standardized Extract from *Vaccinium macrocarpon*.** *Toxics* 2021, **9:**92.
293. Bitter W, Tommassen J, Weisbeek PJ: **Identification and characterization of the *exbB*, *exbD* and *tonB* genes of *Pseudomonas putida* WCS358: their involvement in ferric-pseudobactin transport.** *Mol Microbiol* 1993, **7:**117-130.
294. Godoy P, Ramos-González M-I, Ramos JL: ***Pseudomonas putida* mutants in the *exbBexbDtonB* gene cluster are hypersensitive to environmental and chemical stressors.** *Environ Microbiol* 2004, **6:**605-610.
295. Llamas MA, Ramos JL, Rodríguez-Herva JJ: **Mutations in each of the tol genes of Pseudomonas putida reveal that they are critical for maintenance of outer membrane stability.** *J Bacteriol* 2000, **182:**4764-4772.
296. Ainsaar K, Tamman H, Kasvandik S, Tenson T, Hõrak R: **The TonB(m)-PocAB System Is Required for Maintenance of Membrane Integrity and Polar Position of Flagella in *Pseudomonas putida*.** *J Bacteriol* 2019, **201**.
297. Yu S, Plan MR, Winter G, Kromer JO: **Metabolic Engineering of *Pseudomonas putida* KT2440 for the Production of para-Hydroxy Benzoic Acid.** *Front Bioeng Biotechnol* 2016, **4:**90.
298. Koehorst JJ, van Dam JCJ, van Heck RGA, Saccenti E, dos Santos VAM, Suárez-Diez M, Schaap PJ: **Comparison of 432 *Pseudomonas* strains through integration of genomic, functional, metabolic and expression data.** *Sci Rep* 2016, **6**.

299. Martinez-Garcia E, Nikel PI, Chavarria M, de Lorenzo V: **The metabolic cost of flagellar motion in *Pseudomonas putida* KT2440.** *Environ Microbiol* 2014, **16:**291-303.
300. Martínez-García E, Nikel PI, Aparicio T, de Lorenzo V: ***Pseudomonas* 2.0: genetic upgrading of *P. putida* KT2440 as an enhanced host for heterologous gene expression.** *Microb Cell Fact* 2014, **13:**159.
301. Lieder S, Nikel PI, de Lorenzo V, Takors R: **Genome reduction boosts heterologous gene expression in *Pseudomonas putida*.** *Microb Cell Fact* 2015, **14:**23.
302. Dong F, Simoska O, Gaffney E, Minteer SD: **Applying synthetic biology strategies to bioelectrochemical systems.** *Electrochem Sci Adv* 2022, **2:**e2100197.
303. Bagg A, Neilands JB: **Ferric uptake regulation protein acts as a repressor, employing iron(II) as a cofactor to bind the operator of an iron transport operon in *Escherichia coli*.** *Biochem* 1987, **26:**5471-5477.
304. Barton HA, Johnson Z, Cox CD, Vasil AI, Vasil ML: **Ferric uptake regulator mutants of *Pseudomonas aeruginosa* with distinct alterations in the iron-dependent repression of exotoxin A and siderophores in aerobic and microaerobic environments.** *Mol Microbiol* 1996, **21:**1001-1017.
305. Kaushik MS, Singh P, Tiwari B, Mishra AK: **Ferric Uptake Regulator (FUR) protein: properties and implications in cyanobacteria.** *Ann Microbiol* 2016, **66:**61-75.
306. Pasqua M, Visaggio D, Lo Sciuto A, Genah S, Banin E, Visca P, Imperi F: **Ferric Uptake Regulator Fur Is Conditionally Essential in *Pseudomonas aeruginosa*.** *J Bacteriol* 2017, **199:**e00472-00417.
307. Nishino K, Yamasaki S, Nakashima R, Zwama M, Hayashi-Nishino M: **Function and Inhibitory Mechanisms of Multidrug Efflux Pumps.** *Front Microbiol* 2021, **12**.
308. Horiyama T, Nishino K: **AcrB, AcrD, and MdtABC multidrug efflux systems are involved in enterobactin export in *Escherichia coli*.** *PLoS One* 2014, **9:**e108642.
309. Poole K, Krebes K, McNally C, Neshat S: **Multiple antibiotic resistance in *Pseudomonas aeruginosa*: evidence for involvement of an efflux operon.** *J Bacteriol* 1993, **175:**7363-7372.
310. Antoniewicz MR: **Tandem mass spectrometry for measuring stable-isotope labeling.** *Curr Opin Biotechnol* 2013, **24:**48-53.
311. Defossez E, Bourquin J, von Reuss S, Rasmann S, Glauser G: **Eight key rules for successful data-dependent acquisition in mass spectrometry-based metabolomics.** *Mass Spectrom Rev* 2023, **42:**131-143.
312. van der Laan T, Boom I, Maliepaard J, Dubbelman A-C, Harms AC, Hankemeier T: **Data-Independent Acquisition for the Quantification and Identification of Metabolites in Plasma.** *Metabolites* 2020, **10:**514.
313. Ludwig C, Gillet L, Rosenberger G, Amon S, Collins BC, Aebersold R: **Data-independent acquisition-based SWATH-MS for quantitative proteomics: a tutorial.** *Mol Syst Biol* 2018, **14:**e8126.
314. Gillet LC, Navarro P, Tate S, Röst H, Selevsek N, Reiter L, Bonner R, Aebersold R: **Targeted data extraction of the MS/MS spectra generated by data-independent acquisition: a new concept for consistent and accurate proteome analysis.** *Mol Cell Proteomics* 2012, **11:**O111.016717.

Appendix

Appendix A. Growth curves of *P. putida* KT2440 from single colony inoculation in different carbon source under aerobic condition xxii

Appendix B. Growth curves of wild-type *P. putida* KT2440 and different pathway mutants (glcP, gaP, 2kgaP) in shake flask with glucose as substrate xxiii

Appendix C. Example of full current density curves produced by glcP, gaP and 2kgaP strains using glucose as substrate..... xxiv

Appendix D. Optical densities of *P. putida* KT2440 wild-type and Δ*gcd* cultures in BES with various aldoses..... xxv

Appendix E. List of proteins with highly significant expression change during bioelectrochemical cultivation of *P. putida* with fructose as substrate. xxvi

Appendix F. List of proteins with highly significant expression change during open-circuit cultivation of *P. putida* with fructose as substrate xxviii

Appendix G. Changes in protein expression of the central carbon metabolism in *P. putida* KT2440 during open-circuit cultivation in fructose (t_1/t_0). xxix

Appendix H. Changes in protein expression of the electron transport in *P. putida* KT2440 during open-circuit cultivation in fructose (t_1/t_0)..... xxx

Appendix A. Growth curves of *P. putida* KT2440 from single colony inoculation in different (**A**) carbohydrates and sugar alcohols, and (**B**) organic acids, under aerobic condition. Data are average of three biological replicates; error bars represent the standard deviation of the sample mean (n=3).

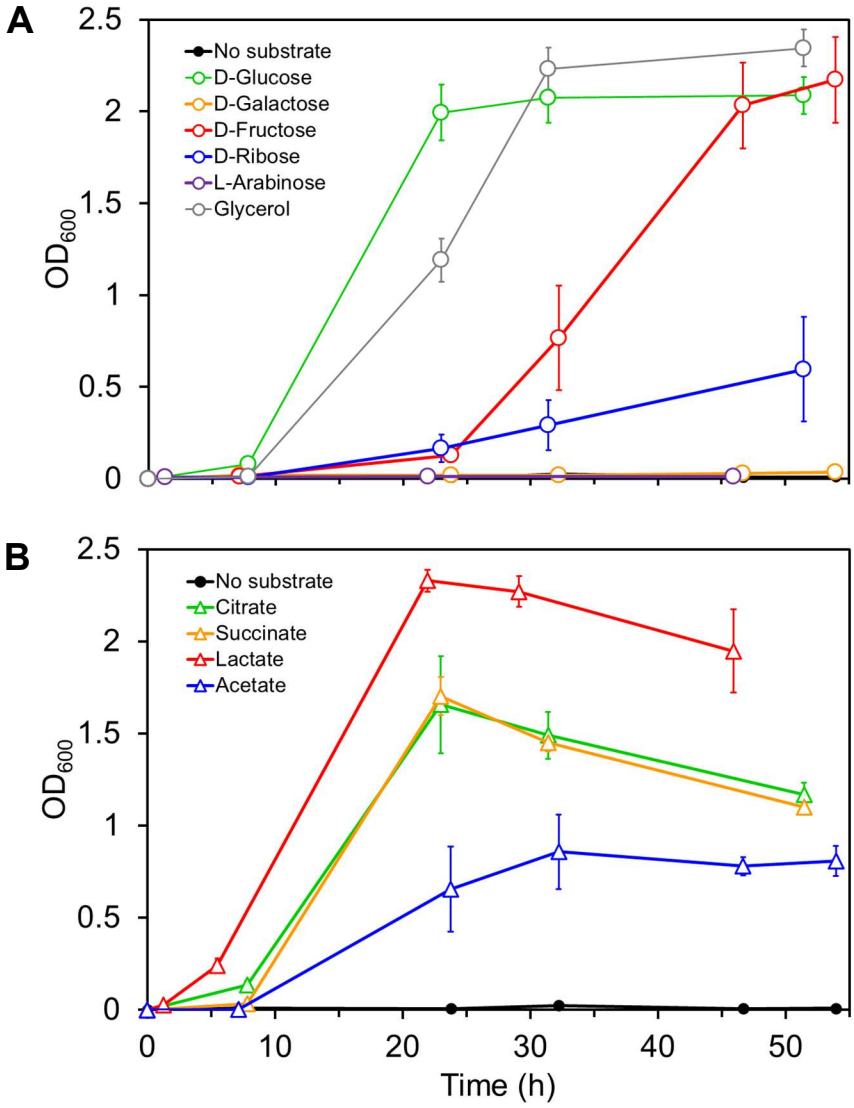

Appendix B. Growth curves of wild-type *P. putida* KT2440 and different pathway mutants (glcP, gaP, 2kgaP) in shake flask with glucose as substrate; (**A**) OD_{600} vs. time, and (**B**) ln(OD) vs. time. Data are average of three biological replicates; error bars represent the standard deviation of the sample mean (n=3).

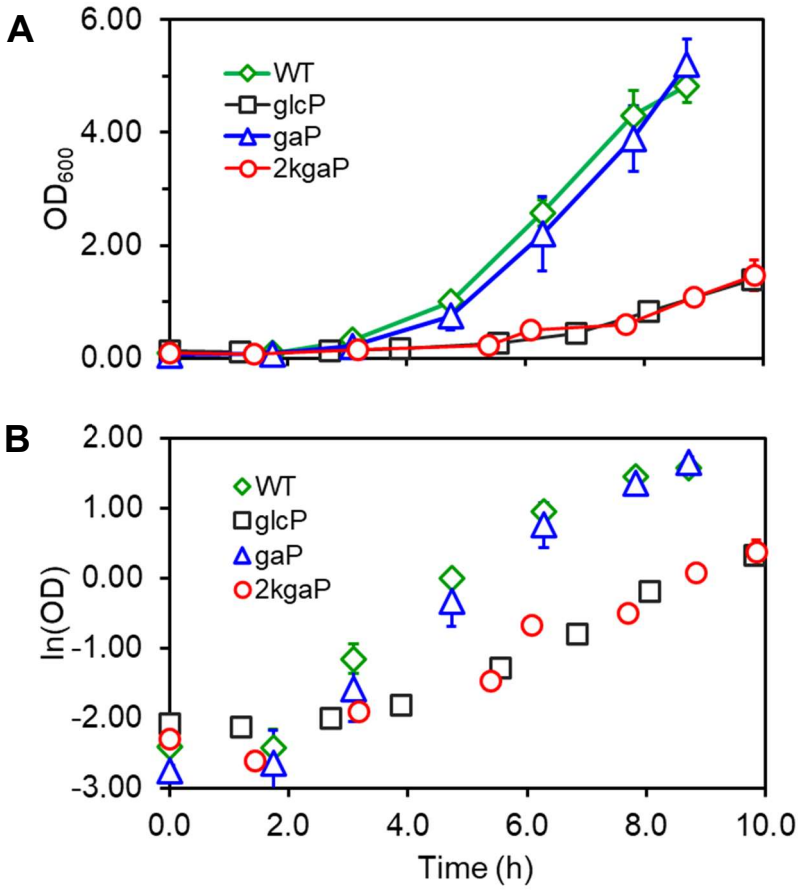

Appendix C. Example of full current density curves produced by glcP, gaP and 2kgaP strains using glucose as substrate (n=1 for each strain)

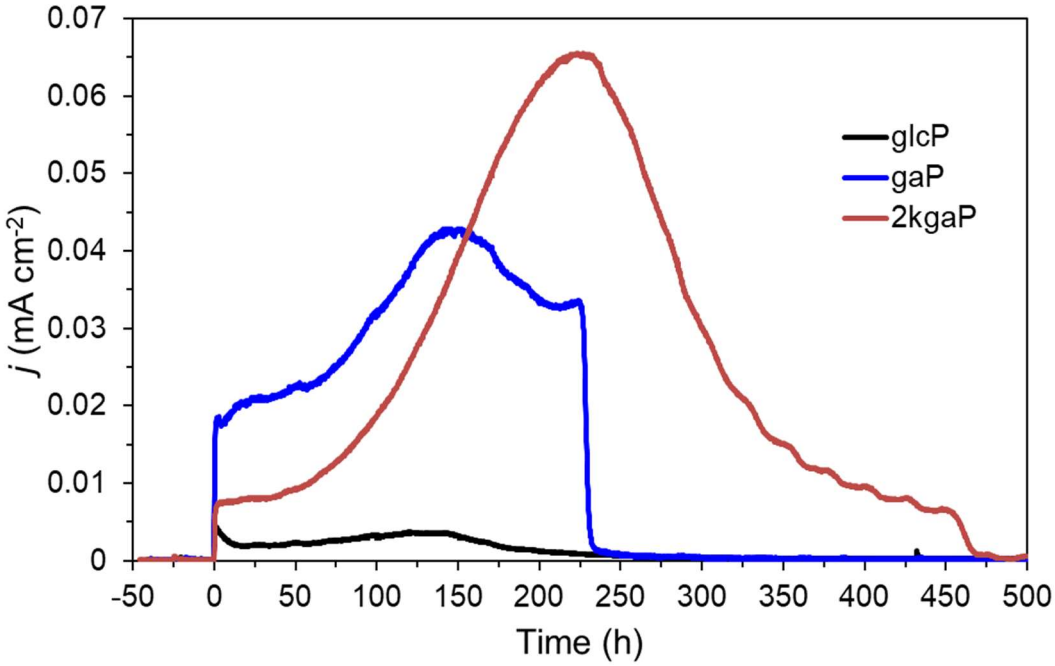

Appendix D. Optical densities of *P. putida* KT2440 (**A**) wild-type and (**B**) Δ*gcd* cultures in BES with various aldoses (n=1 for each sugar).

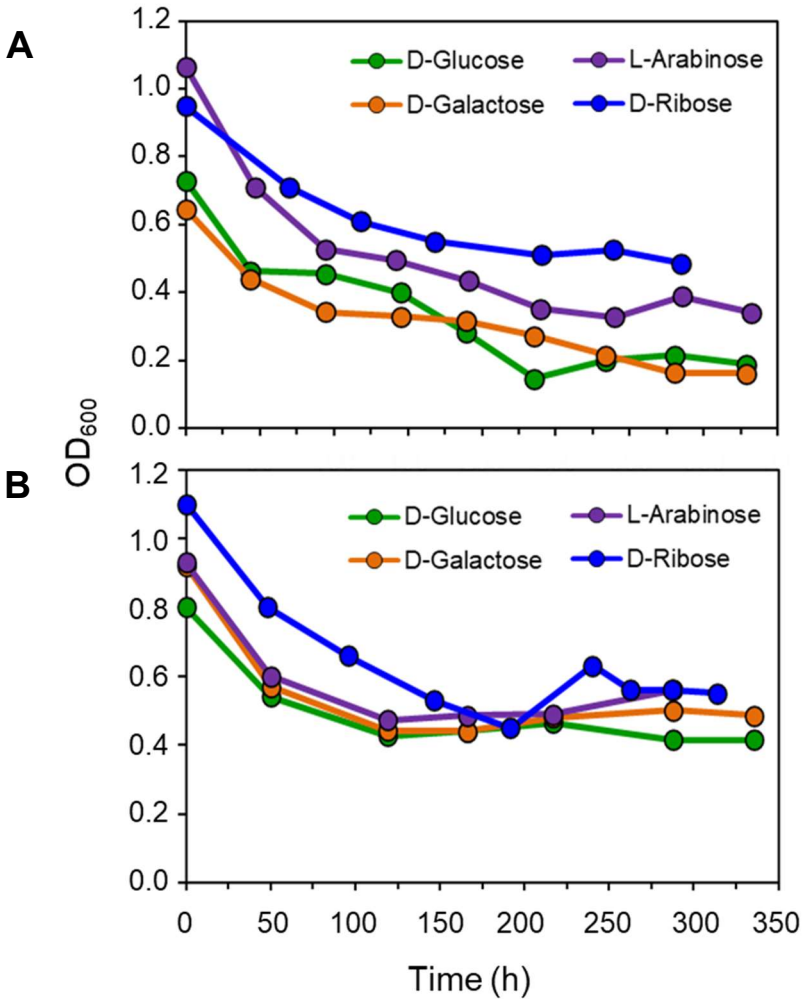

Appendix E. List of proteins with highly significant expression change during bioelectrochemical cultivation of *P. putida* with fructose as substrate. Red, upregulated; blue, downregulated. p-value: *, <0.5; **, <0.01; ***, <0.001.

	Protein	Description	log_2(FC)	p-value
		t_1/t_0		
U1	PP_5324	Response regulator	1.671	***
U2	PP_4944	Carbamoyltransferase	1.123	***
U3	PP_0973	Nucleoid-associated protein	1.146	***
U4	AtpC	ATP synthase epsilon chain	1.219	***
U5	TufA	Elongation factor Tu-A	1.338	***
U6	GyrB	DNA gyrase subunit B	1.546	***
U7	PP_2213	Putative acyl-CoA synthetase	2.970	***
U8	PstB2	Phosphate import ATP-binding protein	2.359	***
U9	PP_1398	Flavin_Reduct domain-containing protein	3.764	**
U10	PP_2601	Transcriptional regulator, IclR family	3.114	**
U11	PP_0111	Electron transport protein SCO1/SenC	3.051	*
U12	CoaD	Phosphopantetheine adenylyltransferase	3.130	*
U13	CumA	Multicopper oxidase	3.564	*
U14	FtsK	DNA translocase	3.038	*
U15	PP_1786	Putative Glycosyl transferase	3.479	*
U16	VisC	Putative oxidoreductase involved in anerobic synthesis of ubiquinone, FAD/NAD(P)-binding domain	3.138	*
U17	LivM	Branched chain amino acid transporter-permease subunit	4.138	*
D1	RpsS	30S ribosomal protein S19	-3.224	***
D2	DppA-I	Dipeptide ABC transporter-periplasmic binding protein	-2.864	***
D3	RpsO	30S ribosomal protein S15	-4.004	**
D4	Pgk	Phosphoglycerate kinase	-3.297	**
D5	YpfJ	Zinc metalloprotease	-3.347	*
D6	YdcS	Polyamine ABC transporter, periplasmic polyamine-binding protein	-4.107	*
D7	LivK	Branched-chain amino acids ABC transporter-periplasmic leucine binding subunit	-3,809	*
D8	PP_3127	Putative Exopolysaccharide transport protein	-3.176	*
D9	PpnP	Pyrimidine/purine nucleoside phosphorylase	-3.283	*
D10	RplX	50S ribosomal protein L24	-3.118	*
D11	PP_2264	Putative Sugar ABC transporter, periplasmic sugar-binding protein	-3.544	*
D12	PP_3444	Glyoxalase family protein	-3.410	*
D13	PP_4593	Uncharacterized protein	-3.035	*
D14	PpiA	Peptidyl-prolyl cis-trans isomerase	-4.472	*
D15	SurA	Periplasmic chaperone	-4.978	*
D16	Prc	Tail-specific protease	-5.682	*
D17	PP_5432	Uncharacterized protein	-6.040	*
		t_2/t_0		
U18	AlaC	Aminotransferase	2.626	***
U19	PP_4104	Glutathione S-transferase family protein	1.541	***

U20	PP_2213	Putative acyl-CoA synthetase	2.752	***
U21	PP_0939	Carbon-nitrogen hydrolase family protein	2.225	***
U22	TsaC	Threonylcarbamoyl-AMP synthase	3.116	**
U23	PP_4573	ATPase, AAA family	3.019	*
U24	PP_4949	Putative peptidase, TldD/PmbA family	3.241	*
U25	Phr	Deoxyribodipyrimidine photolyase	3.272	*
U26	YadG	Putative ABC transporter-ATP binding subunit	3.212	*
U27	SctS	Sulfur compound ABC transporter-permease subunit	3.394	*
U28	Rnc	Ribonuclease 3	3.749	*
U29	LivM	Branched chain amino acid transporter-permease subunit	4.519	*
U30	YbiT	Putative ATP-binding component of a transport system	3.885	*
D18	HupA	DNA-binding protein HU-alpha	-4.127	***
D19	PP_4981	UPF0312 protein	-3.486	**
D20	GrpE	Stress-response protein GrpE	-3.300	**
D21	Ohr	Organic hydroperoxide resistance protein	-3.199	*
D22	HisD	Histidinol dehydrogenase	-3.405	*
D23	RpsS	30S ribosomal protein S19	-3.594	*
D24	PP_4707	OsmY-related protein	-4.689	*
D25	YpfJ	Zinc metalloprotease	-5.006	**
D26	MucA	Sigma factor AlgU negative regulatory protein	-3.719	*
D27	RpmD	50S ribosomal protein L30	-3.425	*
D28	PP_3127	Putative Exopolysaccharide transport protein	-3.168	*
D29	PP_0797	DUF2383 domain-containing protein	-3.476	*
D30	PP_3904	Uncharacterized protein	-3.307	*
D31	PP_0750	Uncharacterized protein	-3.373	*
D32	PP_4561	UPF0337 protein	-3.277	*
D33	GuaD	Guanine deaminase	-3.360	*
D34	SixA	Phosphohistidine phosphatase	-3.344	*
D35	PP_4785	Uncharacterized protein	-3.558	*
D36	PP_3693	Putative Transcriptional regulator MvaT, P16 subunit	-3.682	*
D37	PP_1352	UPF0234 protein	-3.915	*
D38	GtsA	Mannose/glucose ABC transporter, glucose-binding periplasmic protein	-4.133	*
D39	LivK	Branched-chain amino acids ABC transporter-periplasmic leucine binding subunit	-5,022	*
D40	PP_5432	Uncharacterized protein	-4.876	*
D41	PpnP	Pyrimidine/purine nucleoside phosphorylase	-4.708	*
D42	TpiA	Triosephosphate isomerase	-4.528	*
D43	SurA	Periplasmic chaperone	-4.551	*
D44	GltI	Glutamate / aspartate ABC transporter-periplasmic binding protein	-4.371	*
D45	PP_4421	Putative aminotransferase	-4.346	*
D46	PP_0203	Putative dipeptidase	-5.407	*
D47	PP_5156	DUF4399 domain-containing protein	-3.101	*
D48	Pgl	6-phosphogluconolactonase	-3.078	*

Appendix F. List of proteins with highly significant expression change during open-circuit cultivation of *P. putida* with fructose as substrate. Red, upregulated; blue, downregulated. p-value: *, <0.5; **, <0.01; ***, <0.001.

	Protein	Description	log_2(FC)	p-value
		t_1/t_0		
u1	AceF	Acetyltransferase component of pyruvate dehydrogenase complex	3.195	*
d1	CspA-II	Nucleic acid cold-shock chaperone	-3.074	***
d2	PP_3765	H-NS family protein MvaT	-3.964	***
d3	GpmI	2,3-bisphosphoglycerate-independent phosphoglycerate mutase	-1.979	***
d4	RplQ	50S ribosomal protein L17	-3.701	**
d5	DksA	RNA polymerase-binding transcription factor	-2.846	**
d6	PP_4054	Uncharacterized protein	-3.386	**
d7	HupN	Putative DNA-binding protein HU, form N	-3.479	*
d8	PP_2161	Uncharacterized protein	-3.972	*
d9	RplS	50S ribosomal protein L19	-4.747	*
d10	RpmC	50S ribosomal protein L29	-5.784	*
d11	RpsG	30S ribosomal protein S7	-4.272	*
d12	GroS	10 kDa chaperonin	-3.398	*
d13	RpsJ	30S ribosomal protein S10	-3.130	*
d14	RpsE	30S ribosomal protein S5	-3.803	*
d15	GgT	Gamma-glutamyltranspeptidase	-3.443	*
d16	PP_4707	OsmY-related protein	-3.302	*
d17	FabV	Enoyl-[acyl-carrier-protein] reductase [NADH]	-3.206	*
		t_2/t_0		
u2	AceF	Acetyltransferase component of pyruvate dehydrogenase complex	3.248	*
u3	MetK	S-adenosylmethionine synthase	3.192	*
d18	InfC	Translation initiation factor IF-3	-2.844	***
d19	SlyD	Peptidyl-prolyl cis-trans isomerase	-3.400	**
d20	GapA	Glyceraldehyde-3-phosphate dehydrogenase	-3.191	**
d21	PP_3431	ThiJ/PfpI family protein	-3.196	**
d22	Eda	KHG/KDPG aldolase	-3.366	**
d23	PP_1366	Transcriptional regulator MvaT, P16 subunit	-3.199	**
d24	Tsf	Elongation factor Ts	-3.478	**
d25	PP_3765	H-NS family protein MvaT	-3.528	*
d26	PP_4867	Branched-chain amino acid ABC transporter, periplasmic amino acid-binding protein (BraC-like)	-4.019	*
d27	Eno	Enolase	-4.357	*
d28	EtfB	Electron transfer flavoprotein subunit beta	-3.589	*
d29	RplB	50S ribosomal protein L2	-3.522	*
d30	HupN	Putative DNA-binding protein HU, form N	-3.286	*
d31	PP_2187	Universal stress protein family	-3.118	*

Appendix G. Changes in protein expression of the central carbon metabolism in *P. putida* KT2440 during open-circuit cultivation in fructose (t_1/t_0). Red, upregulated; blue, downregulated, black, not significantly changed; gray, undetermined. D-Fru, fructose; F1P, fructose 1-phosphate; D-Man, mannose; M6P, mannose 6-phosphate; G6P, glucose 6-phosphate; F6P, fructose 6-phosphate; F16P, fructose 1,6-bisphosphate; DHAP, dihydroxyacetone phosphate; RL5P, ribulose 5-phosphate; 6PG, 6-phosphogluconate; KDPG, 2-dehydro-3-deoxy-phosphogluconate; GA3P, glyceraldehyde 3-phosphate; 13BPG, 1,3-bisphosphoglycerate; 3PG, 3-phosphoglycerate; 2PG, 2-phosphoglycerate; PEP, phosphoenolpyruvate; Pyr, pyruvate; Ace-CoA, acetyl coenzyme A; Cit, citrate; Isocit, isocitrate; 2KG, 2-ketoglutarate; Suc-CoA, Succinyl coenzyme A; Suc, succinate; Fum, fumarate; Mal, (L-)malate; Oxa, oxaloacetate; Glyox, glyoxylate; Ala, alanine; Asp, aspartate; Glu: glutamate; Ser, serine.

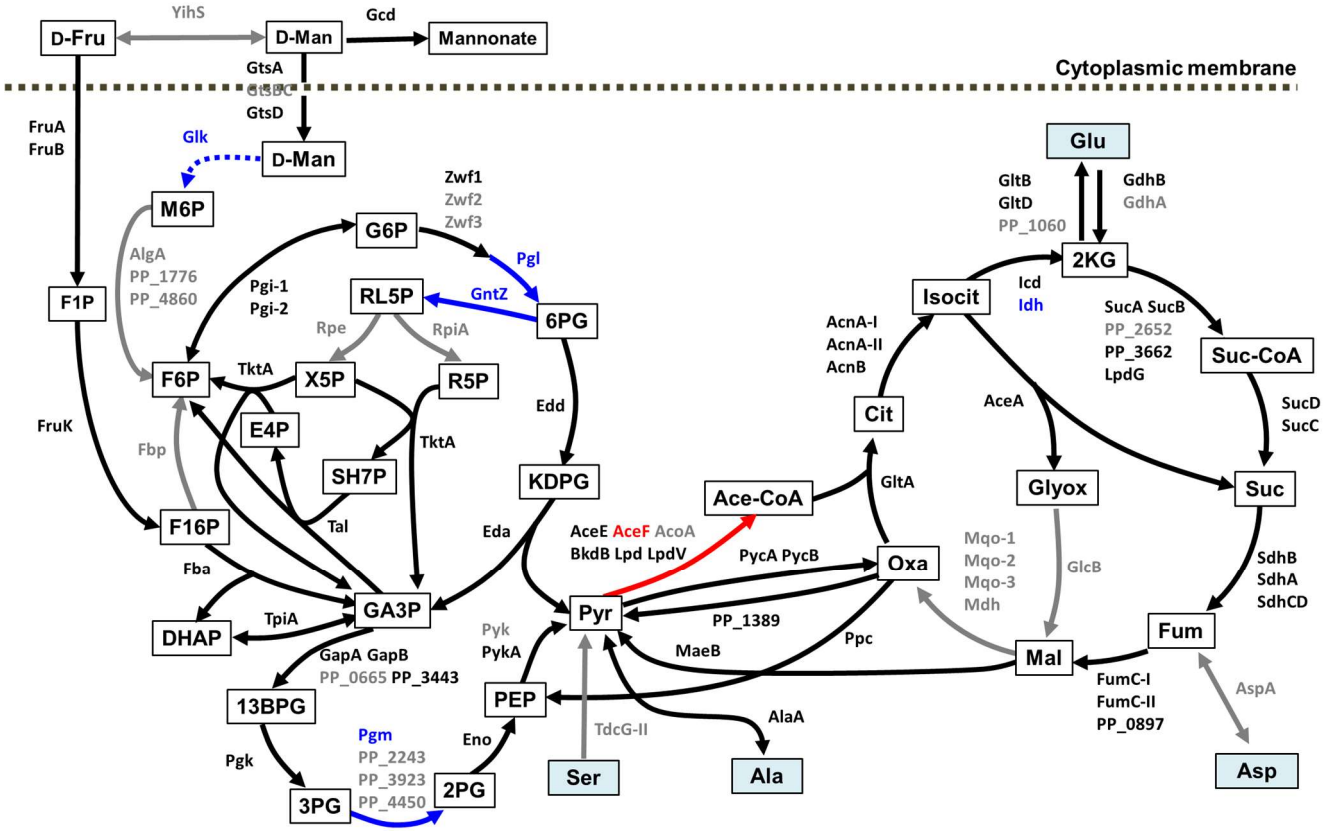

Appendix H. Changes in protein expression of the electron transport chain in *P. putida* KT2440 during open-circuit cultivation in fructose (t_1/t_0). Red, upregulated; blue, downregulated, black, not significantly changed; gray, undetermined.

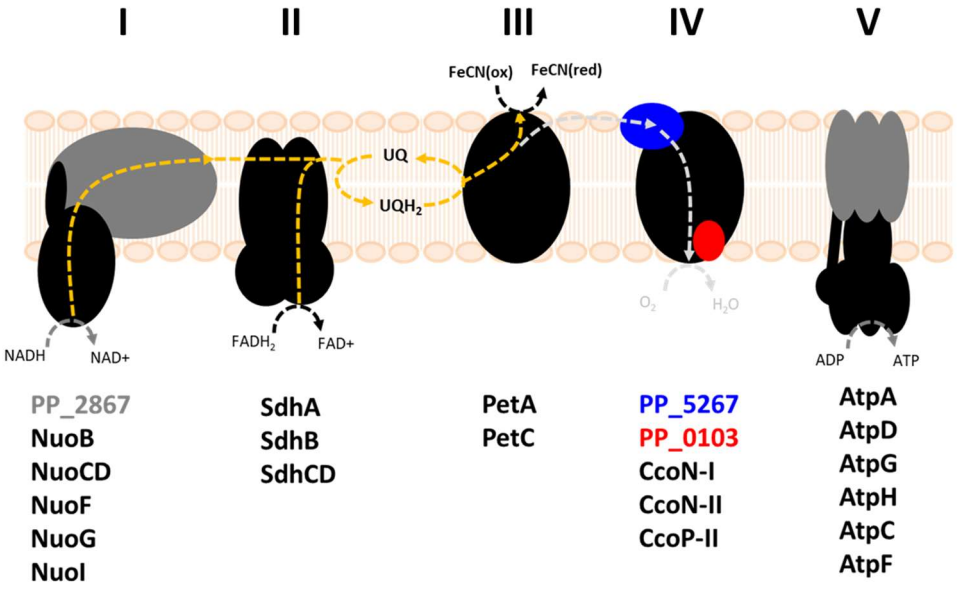

Curriculum vitae

Professional Activities

Jun 2018 – Oct 2021 — **Research Assistant (in the framework of PhD degree)**
Systems Biotechnology, Solar Materials, Helmholtz Center for Environmental Research, Leipzig
Electro-fermentation of different carbohydrates and metabolism of bacterial culture (*Pseudomonas putida*) in anaerobic reactor

Mar 2017 – Aug 2017 — **Internship (in the framework of Master study)**
Bioelectrochemical Systems, Institut für Mikrosystemtechnik, Universität Freiburg, Freiburg im Breisgau
Optimization of microbial electrosynthesis cell design and electrode material for methane production of methanogens

Jun 2016 – Aug 2016 — **Internship (in the framework of Master study)**
The Rosenbaum Lab, Institute of Applied Microbiology, RWTH Aachen, Aachen
Optimization of flat-plate microbial fuel cell for electroactive bacteria

Apr 2014 – Jun 2014 — **Internship (in the framework of Bachelor study)**
Division of Life Sciences, Korea Polar Research Institute, South Korea
Isolation, physiological and biochemical characterization of Antarctic marine bacteria

Academic Phases

Jun 2018 – Present — **Doctoral Candidate**
in Biotechnology
Martin-Luther-Universität Halle-Wittenberg

Oct 2015 – Nov 2017 — **Master of Science and Technology**
in Biomedical Biotechnology
University of Science and Technology of Hanoi

Oct 2011 – Jul 2014 — **Bachelor of Science and Technology**
in Biotechnology-Pharmacology
University of Science and Technology of Hanoi

List of publications during candidature

Published journal papers

- Bin Lai*, Anh Vu Nguyen, and Jens Olaf Krömer*. **Characterizing the Anoxic Phenotype of *Pseudomonas putida* Using a Bioelectrochemical System**. *Methods Protoc* 2019, **2**(2). DOI: 10.3390/mps2020026

Publication citation in this dissertation – this publication was modified and incorporated as Chapter 4, Section 4.1. to 4.3. in this dissertation.

- Anh Vu Nguyen, Bin Lai*, Lorenz Adrian, Jens Olaf Krömer*. **The anoxic electrode-driven fructose catabolism of *Pseudomonas putida* KT2440**. *Microb Biotechnol.* 2021, 14(4):1784-1796. DOI: 10.1111/1751-7915.13862

Publication citation in this dissertation – this publication was modified and incorporated as Chapter 5, Section 5.2. and 5.3. in this dissertation.

- Laura Pause, Anna Weimer, Nicolas Thilo Wirth, Anh Vu Nguyen, Claudius Lenz, Michael Kohlstedt, Christopher Wittmann, Pablo Ivan Nikel, Bin Lai*, Jens Olaf Krömer. **Anaerobic glucose uptake in *Pseudomonas putida* KT2440 in a bioelectrochemical system**. *Microb Biotechnol.* 2024. DOI: 10.1111/1751-7915.14375

Publication citation in this dissertation – parts of this work was modified and incorporated as Chapter 5, Section 5.1. in this dissertation.

Conference

Anh Vu Nguyen, Bin Lai*, Lorenz Adrian, and Jens Olaf Krömer*. **The anoxic, electrode-driven fructose catabolism of *Pseudomonas putida* KT2440**. Electromicrobiology 2021, November 3rd-5th, Aarhus, Denmark, poster.